Title

Measurement of the production cross section for Z/γ* in association with jets in pp collisions at s=7 TeV with the ATLAS detector

Journal

Physical Review D, 85(3)

ISSN

2470-0010

Authors

Aad, G
Abbott, B
Abdallah, J
et al.

Publication Date

2012-02-01

DOI

10.1103/physrevd.85.032009

Measurement of the production cross section for $Z/\gamma*$ in association with jets in pp collisions at $\sqrt{s} = 7$ TeV with the ATLAS detector

G. Aad *et al.**
(ATLAS Collaboration)

(Received 11 November 2011; published 28 February 2012)

Results are presented on the production of jets of particles in association with a Z/γ^* boson, in proton-proton collisions at $\sqrt{s} = 7$ TeV with the ATLAS detector. The analysis includes the full 2010 data set, collected with a low rate of multiple proton-proton collisions in the accelerator, corresponding to an integrated luminosity of 36 pb^{-1}. Inclusive jet cross sections in Z/γ^* events, with Z/γ^* decaying into electron or muon pairs, are measured for jets with transverse momentum $p_T > 30$ GeV and jet rapidity $|y| < 4.4$. The measurements are compared to next-to-leading-order perturbative QCD calculations, and to predictions from different Monte Carlo generators implementing leading-order matrix elements supplemented by parton showers.

DOI: 10.1103/PhysRevD.85.032009 PACS numbers: 12.38.Aw, 12.38.Qk, 13.87.Ce, 14.70.Hp

I. INTRODUCTION

The study of the production of jets of particles in association with a Z/γ^* boson in proton-proton collisions provides a stringent test of perturbative quantum chromodynamics (pQCD). In addition, the proper understanding of these processes in the standard model (SM) is a fundamental element of the LHC physics program, since they constitute backgrounds in searches for new physics. These SM background contributions are estimated using next-to-leading order (NLO) pQCD calculations, and Monte Carlo (MC) predictions that include leading-order (LO) matrix elements supplemented by parton showers. The latter are affected by large scale uncertainties and need to be tuned and validated using data. Measurements of Z/γ^* + jets production have been previously reported in proton-antiproton collisions at $\sqrt{s} = 1.96$ TeV [1] and in proton-proton collisions at $\sqrt{s} = 7$ TeV [2].

This article presents measurements of jet production in events with a Z/γ^* boson in the final state, using 36 ± 1 pb^{-1} of data collected by the ATLAS experiment in 2010 at $\sqrt{s} = 7$ TeV. In this period, the accelerator operated with a moderate instantaneous luminosity of up to 2.1×10^{32} cm^{-2} s^{-1}, and a long spacing of 150 ns between proton bunches, leading to relatively low collision rates and low rates of multiple proton-proton interactions per bunch crossing (pileup) and out-of-time pileup, which makes this data sample especially suitable for cross section measurements at low jet transverse momentum p_T [3].

Events are selected with a Z/γ^* decaying into a pair of electrons (e^+e^-) or muons $(\mu^+\mu^-)$, and the measurements are corrected for detector effects. Inclusive jet differential cross sections are measured as functions of jet transverse momentum, p_T, and rapidity, $|y|$, and total cross sections as functions of jet multiplicity, N_{jet}, in well-defined kinematic regions for the leptons and jets in the final state. Differential cross sections are also measured as functions of p_T and $|y|$ of the leading jet (highest p_T) and second leading jet in Z/γ^* events with at least one and two jets in the final state, respectively. For the latter, the cross section is measured as a function of the invariant mass and the angular separation of the two leading jets. The data are compared to NLO pQCD predictions [4,5], including non-perturbative contributions, and to predictions from several MC programs.

The paper is organized as follows. The detector is described in the next section. Section III discusses the event selection, while Sec. IV provides details of the simulations used in the measurements and Secs. V and VI describe the reconstruction of jets and leptons, respectively. The estimation of background contributions is described in Sec. VII. Selected uncorrected distributions are presented in Sec. VIII, and the procedure used to correct the measurements for detector effects is explained in Sec. IX. The study of systematic uncertainties is discussed in Sec. X. The NLO pQCD predictions are described in Sec. XI. The measured cross sections are presented separately for the electron and muon channels in Sec. XII, where the combination of the electron and muon results is also discussed. Finally, Sec. XIII provides a summary.

II. EXPERIMENTAL SETUP

The ATLAS detector [6] covers almost the whole solid angle around the collision point with layers of tracking detectors, calorimeters and muon chambers. The ATLAS inner detector (ID) has full coverage in ϕ and covers the pseudorapidity range $|\eta| < 2.5$. It consists of a silicon

*Full author list given at the end of the article.

pixel detector, a silicon microstrip detector (SCT), and a straw tube tracker (TRT) which also measures transition radiation for particle identification, all immersed in a 2 tesla axial magnetic field produced by a solenoid.

High-granularity liquid-argon (LAr) electromagnetic sampling calorimeters, with very good energy and position resolution [7], cover the pseudorapidity range $|\eta| < 3.2$. The hadronic calorimetry in the range $|\eta| < 1.7$ is provided by a scintillator-tile calorimeter, consisting of a large barrel and two smaller extended barrel cylinders, one on either side of the central barrel. In the end caps ($|\eta| > 1.5$), LAr hadronic calorimeters match the outer $|\eta|$ limits of the end cap electromagnetic calorimeters. The LAr forward calorimeters provide both electromagnetic and hadronic energy measurements, and extend the coverage to $|\eta| < 4.9$.

The muon spectrometer measures the deflection of muon tracks in the large superconducting air-core toroid magnets in the pseudorapidity range $|\eta| < 2.7$, instrumented with separate trigger and high-precision tracking chambers. Over most of the η range, a precision measurement of the track coordinates in the principal bending direction of the magnetic field is provided by monitored drift tubes. At large pseudorapidities, cathode strip chambers with higher granularity are used in the innermost plane over $2.0 < |\eta| < 2.7$. The muon trigger system, which covers the pseudorapidity range $|\eta| < 2.4$, consists of resistive plate chambers in the barrel ($|\eta| < 1.05$) and thin gap chambers in the end cap regions ($1.05 < |\eta| < 2.4$), with a small overlap in the $|\eta| = 1.05$ region.

III. $Z/\gamma^* \to \ell^+\ell^-$ SELECTION

The data samples considered in this paper were collected with tracking detectors, calorimeters, muon chambers, and magnets fully operational, and correspond to a total integrated luminosity of 36 pb^{-1}.

In the case of the $Z/\gamma^* \to e^+e^-$ analysis, events are selected online using a trigger that requires the presence of at least one identified electron candidate in the calorimeter with transverse energy above 15 GeV in the region $|\eta| < 2.5$. The events are then selected to have two oppositely charged reconstructed electrons (*medium* quality electrons, as described in Ref. [8]) with transverse energy $E_{\mathrm{T}}^e > 20$ GeV, pseudorapidity in the range $|\eta^e| < 2.47$ (where the transition region between calorimeter sections $1.37 < |\eta^e| < 1.52$ is excluded), and a dilepton invariant mass in the range 66 GeV $< m_{e^+e^-} <$ 116 GeV, which optimizes the signal sensitivity.

The $Z/\gamma^* \to \mu^+\mu^-$ sample is collected online using a trigger that requires the presence of at least one muon candidate reconstructed in the muon spectrometer, consistent with having originated from the interaction region with $p_{\mathrm{T}} > 10$ GeV or $p_{\mathrm{T}} > 13$ GeV, depending on the data period, and with the majority of the data taken with the higher threshold, and $|\eta| < 2.4$. The muon candidates are associated with track segments reconstructed in the inner detectors which, combined with the muon spectrometer information, define the final muon track. Combined muon tracks with $p_{\mathrm{T}}^{\mu} > 20$ GeV and $|\eta^{\mu}| < 2.4$ are selected. A number of quality requirements are applied to the muon candidates [9]: the associated inner detector track segment is required to have a minimum number of hits in the pixel, SCT and TRT detectors; and the muon transverse and longitudinal impact parameters, d_0 and z_0, with respect to the reconstructed primary vertex are required to be $d_0/\sigma(d_0) < 3$ and $z_0 < 10$ mm in the $r-\phi$ and $r-z$ planes, respectively, where $\sigma(d_0)$ denotes the d_0 resolution. The muons are required to be isolated: the scalar sum of the transverse momenta of the tracks in an $\eta-\phi$ cone of radius 0.2 around the muon candidate is required to be less than 10% of the muon p_{T}. Events are selected with two oppositely charged muons and an invariant mass 66 GeV $< m_{\mu^+\mu^-} <$ 116 GeV.

In both analyses, events are required to have a reconstructed primary vertex of the interaction with at least 3 tracks associated to it, which suppresses beam-related background contributions and cosmic rays. The selected dilepton samples contain a total of 9705 and 12 582 events for the electron and muon channels, respectively.

IV. MONTE CARLO SIMULATION

Monte Carlo event samples are used to compute detector acceptance and reconstruction efficiencies, determine

TABLE I. Number of events for the $Z/\gamma^* \to e^+e^-$ and $Z/\gamma^* \to \mu^+\mu^-$ analyses as a function of inclusive jet multiplicity. The data are compared to the predictions for the signal (as determined by ALPGEN) and background processes (see Secs. IV and VII). No uncertainties are indicated. The statistical uncertainty on the total prediction is negligible, and the corresponding systematic uncertainty varies between 10% and 23% with increasing N_{jet}.

		$Z/\gamma^* \to e^+e^-$ channel			
		≥ 1 jet	≥ 2 jets	≥ 3 jets	≥ 4 jets
$Z/\gamma^* \to e^+e^-$	ALPGEN	1357	307	64.4	12.7
$W \to e\nu$	ALPGEN	4.3	1.0	0.31	0.11
$Z/\gamma^* \to \tau^+\tau^-$	ALPGEN	0.9	0.25	0.03	0.005
WW, WZ, ZZ	ALPGEN	9.6	4.8	1.7	0.45
$t\bar{t}$	MC@NLO	11.7	9.2	4.3	1.3
Multijets	From data	49	12.6	2.2	0.7
SM prediction		1432	334	72.9	15.2
data (36 pb^{-1})		1514	333	62	15
		$Z/\gamma^* \to \mu^+\mu^-$ channel			
		≥ 1 jet	≥ 2 jets	≥ 3 jets	≥ 4 jets
$Z/\gamma^* \to \mu^+\mu^-$	ALPGEN	1869	421	87.2	17.7
$W \to \mu\nu$	ALPGEN	0.3	0.06	0.04	0.04
$Z/\gamma^* \to \tau^+\tau^-$	ALPGEN	0.68	0.11	0.03	<0.01
WW, WZ, ZZ	ALPGEN	12.8	6.8	2.3	0.57
$t\bar{t}$	MC@NLO	13.6	10.7	4.6	1.4
Multijets	From data	1	0.3	0.1	0.01
SM prediction		1898	439	94.2	19.8
Data (36 pb^{-1})		1885	422	93	20

background contributions, correct the measurements for detector effects, and estimate systematic uncertainties on the final results.

Samples of simulated $Z/\gamma^*(\rightarrow e^+e^-)+\text{jets}$ and $Z/\gamma^*(\rightarrow \mu^+\mu^-)+\text{jets}$ events with a dilepton invariant mass above 40 GeV are generated using ALPGEN v2.13 [10] (including LO matrix elements for up to $2 \rightarrow 5$ parton scatters) interfaced to HERWIG v6.510 [11] for parton shower and fragmentation into particles, and to JIMMY v4.31 [12] to model underlying event (UE) contributions. Similar samples are generated using SHERPA 1.2.3 [13] with an UE modeling according to Ref. [14]. For the ALPGEN samples CTEQ6L1 [15] parton density functions (PDFs) are employed, while for SHERPA CTEQ6.6 [16] is used. The ALPGEN and SHERPA samples are normalized to the next-to-next-to-leading order (NNLO) pQCD inclusive Drell-Yan prediction of 1.07 ± 0.05 nb, as determined by the FEWZ [17] program using the MSTW2008 PDFs. In addition, $Z/\gamma^*+\text{jets}$ samples ($q\bar{q} \rightarrow Z/\gamma^* g$ and $qg \rightarrow Z/\gamma^* q$ processes with $\hat{p}_T > 10$ GeV, where $\hat{p}_T$ is the transverse momentum defined in the rest frame of the hard interaction) are produced using PYTHIA v6.423 [18] and HERWIG plus JIMMY with MRST2007LO* [19] PDFs. For the ALPGEN and HERWIG plus JIMMY MC samples the AUET1 [20] tuned set of parameters is used to model the UE activity in the final state. In the case of the PYTHIA samples, the AMBT1 [21] tune is employed.

Background samples from $W+\text{jets}$ and $Z/\gamma^*(\rightarrow \tau^+\tau^-)+\text{jets}$ final states, and diboson (WW, WZ, ZZ) processes are generated using ALPGEN with CTEQ6L1 PDFs normalized to NNLO [17] and NLO [4] pQCD predictions, respectively. TAUOLA v1.0.2 [22] is used for tau decays. Simulated top-quark production samples are generated using MC@NLO [23] and CTEQ6.6 PDFs.

The MC samples are generated with minimum bias interactions from PYTHIA overlaid on top of the hard-scattering event in order to account for the presence of

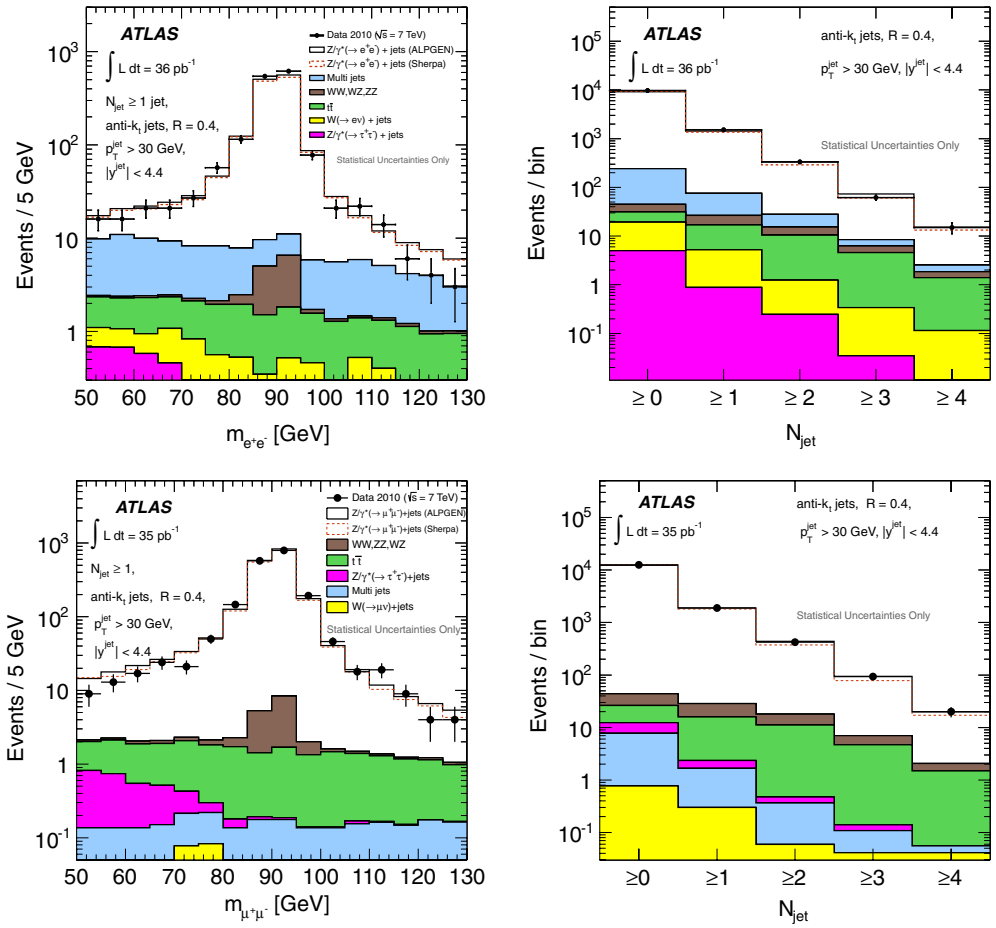

FIG. 1 (color online). Uncorrected dilepton invariant mass in (top) $Z/\gamma^* \rightarrow e^+e^-$ and (bottom) $Z/\gamma^* \rightarrow \mu^+\mu^-$ events with at least one jet in the final state, shown in a wider dilepton mass region than the one selected (left), and uncorrected inclusive jet multiplicity (right), for jets with $p_T > 30$ GeV and $|y| < 4.4$ (black dots), and in the mass range 66 GeV $< m_{\ell^+\ell^-} <$ 116 GeV ($\ell = e, \mu$). Only statistical uncertainties are shown. The data are compared to predictions for signal (ALPGEN and SHERPA, both normalized to the FEWZ value for the total cross section) and background processes (filled histograms).

the pileup experienced in the data. The number of minimum bias (MB) interactions follows a Poisson distribution with a mean of two, which is appropriate for the 2010 data. The MC generated samples are then passed through a full simulation [24] of the ATLAS detector and trigger system, based on GEANT4 [25]. The simulated events are reconstructed and analyzed with the same analysis chain as for the data, using the same trigger and event selection criteria, and reweighted such that the distribution of the number of primary vertices matches that of the data.

The multijets background contributions in the electron and muon channels are determined using data, as discussed in Sec. VII.

V. JET RECONSTRUCTION

Jets are defined using the anti-k_t jet algorithm [26] with the distance parameter set to $R = 0.4$. Energy depositions reconstructed as calorimeter clusters are the inputs to the jet algorithm in data and MC simulated events. The same jet algorithm is applied to final state particles in the MC generated events to define jets at particle level [27]. The jet kinematics in data and MC simulated events are corrected to account for the following effects: the presence of additional proton-proton interactions per bunch crossing, leading to an additional energy offset of (500 ± 160) MeV within the jet cone for each extra interaction [28]; the position of the primary vertex of the interaction; and the measurement biases induced by calorimeter noncompensation, additional dead material, and out-of-cone effects. The measured jet p_T is corrected for detector effects back to the true jet energy [29] using an average correction, computed as a function of the jet transverse momentum and pseudorapidity, and extracted from inclusive jet MC samples. The measured jet p_T is reconstructed with a resolution of about 10% at low p_T which improves to 6% for p_T about 200 GeV. The measured jet angular variables y and ϕ are reconstructed with no significant shift and a resolution better than 0.05, which improves as the jet transverse momentum increases.

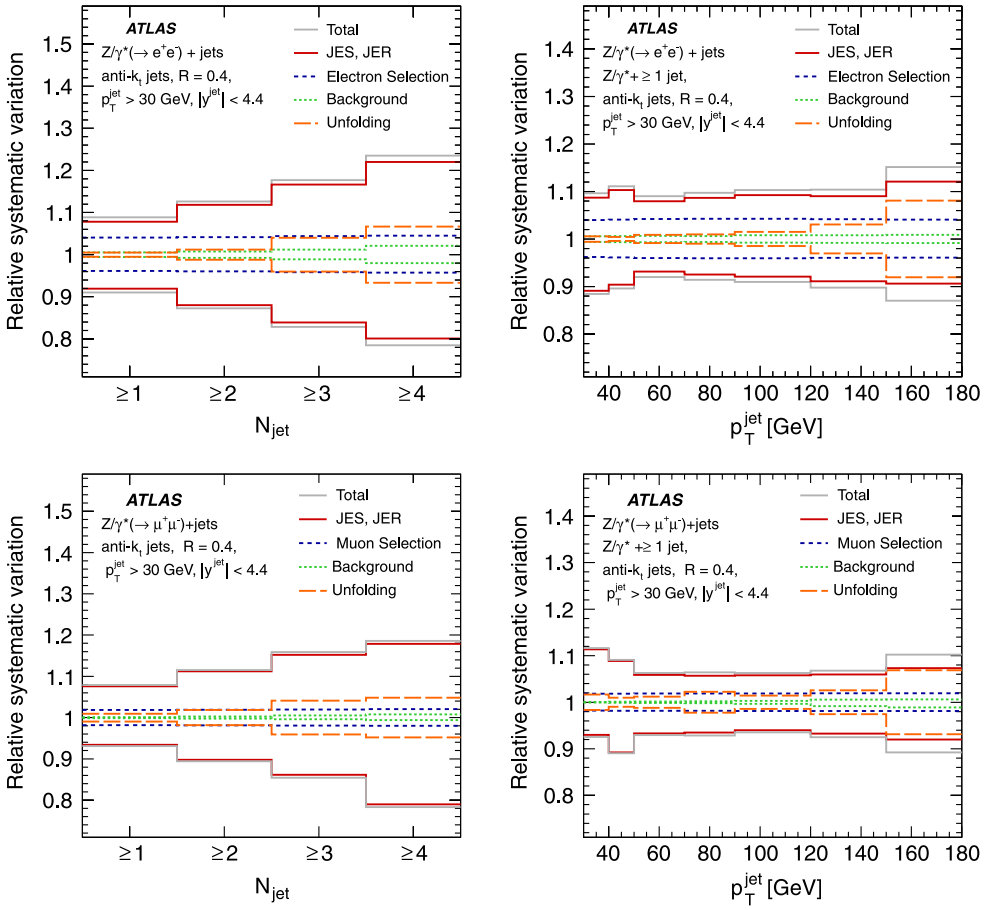

FIG. 2 (color online). Relative systematic uncertainties from different sources in the (top) $Z/\gamma^*(\rightarrow e^+e^-)$ + jets and (bottom) $Z/\gamma^*(\rightarrow \mu^+\mu^-)$ + jets analyses for the measured cross section as a function of inclusive jet multiplicity, and the inclusive differential cross sections as a function of p_T, for events with at least one jet with $p_T > 30$ GeV and $|y| < 4.4$ in the final state (see Sec. X). The total systematic uncertainty is obtained by summing all contributions in quadrature.

TABLE II. Measured cross section $\sigma_{N_{\text{jet}}}$ as a function of the inclusive jet multiplicity, for events with at least one jet with $p_T > 30$ GeV and $|y| < 4.4$ in the final state. In this and subsequent Tables III and XIII the results are presented for the $Z/\gamma^*(\rightarrow e^+e^-)$ and $Z/\gamma^*(\rightarrow \mu^+\mu^-)$ analyses separately, as extrapolated to the Born level in the common acceptance region $p_T > 20$ GeV and $|\eta| < 2.5$ for the lepton kinematics, and their combination. The multiplicative parton-to-hadron correction factors δ^{had} are applied to the NLO pQCD predictions.

	$\sigma_{N_{\text{jet}}}$ [pb]			
N_{jet}	$Z/\gamma^*(\rightarrow e^+e^-)$	$Z/\gamma^*(\rightarrow \mu^+\mu^-)$	$Z/\gamma^*(\rightarrow \ell^+\ell^-)$	$\delta^{\text{had}} \pm$ (total unc)
	$\sigma \pm$ (stat) $\pm$ (syst)	$\sigma \pm$ (stat) $\pm$ (syst)	$\sigma \pm$ (total unc)	parton $\rightarrow$ hadron
≥ 1 jet	$69 \pm 2 \pm 7$	$65 \pm 2^{+6}_{-5}$	65^{+6}_{-5}	0.99 ± 0.02
≥ 2 jets	$14.3 \pm 0.9 \pm 1.9$	$13.9 \pm 0.7^{+1.7}_{-1.6}$	14.0 ± 1.8	0.98 ± 0.03
≥ 3 jets	$2.4 \pm 0.4 \pm 0.4$	$2.9 \pm 0.3^{+0.5}_{-0.4}$	2.7 ± 0.5	0.98 ± 0.05
≥ 4 jets	$0.6 \pm 0.2 \pm 0.1$	$0.6 \pm 0.2 \pm 0.1$	0.6 ± 0.2	1.03 ± 0.05

TABLE III. Measured cross section ratio $\sigma_{N_{\text{jet}}}/\sigma_{N_{\text{jet}}-1}$ as a function of the inclusive jet multiplicity, for events with at least one jet with $p_T > 30$ GeV and $|y| < 4.4$ in the final state.

	$\sigma_{N_{\text{jet}}}/\sigma_{N_{\text{jet}}-1}$			
N_{jet}	$Z/\gamma^*(\rightarrow e^+e^-)$ ratio $\pm$ (stat) $\pm$ (syst)	$Z/\gamma^*(\rightarrow \mu^+\mu^-)$ ratio $\pm$ (stat) $\pm$ (syst)	$Z/\gamma^*(\rightarrow \ell^+\ell^-)$ ratio $\pm$ (total unc)	$\delta^{\text{had}} \pm$ (total unc) parton $\rightarrow$ hadron
≥ 1 jet	$0.139 \pm 0.002 \pm 0.011$	$0.135 \pm 0.003^{+0.010}_{-0.009}$	$0.135^{+0.011}_{-0.009}$	0.99 ± 0.03
≥ 2 jets	$0.208 \pm 0.007^{+0.008}_{-0.009}$	$0.215 \pm 0.010^{+0.008}_{-0.009}$	$0.215^{+0.010}_{-0.011}$	0.99 ± 0.01
≥ 3 jets	$0.17 \pm 0.02 \pm 0.01$	$0.21 \pm 0.02 \pm 0.01$	0.20 ± 0.02	1.00 ± 0.02
≥ 4 jets	$0.23 \pm 0.04 \pm 0.01$	$0.20 \pm 0.05^{+0.01}_{-0.02}$	0.21 ± 0.03	1.05 ± 0.03

TABLE IV. Measured inclusive jet differential cross section $d\sigma/dp_T$ as a function of p_T, for events with at least one jet with $p_T > 30$ GeV and $|y| < 4.4$ in the final state.

	$d\sigma/dp_{\text{T}}$ [pb/GeV] (inclusive)			
p_T	$Z/\gamma^*(\rightarrow e^+e^-)$	$Z/\gamma^*(\rightarrow \mu^+\mu^-)$	$Z/\gamma^*(\rightarrow \ell^+\ell^-)$	$\delta^{\text{had}} \pm$ (total unc)
[GeV]	$\sigma \pm$ (stat) $\pm$ (syst)	$\sigma \pm$ (stat) $\pm$ (syst)	$\sigma \pm$ (total unc)	parton $\rightarrow$ hadron
30–40	$3.2 \pm 0.1^{+0.3}_{-0.4}$	$2.9 \pm 0.1^{+0.4}_{-0.2}$	$3.0^{+0.4}_{-0.3}$	1.00 ± 0.04
40–50	$1.9 \pm 0.1 \pm 0.2$	$1.9 \pm 0.1 \pm 0.2$	1.9 ± 0.2	0.99 ± 0.02
50–70	$0.89 \pm 0.05^{+0.09}_{-0.08}$	$0.81 \pm 0.04 \pm 0.06$	0.83 ± 0.07	0.99 ± 0.02
70–90	$0.42 \pm 0.03 \pm 0.04$	$0.42 \pm 0.03 \pm 0.03$	0.42 ± 0.04	0.98 ± 0.01
90–120	$0.17 \pm 0.02 \pm 0.02$	$0.18 \pm 0.02 \pm 0.01$	0.17 ± 0.02	0.98 ± 0.01
120–150	$0.073 \pm 0.011 \pm 0.008$	$0.055 \pm 0.008^{+0.004}_{-0.005}$	$0.061^{+0.009}_{-0.008}$	1.00 ± 0.02
150–180	$0.037 \pm 0.008^{+0.006}_{-0.005}$	$0.040 \pm 0.007^{+0.004}_{-0.005}$	0.039 ± 0.007	1.01 ± 0.05

TABLE V. Measured jet differential cross section $d\sigma/dp_T$ as a function of the leading-jet p_T, for events with at least one jet with $p_T > 30$ GeV and $|y| < 4.4$ in the final state.

	$d\sigma/dp_T$ [pb/GeV] (leading jet)			
p_T	$Z/\gamma^*(\rightarrow e^+e^-)$	$Z/\gamma^*(\rightarrow \mu^+\mu^-)$	$Z/\gamma^*(\rightarrow \ell^+\ell^-)$	$\delta^{\text{had}} \pm$ (total unc)
[GeV]	$\sigma \pm$ (stat) $\pm$ (syst)	$\sigma \pm$ (stat) $\pm$ (syst)	$\sigma \pm$ (total unc)	parton $\rightarrow$ hadron
30–40	$2.4 \pm 0.1^{+0.2}_{-0.3}$	$2.2 \pm 0.1^{+0.3}_{-0.2}$	$2.3^{+0.3}_{-0.2}$	1.00 ± 0.03
40–50	$1.5 \pm 0.1 \pm 0.2$	$1.5 \pm 0.1^{+0.1}_{-0.2}$	1.5 ± 0.2	1.00 ± 0.03
50–70	$0.74 \pm 0.04^{+0.07}_{-0.06}$	$0.65 \pm 0.03 \pm 0.05$	0.67 ± 0.06	0.99 ± 0.02
70–90	$0.36 \pm 0.03^{+0.04}_{-0.03}$	$0.35 \pm 0.03 \pm 0.03$	0.35 ± 0.03	0.98 ± 0.02
90–120	$0.15 \pm 0.02 \pm 0.02$	$0.15 \pm 0.01 \pm 0.01$	0.15 ± 0.02	0.98 ± 0.01
120–150	$0.068 \pm 0.011^{+0.008}_{-0.007}$	$0.051 \pm 0.008 \pm 0.004$	0.056 ± 0.008	1.00 ± 0.02
150–180	$0.034 \pm 0.007^{+0.006}_{-0.005}$	$0.031 \pm 0.006 \pm 0.004$	0.032 ± 0.006	1.01 ± 0.05

TABLE VI. Measured jet differential cross section $d\sigma/dp_T$ as a function of the second-leading jet p_T, for events with at least two jets with $p_T > 30$ GeV and $|y| < 4.4$ in the final state.

	$d\sigma/dp_T$ [pb/GeV] (second-leading jet)			
p_T	$Z/\gamma^*(\rightarrow e^+e^-)$	$Z/\gamma^*(\rightarrow \mu^+\mu^-)$	$Z/\gamma^*(\rightarrow \ell^+\ell^-)$	$\delta^{\text{had}} \pm$ (total unc)
[GeV]	$\sigma \pm$ (stat) $\pm$ (syst)	$\sigma \pm$ (stat) $\pm$ (syst)	$\sigma \pm$ (total unc)	parton $\rightarrow$ hadron
30–40	$0.66 \pm 0.06^{+0.08}_{-0.10}$	$0.55 \pm 0.04^{+0.08}_{-0.06}$	$0.58^{+0.09}_{-0.07}$	1.00 ± 0.04
40–50	$0.29 \pm 0.04^{+0.05}_{-0.04}$	$0.33 \pm 0.03^{+0.04}_{-0.05}$	0.31 ± 0.05	0.97 ± 0.02
50–70	$0.14 \pm 0.02 \pm 0.02$	$0.13 \pm 0.02 \pm 0.01$	0.14 ± 0.02	0.97 ± 0.01
70–90	$0.053 \pm 0.012^{+0.007}_{-0.006}$	$0.062 \pm 0.011 \pm 0.006$	0.058 ± 0.010	0.95 ± 0.02
90–120	$0.020 \pm 0.006 \pm 0.002$	$0.024 \pm 0.006 \pm 0.002$	0.022 ± 0.005	0.95 ± 0.06

TABLE VII. Measured inclusive jet differential cross section $d\sigma/d|y|$ as a function of $|y|$, for events with at least one jet with $p_T > 30$ GeV and $|y| < 4.4$ in the final state.

	$d\sigma/d\|y\|$ [pb] (inclusive)			
$\|y\|$	$Z/\gamma^*(\rightarrow e^+e^-)$	$Z/\gamma^*(\rightarrow \mu^+\mu^-)$	$Z/\gamma^*(\rightarrow \ell^+\ell^-)$	$\delta^{\text{had}} \pm$ (total unc)
	$\sigma \pm$ (stat) $\pm$ (syst)	$\sigma \pm$ (stat) $\pm$ (syst)	$\sigma \pm$ (total unc)	parton $\rightarrow$ hadron
0.0–0.5	$42 \pm 2 \pm 4$	$40 \pm 2 \pm 3$	40 ± 3	1.00 ± 0.03
0.5–1.0	$39 \pm 2^{+3}_{-4}$	$37 \pm 2 \pm 3$	38 ± 3	1.00 ± 0.03
1.0–1.5	$31 \pm 2 \pm 3$	$31 \pm 1^{+3}_{-2}$	31 ± 3	1.00 ± 0.03
1.5–2.0	$25 \pm 2 \pm 3$	$24 \pm 1 \pm 2$	24^{+3}_{-2}	0.99 ± 0.03
2.0–2.5	$16 \pm 1^{+1}_{-2}$	$17 \pm 1 \pm 2$	17 ± 2	0.99 ± 0.02
2.5–3.0	$12 \pm 1 \pm 2$	$8.8 \pm 0.8 \pm 1.4$	10 ± 2	0.97 ± 0.02
3.0–3.5	$5.7 \pm 0.8^{+1.3}_{-1.2}$	$5.2 \pm 0.6^{+1.1}_{-1.2}$	5.4 ± 1.3	0.95 ± 0.03
3.5–4.0	$1.9 \pm 0.5^{+0.7}_{-0.6}$	$1.8 \pm 0.4^{+0.6}_{-0.7}$	1.8 ± 0.7	0.91 ± 0.03

TABLE VIII. Measured jet differential cross section $d\sigma/d|y|$ as a function of the leading-jet $|y|$, for events with at least one jet with $p_T > 30$ GeV and $|y| < 4.4$ in the final state.

	$d\sigma/d\|y\|$ [pb] (leading jet)			
$\|y\|$	$Z/\gamma^*(\rightarrow e^+e^-)$	$Z/\gamma^*(\rightarrow \mu^+\mu^-)$	$Z/\gamma^*(\rightarrow \ell^+\ell^-)$	$\delta^{\text{had}} \pm$ (total unc)
	$\sigma \pm$ (stat) $\pm$ (syst)	$\sigma \pm$ (stat) $\pm$ (syst)	$\sigma \pm$ (total unc)	parton $\rightarrow$ hadron
0.0–0.5	$34 \pm 2 \pm 3$	$33 \pm 2 \pm 2$	33^{+3}_{-2}	1.00 ± 0.03
0.5–1.0	$31 \pm 2 \pm 3$	$29 \pm 1 \pm 2$	30 ± 2	1.00 ± 0.03
1.0–1.5	$26 \pm 2 \pm 2$	$25 \pm 1 \pm 2$	25 ± 2	1.00 ± 0.03
1.5–2.0	$19 \pm 1 \pm 2$	$18 \pm 1^{+2}_{-1}$	19 ± 2	1.00 ± 0.03
2.0–2.5	$13 \pm 1 \pm 2$	$13 \pm 1^{+2}_{-1}$	13 ± 2	0.99 ± 0.02
2.5–3.0	$10 \pm 1 \pm 2$	$7 \pm 1 \pm 1$	8 ± 1	0.97 ± 0.01
3.0–3.5	$4.1 \pm 0.7^{+0.9}_{-0.8}$	$4.0 \pm 0.6^{+0.8}_{-0.9}$	4.1 ± 1.0	0.94 ± 0.01
3.5–4.0	$1.2 \pm 0.4^{+0.5}_{-0.4}$	$0.9 \pm 0.3 \pm 0.3$	1.0 ± 0.4	0.92 ± 0.02

TABLE IX. Measured jet differential cross section $d\sigma/d|y|$ as a function of the second-leading jet $|y|$, for events with at least two jets with $p_T > 30$ GeV and $|y| < 4.4$ in the final state.

	$d\sigma/d\|y\|$ [pb] (second-leading jet)			
$\|y\|$	$Z/\gamma^*(\rightarrow e^+e^-)$	$Z/\gamma^*(\rightarrow \mu^+\mu^-)$	$Z/\gamma^*(\rightarrow \ell^+\ell^-)$	$\delta^{\text{had}} \pm$ (total unc)
	$\sigma \pm$ (stat) $\pm$ (syst)	$\sigma \pm$ (stat) $\pm$ (syst)	$\sigma \pm$ (total unc)	parton $\rightarrow$ hadron
0.0–0.5	$7.0 \pm 0.8 \pm 0.8$	$6.2 \pm 0.7 \pm 0.6$	$6.5^{+0.9}_{-0.8}$	1.00 ± 0.03
0.5–1.0	$6.7 \pm 0.8 \pm 0.8$	$6.0 \pm 0.7 \pm 0.6$	$6.3^{+0.9}_{-0.8}$	0.99 ± 0.03
1.0–1.5	$4.8 \pm 0.7 \pm 0.6$	$5.0 \pm 0.6^{+0.6}_{-0.5}$	5.0 ± 0.7	1.00 ± 0.03
1.5–2.0	$4.6 \pm 0.7 \pm 0.6$	$3.8 \pm 0.5 \pm 0.4$	4.1 ± 0.6	0.98 ± 0.02
2.0–2.5	$2.2 \pm 0.5^{+0.3}_{-0.4}$	$3.3 \pm 0.5^{+0.5}_{-0.4}$	2.8 ± 0.5	0.98 ± 0.03
2.5–3.0	$1.3 \pm 0.4 \pm 0.2$	$1.9 \pm 0.4^{+0.4}_{-0.3}$	1.6 ± 0.4	0.97 ± 0.05
3.0–3.5	$1.2 \pm 0.4 \pm 0.3$	$0.8 \pm 0.2 \pm 0.2$	0.9 ± 0.3	0.97 ± 0.05

TABLE X. Measured differential cross section $d\sigma/dm^{jj}$ as a function of the dijet invariant mass, for events with at least two jets with $p_T > 30$ GeV and $|y| < 4.4$ in the final state.

	$d\sigma/dm^{jj}$ [pb/GeV]			
m^{jj}	$Z/\gamma^*(\to e^+e^-)$	$Z/\gamma^*(\to \mu^+\mu^-)$	$Z/\gamma^*(\to \ell^+\ell^-)$	$\delta^{\text{had}} \pm$ (total unc)
[GeV]	$\sigma \pm$ (stat) $\pm$ (syst)	$\sigma \pm$ (stat) $\pm$ (syst)	$\sigma \pm$ (total unc)	parton $\to$ hadron
60–90	$0.06 \pm 0.01 \pm 0.01$	$0.06 \pm 0.01 \pm 0.01$	0.06 ± 0.01	1.03 ± 0.04
90–120	$0.11 \pm 0.01 \pm 0.01$	$0.10 \pm 0.01 \pm 0.01$	$0.10^{+0.02}_{-0.01}$	1.01 ± 0.04
120–150	$0.06 \pm 0.01 \pm 0.01$	$0.07 \pm 0.01 \pm 0.01$	0.07 ± 0.01	1.01 ± 0.03
150–180	$0.057 \pm 0.010 \pm 0.008$	$0.043 \pm 0.007^{+0.005}_{-0.004}$	0.047 ± 0.008	1.00 ± 0.04
180–210	$0.042 \pm 0.009^{+0.005}_{-0.006}$	$0.036 \pm 0.007 \pm 0.004$	0.038 ± 0.007	1.00 ± 0.02
210–240	$0.025 \pm 0.007^{+0.004}_{-0.003}$	$0.021 \pm 0.005^{+0.002}_{-0.003}$	0.023 ± 0.005	0.98 ± 0.04
240–270	$0.018 \pm 0.006^{+0.002}_{-0.003}$	$0.017 \pm 0.005 \pm 0.002$	0.017 ± 0.004	0.94 ± 0.06
270–300	$0.015 \pm 0.005 \pm 0.003$	$0.017 \pm 0.005 \pm 0.002$	0.016 ± 0.004	0.95 ± 0.05

TABLE XI. Measured differential cross section $d\sigma/d|\Delta y^{jj}|$ as a function of the dijet rapidity separation, for events with at least two jets with $p_T > 30$ GeV and $|y| < 4.4$ in the final state.

	$d\sigma/d\lvert\Delta y^{jj}\rvert$ [pb]			
$\lvert\Delta y^{jj}\rvert$	$Z/\gamma^*(\to e^+e^-)$	$Z/\gamma^*(\to \mu^+\mu^-)$	$Z/\gamma^*(\to \ell^+\ell^-)$	$\delta^{\text{had}} \pm$ (total unc)
	$\sigma \pm$ (stat) $\pm$ (syst)	$\sigma \pm$ (stat) $\pm$ (syst)	$\sigma \pm$ (total unc)	parton $\to$ hadron
0.0–0.5	$5.3 \pm 0.7 \pm 0.6$	$5.6 \pm 0.6 \pm 0.6$	$5.5^{+0.8}_{-0.7}$	0.98 ± 0.04
0.5–1.0	$6.1 \pm 0.8 \pm 0.7$	$6.6 \pm 0.7 \pm 0.7$	$6.4^{+0.9}_{-0.8}$	1.02 ± 0.04
1.0–1.5	$5.1 \pm 0.7 \pm 0.6$	$5.0 \pm 0.6^{+0.6}_{-0.5}$	5.1 ± 0.7	1.01 ± 0.05
1.5–2.0	$4.5 \pm 0.7 \pm 0.6$	$3.6 \pm 0.5 \pm 0.4$	3.9 ± 0.6	1.00 ± 0.03
2.0–2.5	$2.7 \pm 0.5 \pm 0.4$	$3.0 \pm 0.5^{+0.4}_{-0.3}$	2.9 ± 0.5	0.99 ± 0.04
2.5–3.0	$1.8 \pm 0.4 \pm 0.3$	$1.6 \pm 0.3 \pm 0.2$	1.7 ± 0.4	0.96 ± 0.02
3.0–3.5	$1.6 \pm 0.4 \pm 0.3$	$1.0 \pm 0.3 \pm 0.2$	1.2 ± 0.3	0.95 ± 0.03

TABLE XII. Measured differential cross section $d\sigma/d|\Delta\phi^{jj}|$ as a function of the dijet azimuthal separation, for events with at least two jets with $p_T > 30$ GeV and $|y| < 4.4$ in the final state.

	$d\sigma/d\lvert\Delta\phi^{jj}\rvert$[pb]			
$\lvert\Delta\phi^{jj}\rvert$ [rad.]	$Z/\gamma^*(\to e^+e^-)$	$Z/\gamma^*(\to \mu^+\mu^-)$	$Z/\gamma^*(\to \ell^+\ell^-)$	$\delta^{had} \pm$ (total unc)
	$\sigma \pm$ (stat) $\pm$ (syst)	$\sigma \pm$ (stat) $\pm$ (syst)	$\sigma \pm$ (total unc)	parton $\to$ hadron
$0 - \pi/8$	$1.8 \pm 0.5 \pm 0.3$	$1.7 \pm 0.4 \pm 0.3$	1.7 ± 0.4	0.94 ± 0.04
$\pi/8 - \pi/4$	$2.7 \pm 0.6^{+0.5}_{-0.4}$	$2.9 \pm 0.5^{+0.4}_{-0.3}$	$2.8^{+0.6}_{-0.5}$	0.98 ± 0.05
$\pi/4 - 3\pi/8$	$2.0 \pm 0.5 \pm 0.3$	$2.5 \pm 0.5 \pm 0.3$	2.3 ± 0.5	1.01 ± 0.07
$3\pi/8 - \pi/2$	$2.5 \pm 0.6 \pm 0.4$	$3.2 \pm 0.5 \pm 0.4$	$2.9^{+0.6}_{-0.5}$	0.97 ± 0.03
$\pi/2 - 5\pi/8$	$4.0 \pm 0.7^{+0.5}_{-0.6}$	$3.8 \pm 0.6 \pm 0.5$	3.9 ± 0.7	0.97 ± 0.02
$5\pi/8 - 3\pi/4$	$4.4 \pm 0.8 \pm 0.6$	$4.6 \pm 0.7 \pm 0.6$	$4.5^{+0.8}_{-0.7}$	0.98 ± 0.04
$3\pi/4 - 7\pi/8$	$7.9 \pm 1.0 \pm 0.9$	$6.8 \pm 0.8 \pm 0.7$	7.0 ± 1.0	0.98 ± 0.03
$7\pi/8 - \pi$	$11.4 \pm 1.2 \pm 1.4$	$10.0 \pm 1.0^{+1.1}_{-1.0}$	$10.4^{+1.4}_{-1.3}$	1.00 ± 0.08

In this analysis, jets are selected with corrected $p_T > 30$ GeV and $|y| < 4.4$ to ensure full containment in the instrumented region. Events are required to have at least one jet well separated from the final state leptons from the Z/γ^* decay. Jets within a cone of radius 0.5 around any selected lepton are not considered. Additional quality criteria are applied to ensure that jets are not produced by noisy calorimeter cells, and to avoid problematic detector regions.

The final sample for $Z/\gamma^*(\to e^+e^-) +$ jets contains 1514, 333, 62, and 15 events with at least one, two, three, and four jets in the final state, respectively. Similarly, the $Z/\gamma^*(\to \mu^+\mu^-) +$ jets sample contains 1885, 422, 93, and 20 events with at least one, two, three, and four jets in the final state, respectively.

VI. LEPTON RECONSTRUCTION

Samples of $Z/\gamma^* \to e^+e^-$ and $Z/\gamma^* \to \mu^+\mu^-$ events in data and MC simulation, together with the world average values for the Z boson mass and width, are used to determine the absolute scale and resolution of the

TABLE XIII. Measured differential cross section $d\sigma/d|\Delta R^{jj}|$ as a function of the dijet angular separation ($y-\phi$ space), for events with at least two jets with $p_T > 30$ GeV and $|y| < 4.4$ in the final state.

ΔR^{jj}	$d\sigma/d\|\Delta R^{jj}\|$[pb] $Z/\gamma^*(\to e^+e^-)$	$Z/\gamma^*(\to \mu^+\mu^-)$	$Z/\gamma^*(\to \ell^+\ell^-)$	$\delta^{\text{had}} \pm$ (total unc)
	$\sigma \pm$ (stat) $\pm$ (syst)	$\sigma \pm$ (stat) $\pm$ (syst)	$\sigma \pm$ (total unc)	parton $\to$ hadron
0.4–0.8	$1.8 \pm 0.5 \pm 0.3$	$1.6 \pm 0.4 \pm 0.3$	1.7 ± 0.4	0.91 ± 0.02
0.8–1.2	$1.5 \pm 0.4 \pm 0.2$	$1.9 \pm 0.4 \pm 0.2$	1.7 ± 0.4	1.04 ± 0.09
1.2–1.6	$1.8 \pm 0.5 \pm 0.3$	$2.2 \pm 0.4 \pm 0.3$	2.1 ± 0.4	0.99 ± 0.03
1.6–2.0	$2.2 \pm 0.5 \pm 0.3$	$2.7 \pm 0.5 \pm 0.3$	2.5 ± 0.5	1.02 ± 0.07
2.0–2.4	$3.4 \pm 0.7^{+0.5}_{-0.4}$	$3.5 \pm 0.6 \pm 0.4$	3.5 ± 0.6	1.02 ± 0.07
2.4–2.8	$5.7 \pm 0.9 \pm 0.7$	$5.4 \pm 0.7 \pm 0.6$	5.6 ± 0.8	0.99 ± 0.02
2.8–3.2	$7.8 \pm 1.0 \pm 0.9$	$8.5 \pm 0.9^{+0.9}_{-0.8}$	$8.2^{+1.1}_{-1.0}$	1.01 ± 0.02
3.2–3.6	$5.5 \pm 0.8 \pm 0.7$	$4.7 \pm 0.7 \pm 0.5$	$5.0^{+0.8}_{-0.7}$	0.99 ± 0.03
3.6–4.0	$2.5 \pm 0.6 \pm 0.4$	$1.2 \pm 0.3 \pm 0.2$	1.5 ± 0.3	0.96 ± 0.03
4.0–4.4	$1.5 \pm 0.4 \pm 0.3$	$1.5 \pm 0.4 \pm 0.2$	1.5 ± 0.4	0.97 ± 0.05

energy/momentum of the leptons, to validate calibration- and alignment-related constants in data, and to check the MC description [30]. In addition, the trigger and offline lepton reconstruction efficiencies are studied using control samples in data, and the results are compared to the simulation. The differences observed between data and MC predictions define scale factors which are applied in the analysis to the simulated samples before they are used to correct the measurements for detector effects.

For the electron channel, the trigger and offline electron reconstruction and identification efficiencies for single electrons are estimated using $W \to e\nu$ and $Z/\gamma^* \to e^+e^-$ events in data and compared to MC predictions. In

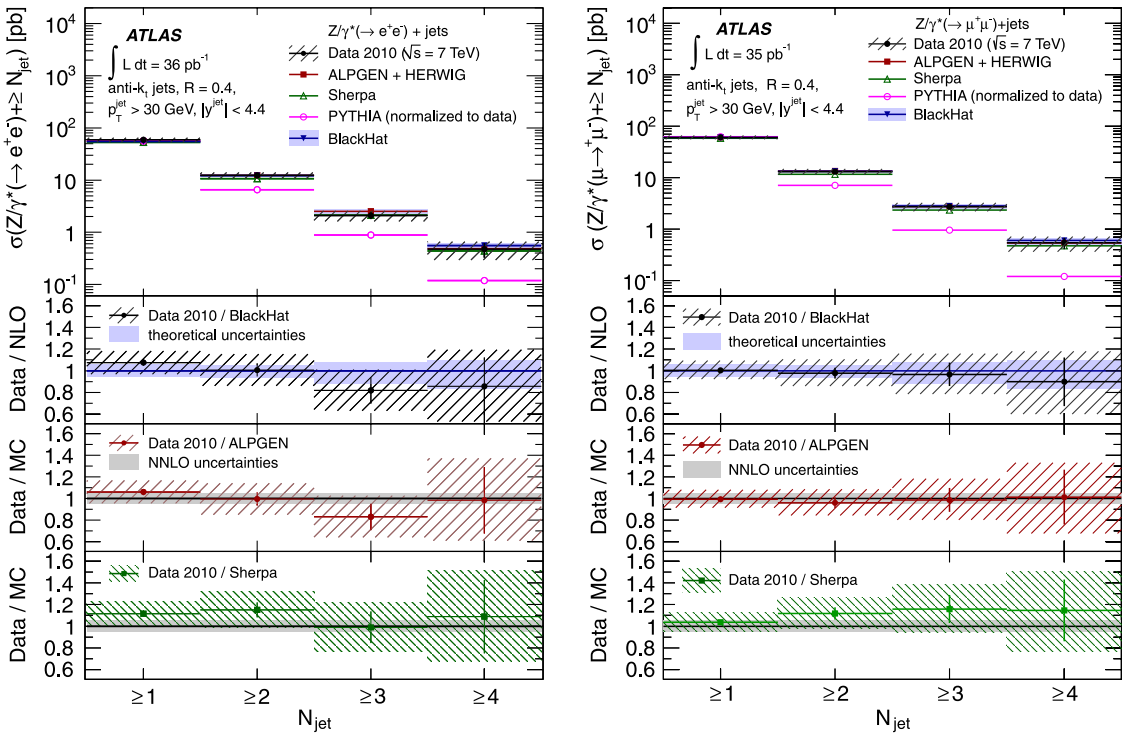

FIG. 3 (color online). Measured cross section $\sigma_{N_{\text{jet}}}$ (black dots) for (left) $Z/\gamma^*(\to e^+e^-)$ + jets and (right) $Z/\gamma^*(\to \mu^+\mu^-)$ + jets production as a function of the inclusive jet multiplicity, for events with at least one jet with $p_T > 30$ GeV and $|y| < 4.4$ in the final state. In this and subsequent Figs. 4 and 14 the error bars indicate the statistical uncertainty and the dashed areas the statistical and systematic uncertainties added in quadrature. The measurements are compared to NLO pQCD predictions from BLACKHAT, as well as the predictions from ALPGEN and SHERPA (both normalized to the FEWZ value for the total cross section), and PYTHIA (normalized to the data as discussed in Sec. XII).

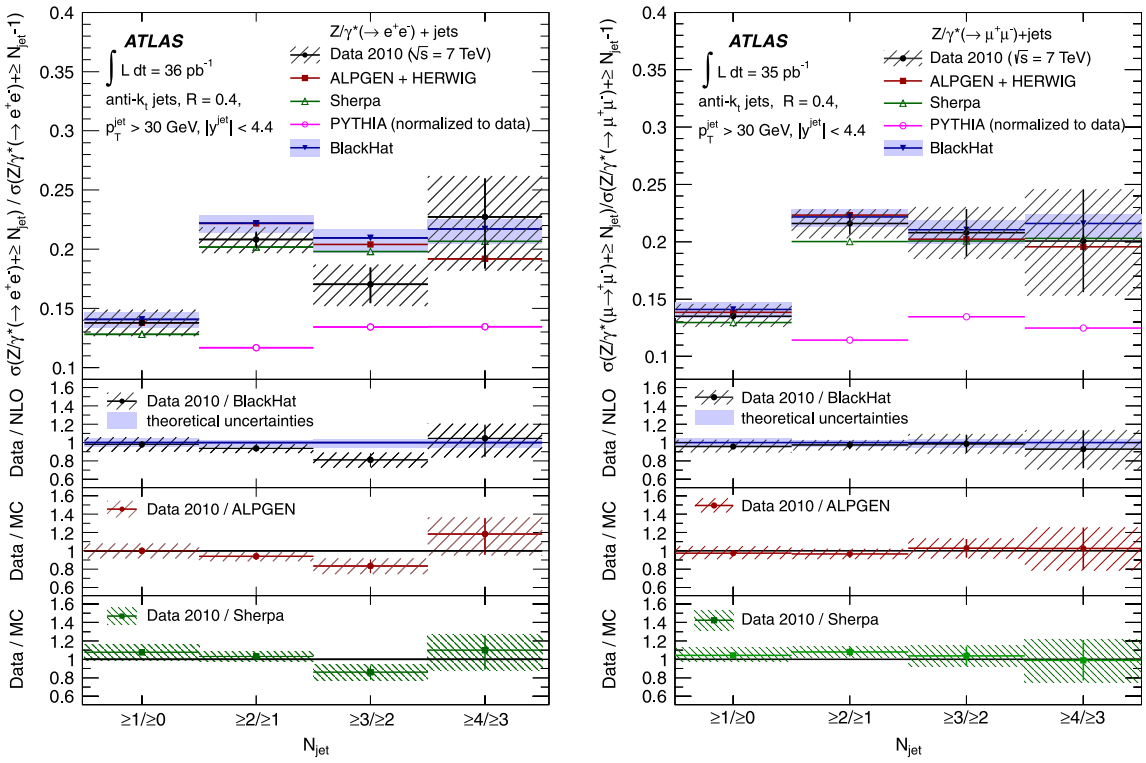

FIG. 4 (color online). Measured ratio of cross sections $(\sigma_{N_{\text{jet}}}/\sigma_{N_{\text{jet}}-1})$ (black dots) for (left) $Z/\gamma^*(\rightarrow e^+e^-)$ + jets and (right) $Z/\gamma^*(\rightarrow \mu^+\mu^-)$ + jets production as a function of the inclusive jet multiplicity, for events with at least one jet with $p_T > 30$ GeV and $|y| < 4.4$ in the final state.

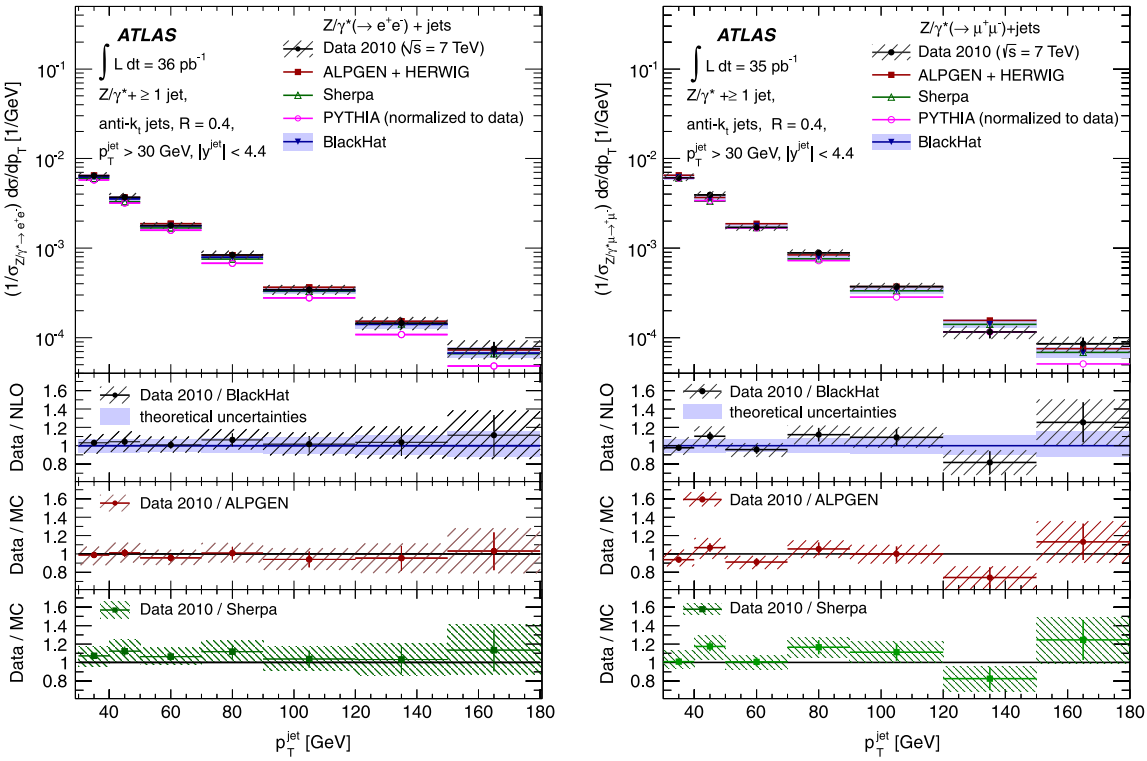

FIG. 5 (color online). Measured normalized inclusive jet cross section $(1/\sigma_{Z/\gamma^*\rightarrow\ell^+\ell^-})d\sigma/dp_T$ (black dots) in (left) $Z/\gamma^*(\rightarrow e^+e^-)$ + jets and (right) $Z/\gamma^*(\rightarrow \mu^+\mu^-)$ + jets production as a function of p_T, in events with at least one jet with $p_T > 30$ GeV and $|y| < 4.4$ in the final state, and normalized by $\sigma_{Z/\gamma^*\rightarrow e^+e^-}$ and $\sigma_{Z/\gamma^*\rightarrow\mu^+\mu^-}$ Drell-Yan cross sections, respectively.

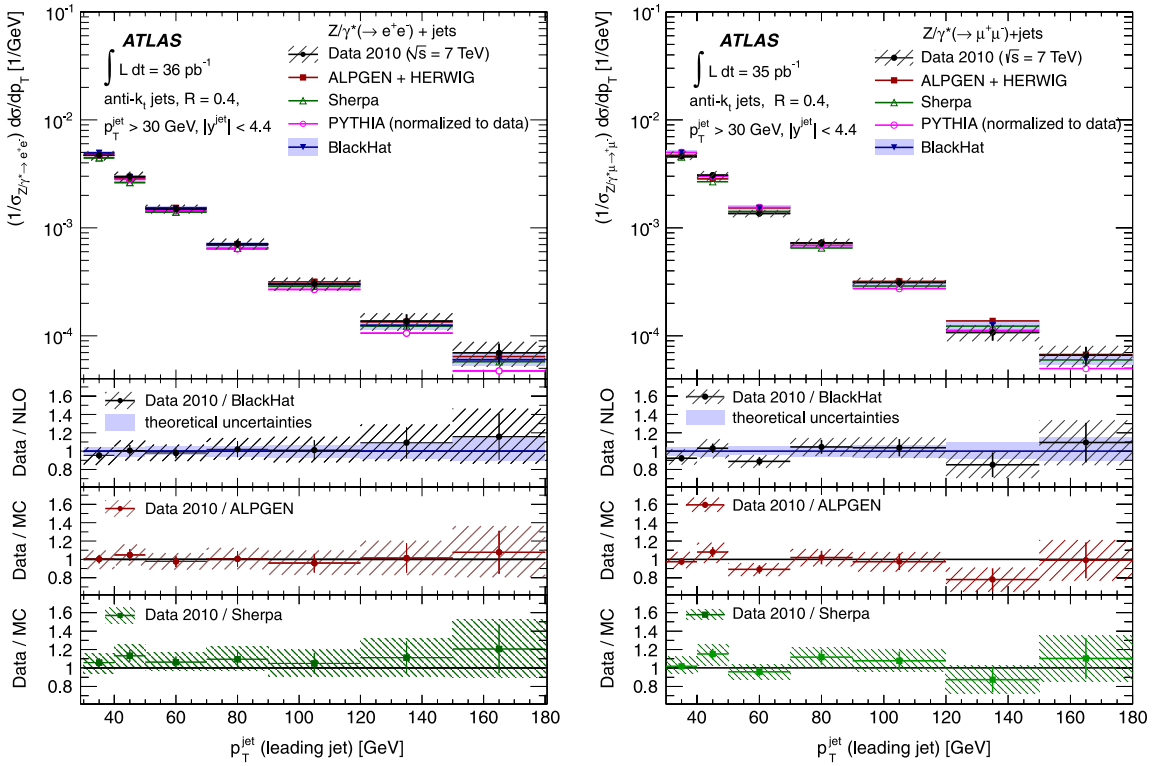

FIG. 6 (color online). Measured normalized jet cross section $(1/\sigma_{Z/\gamma^* \to \ell^+\ell^-})d\sigma/dp_T$ (black dots) in (left) $Z/\gamma^*(\to e^+e^-)$ + jets and (right) $Z/\gamma^*(\to \mu^+\mu^-)$ + jets production as a function of the leading jet p_T, in events with at least one jet with $p_T > 30$ GeV and $|y| < 4.4$ in the final state, and normalized by $\sigma_{Z/\gamma^* \to e^+e^-}$ and $\sigma_{Z/\gamma^* \to \mu^+\mu^-}$ Drell-Yan cross sections, respectively.

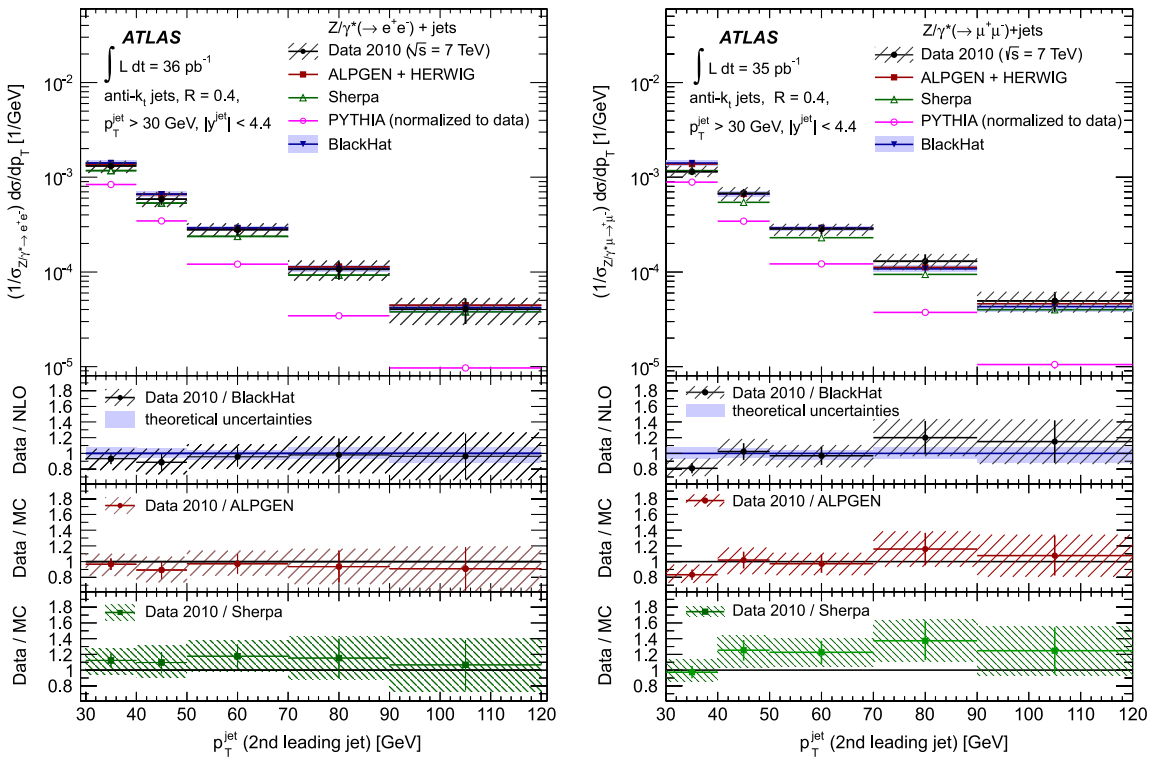

FIG. 7 (color online). Measured normalized jet cross section $(1/\sigma_{Z/\gamma^* \to \ell^+\ell^-})d\sigma/dp_T$ (black dots) in (left) $Z/\gamma^*(\to e^+e^-)$ + jets and (right) $Z/\gamma^*(\to \mu^+\mu^-)$ + jets production as a function of the second-leading jet p_T, in events with at least two jets with $p_T > 30$ GeV and $|y| < 4.4$ in the final state, and normalized by $\sigma_{Z/\gamma^* \to e^+e^-}$ and $\sigma_{Z/\gamma^* \to \mu^+\mu^-}$ Drell-Yan cross sections, respectively.

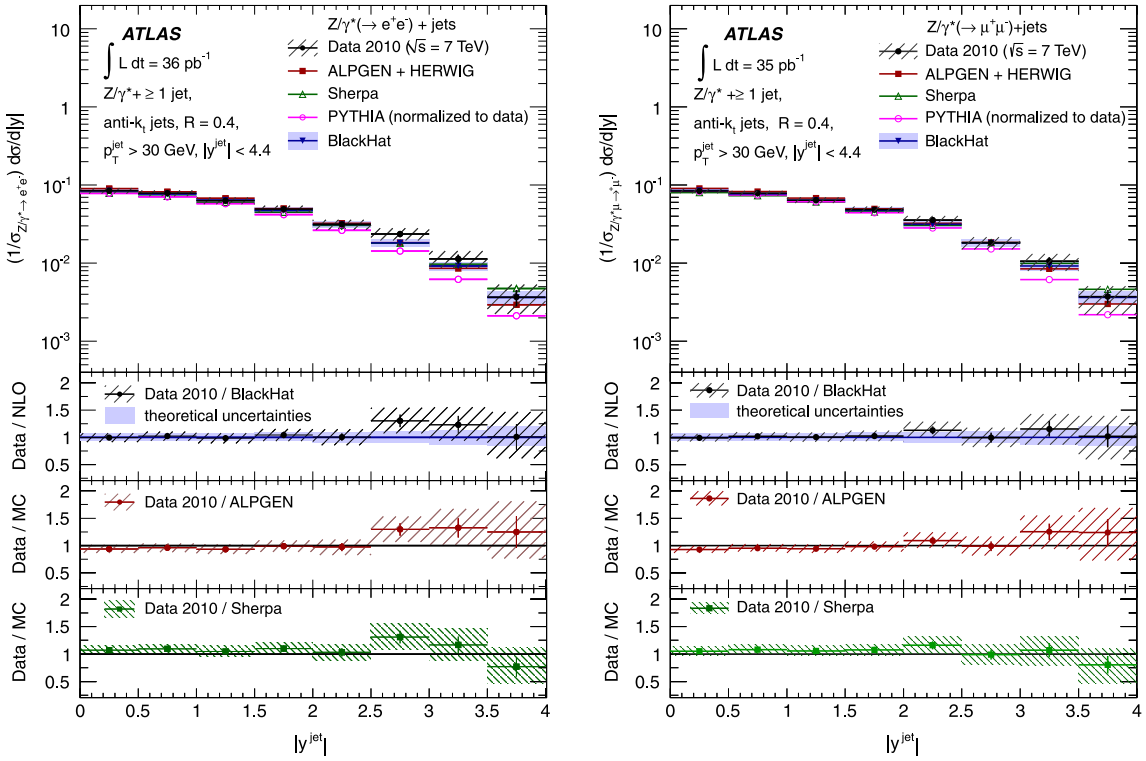

FIG. 8 (color online). Measured normalized inclusive jet cross section $(1/\sigma_{Z/\gamma^* \to \ell^+\ell^-})d\sigma/d|y|$ (black dots) in (left) $Z/\gamma^*(\to e^+e^-)$ + jets and (right) $Z/\gamma^*(\to \mu^+\mu^-)$ + jets production as a function of $|y|$, in events with at least one jet with $p_T > 30$ GeV and $|y| < 4.4$ in the final state, and normalized by $\sigma_{Z/\gamma^* \to e^+e^-}$ and $\sigma_{Z/\gamma^* \to \mu^+\mu^-}$ Drell-Yan cross sections, respectively.

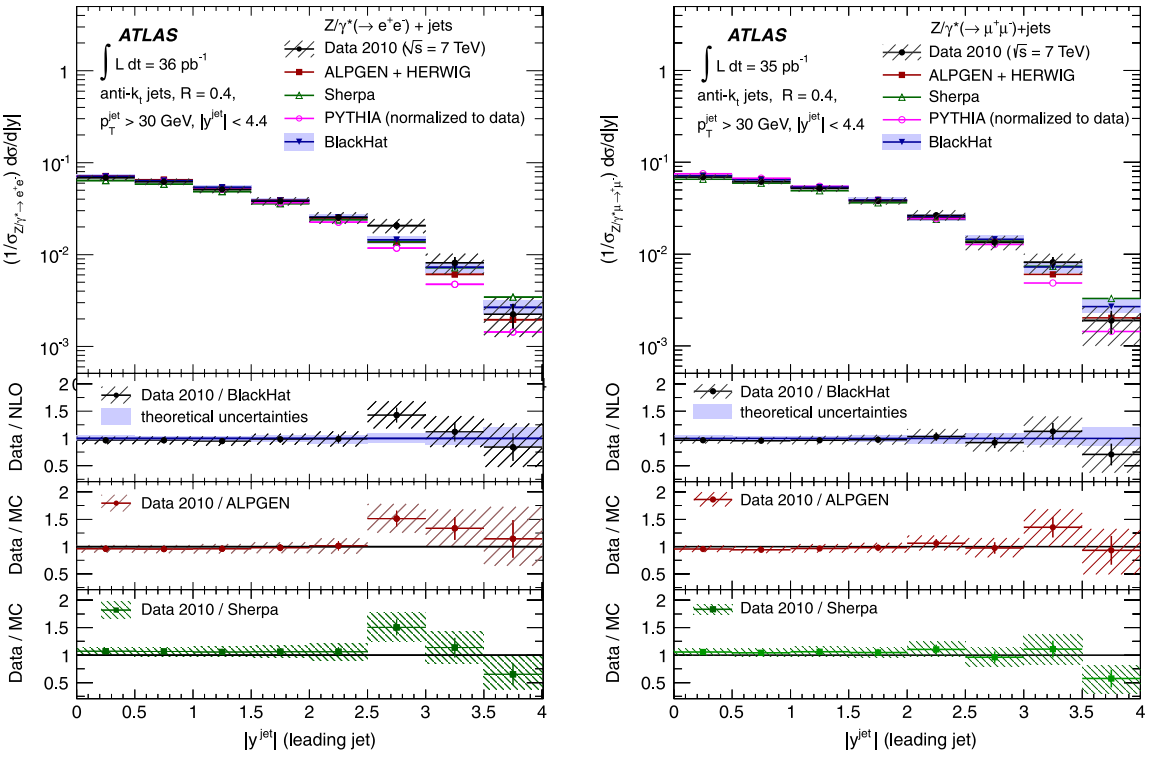

FIG. 9 (color online). Measured normalized jet cross section $(1/\sigma_{Z/\gamma^* \to \ell^+\ell^-})d\sigma/d|y|$ (black dots) in (left) $Z/\gamma^*(\to e^+e^-)$ + jets and (right) $Z/\gamma^*(\to \mu^+\mu^-)$ + jets production as a function of the leading jet $|y|$, in events with at least one jet with $p_T > 30$ GeV and $|y| < 4.4$ in the final state, and normalized by $\sigma_{Z/\gamma^* \to e^+e^-}$ and $\sigma_{Z/\gamma^* \to \mu^+\mu^-}$ Drell-Yan cross sections, respectively.

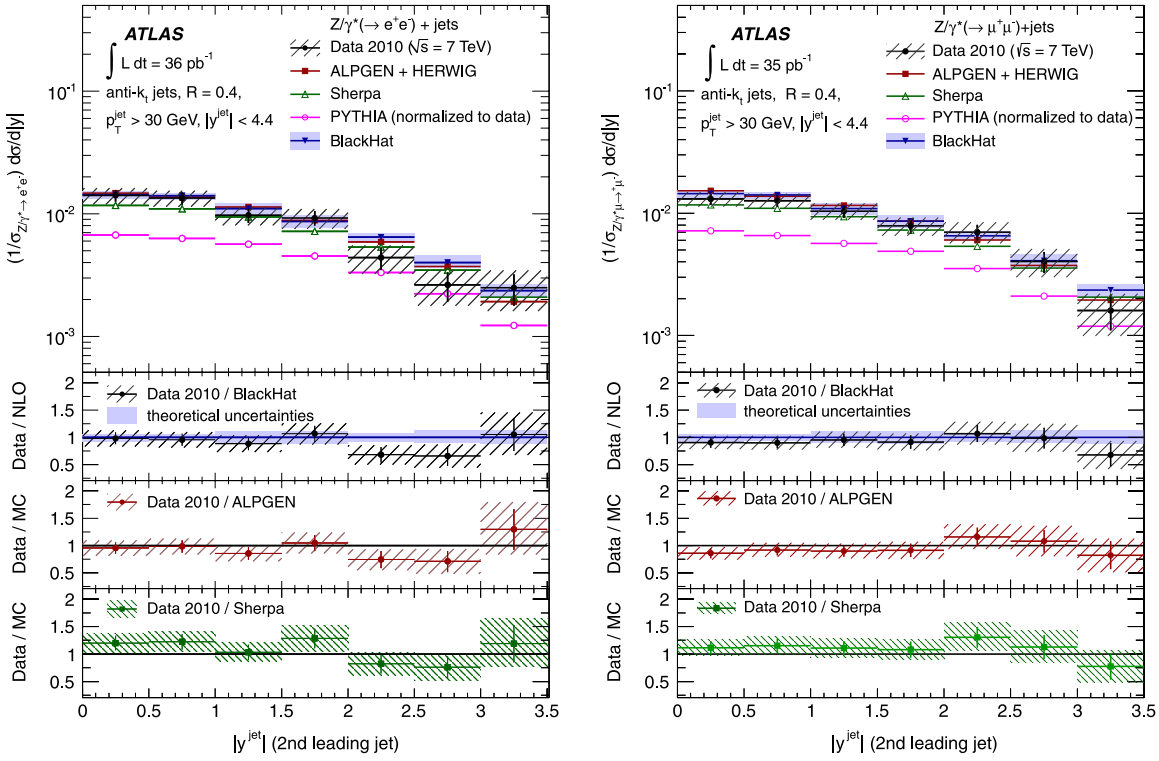

FIG. 10 (color online). Measured normalized jet cross section $(1/\sigma_{Z/\gamma^* \to \ell^+\ell^-}) d\sigma/d|y|$ (black dots) in (left) $Z/\gamma^*(\to e^+e^-)$ + jets and (right) $Z/\gamma^*(\to \mu^+\mu^-)$ + jets production as a function of the second-leading jet $|y|$, in events with at least two jets with $p_T > 30$ GeV and $|y| < 4.4$ in the final state, and normalized by $\sigma_{Z/\gamma^* \to e^+e^-}$ and $\sigma_{Z/\gamma^* \to \mu^+\mu^-}$ Drell-Yan cross sections, respectively.

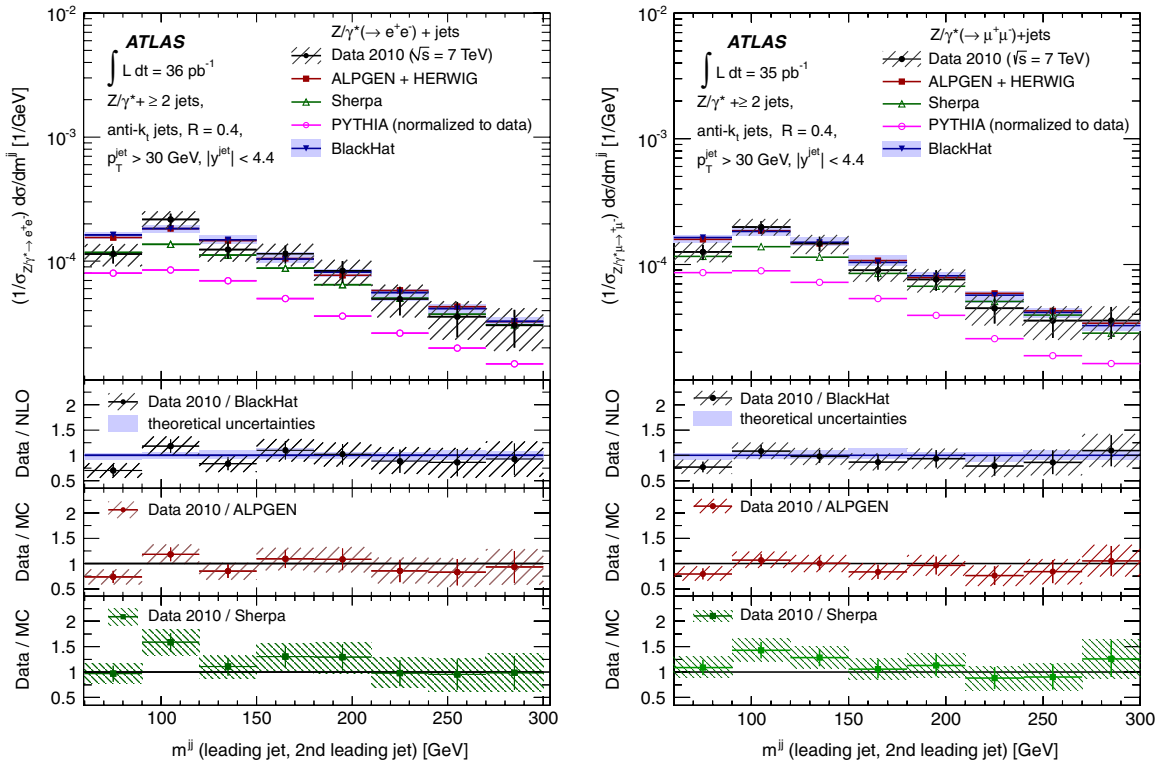

FIG. 11 (color online). Measured normalized dijet cross section $(1/\sigma_{Z/\gamma^* \to \ell^+\ell^-}) d\sigma/dm^{jj}$ (black dots) in (left) $Z/\gamma^*(\to e^+e^-)$ + jets and (right) $Z/\gamma^*(\to \mu^+\mu^-)$ + jets production as a function of the invariant mas of the two leading jets m^{jj}, in events with at least two jets with $p_T > 30$ GeV and $|y| < 4.4$ in the final state, and normalized by $\sigma_{Z/\gamma^* \to e^+e^-}$ and $\sigma_{Z/\gamma^* \to \mu^+\mu^-}$ Drell-Yan cross sections, respectively.

the kinematic range for the electrons considered in the analysis (see Sec. III), the trigger and offline efficiencies per electron are above 99% and 93%, respectively. The study indicates a good agreement between data and simulated trigger efficiencies with a MC-to-data scale factor of 0.995 ± 0.005. The simulation tends to overestimate the offline efficiencies. Scale factors in the range between 0.901 ± 0.045 and 0.999 ± 0.016, depending on η^e and E_{T}^e, for $E_{\mathrm{T}}^e > 20$ GeV, are applied per lepton to the MC samples to account for this effect.

In the muon analysis, the trigger and offline muon reconstruction efficiencies are also estimated using the data and are compared to simulation. The measured average single muon trigger efficiency is about 85%, independent of p_{T}^{μ}, and varies from 80% for $|\eta^{\mu}| < 0.63$ and 73% for $0.63 < |\eta^{\mu}| < 1.05$ to 94% for $1.05 < |\eta^{\mu}| < 2.4$, limited mainly by the trigger chamber geometric acceptance. The measured average offline muon reconstruction efficiency is about 92% and approximately independent of p_{T}^{μ}. The MC simulation predicts efficiencies very similar to those in the data, but tends to overestimate the average offline reconstruction efficiency by about 1%. This originates from the transition region between the barrel part and the endcap wheels at $|\eta| \sim 1$, where the simulation overestimates the offline reconstruction efficiency by about 6%. The latter is attributed to the limited accuracy of the magnetic field map used in this region which leads to a small mismeasurement of the standalone muon momentum and an overestimation in the simulated efficiency. Scale factors are applied in the analysis that take this effect into account.

VII. BACKGROUND ESTIMATION

The background contribution to the electron and muon analyses from SM processes is estimated using MC simulated samples, as discussed in Sec. IV, with the exception of the multijets background that is estimated using data.

The multijets background contribution in the $Z/\gamma^* \times (\rightarrow e^+e^-)$ + jets analysis is estimated using a control data sample with two electron candidates which pass a loose selection but fail to pass the *medium* identification requirements. This sample is dominated by jets faking electrons in the final state and is employed to determine the shape of the multijets background under each of the

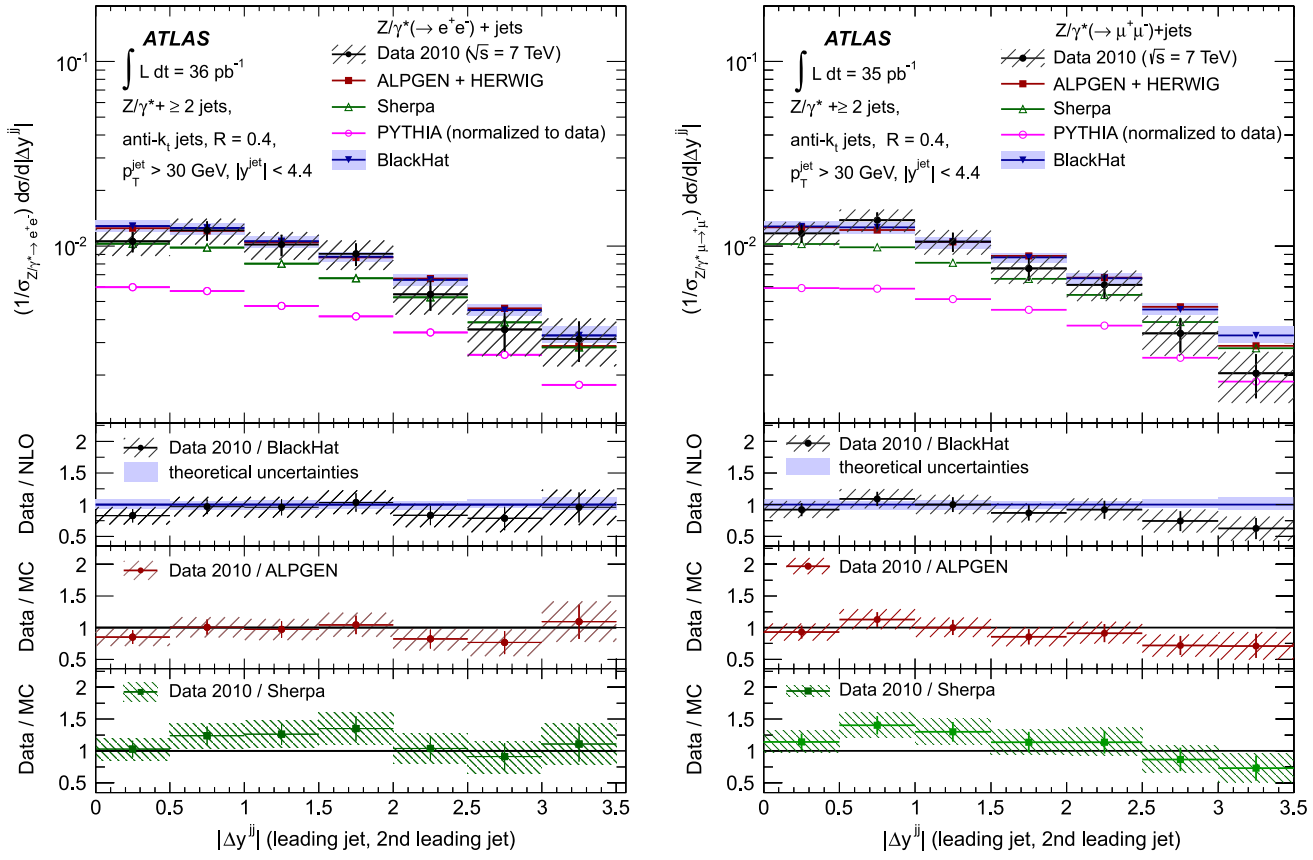

FIG. 12 (color online). Measured normalized dijet cross section $(1/\sigma_{Z/\gamma^* \to \ell^+\ell^-}) d\sigma/d|\Delta y^{jj}|$ (black dots) in (left) $Z/\gamma^*(\rightarrow e^+e^-)$ + jets and (right) $Z/\gamma^*(\rightarrow \mu^+\mu^-)$ + jets production as a function of the rapidity separation of the two leading jets $|\Delta y^{jj}|$, in events with at least two jets with $p_T > 30$ GeV and $|y| < 4.4$ in the final state, and normalized by $\sigma_{Z/\gamma^* \to e^+e^-}$ and $\sigma_{Z/\gamma^* \to \mu^+\mu^-}$ Drell-Yan cross sections, respectively.

measured distributions. The normalization of the multijets background events in the signal region is extracted from a fit to the measured inclusive dilepton invariant mass spectrum with nominal lepton requirements, using as input the observed shape of the multijets contribution in data and the MC predictions for the shape of the signal and the rest of the SM background processes. The multijets background contribution to the measured inclusive jet multiplicity varies between $3.2 \pm 0.5(\text{stat})^{+0.3}_{-0.2}(\text{syst})\%$ for $N_{\text{jet}} \geq 1$ and $4.5 \pm 1.9(\text{stat})^{+0.4}_{-0.2}(\text{syst})\%$ for $N_{\text{jet}} \geq 4$. The quoted total systematic uncertainty includes: uncertainties related to the details of the parameterization and the mass range used to fit the measured dilepton invariant mass spectrum; uncertainties on the shape of the dilepton invariant mass distribution, as determined in the control sample; and uncertainties on the shape of the simulated dilepton invariant mass distribution for the other SM processes.

In the $Z/\gamma^*(\rightarrow \mu^+\mu^-)$ + jets case, the multijets background mainly originates from heavy-flavour jet production processes, with muons from bottom and charm quark decays, as well as from the decay-in-flight of pions and kaons, which are highly suppressed by the isolation requirement applied to the muon candidates. The isolation criterion of the muon pair, defined as the isolation of the least-isolated muon candidate, is used together with the dimuon invariant mass to estimate the remaining multijets background contribution. The MC simulation indicates that, for multijet processes, the muon isolation is not correlated with the dimuon invariant mass, and so the ratio of isolated to nonisolated muon pairs (as defined with an inverted isolation criterion) does not depend on the dimuon mass. The multijets background with isolated muons with $66\ \text{GeV} < m_{\mu^+\mu^-} < 116\ \text{GeV}$ is therefore extracted from data as the ratio between the number of isolated and nonisolated dimuon candidates in the region $40\ \text{GeV} < m_{\mu^+\mu^-} < 60\ \text{GeV}$ multiplied by the number of nonisolated dimuon candidates in the range $66\ \text{GeV} < m_{\mu^+\mu^-} < 116\ \text{GeV}$. A small contribution from top pair production processes is subtracted from the data according to MC predictions. The multijets background contribution to the $Z/\gamma^*(\rightarrow \mu^+\mu^-)$ + jets analysis is of the order of 1 per mille and therefore negligible.

In the electron channel, the total background increases from 5% to 17% as the jet multiplicity increases and is dominated by multijet processes, followed by contributions from $t\bar{t}$ and diboson production at large jet multiplicities. In the muon channel, the SM background contribution increases from 2% to 10% as the jet multiplicity increases, dominated by $t\bar{t}$ and diboson processes. Table I shows, for the electron and muon analyses

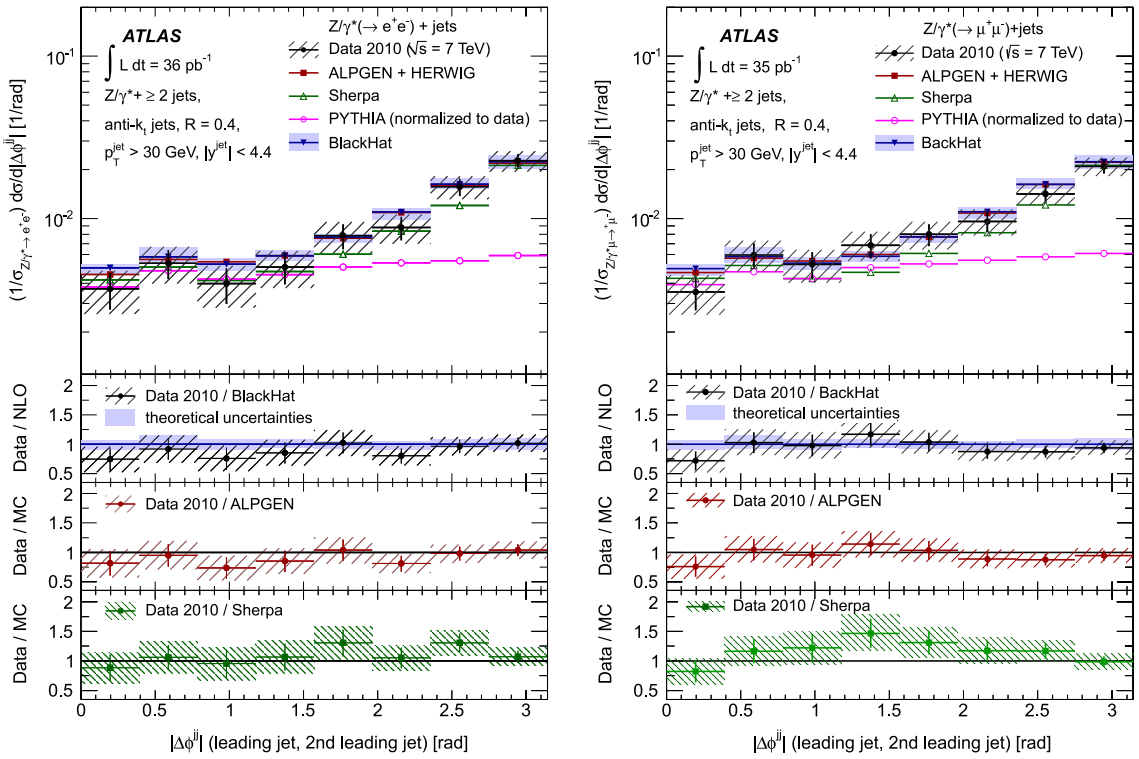

FIG. 13 (color online). Measured normalized dijet cross section $(1/\sigma_{Z/\gamma^*\rightarrow\ell^+\ell^-})d\sigma/d|\Delta\phi^{jj}|$ (black dots) in (left) $Z/\gamma^*(\rightarrow e^+e^-)$ + jets and (right) $Z/\gamma^*(\rightarrow\mu^+\mu^-)$+jets production as a function of the azimuthal separation of the two leading jets $|\Delta\phi^{jj}|$, in events with at least two jets with $p_T > 30\text{GeV}$ and $|y| < 4.4$ in the final state, and normalized by $\sigma_{Z/\gamma^*\rightarrow e^+e^-}$ and $\sigma_{Z/\gamma^*\rightarrow\mu^+\mu^-}$ Drell-Yan cross sections, respectively.

separately, the observed number of events for the different jet multiplicities in the final state compared to predictions for signal and background processes.

VIII. UNCORRECTED DISTRIBUTIONS

The uncorrected $Z/\gamma^*(\rightarrow e^+e^-)$ + jets and $Z/\gamma^*(\rightarrow \mu^+\mu^-)$ + jets data are compared to the predictions for signal and background contributions. For the signal, both ALPGEN and SHERPA predictions are considered. As an example, Fig. 1 shows, separately for the electron and muon channels, the measured dilepton invariant mass in events with at least one jet in the final state, as well as the measured uncorrected inclusive jet multiplicity. Other observables considered include: the uncorrected inclusive jet p_T, y, and ϕ distributions; the corresponding p_T, y, and ϕ distributions of the leading, second-leading and third-leading jet in events with at least one, two and three jets in the final state, respectively; the invariant mass of the two leading jets, m^{jj}, and their rapidity difference, Δy^{jj}, their azimuthal separation, $\Delta\phi^{jj}$, and the angular separation in $y-\phi$ space, $\Delta R^{jj} = \sqrt{(\Delta y^{jj})^2 + (\Delta\phi^{jj})^2}$, in events with at least two jets in the final state. In all cases, the data yields are described, within statistical uncertainties, by the MC predictions for the signal plus the estimated SM background contributions.

IX. CORRECTION FOR DETECTOR EFFECTS

The jet measurements are corrected for detector effects back to the particle level using a bin-by-bin correction procedure, based on MC simulated samples, that corrects for jet selection efficiency and resolution effects and also accounts for the efficiency of the Z/γ^* selection.

The corrected measurements refer to particle level jets identified using the anti-k_t algorithm with $R = 0.4$, for jets with $p_T > 30$ GeV and $|y| < 4.4$. At particle level, the lepton kinematics in the MC generated samples include the contributions from the photons radiated within a cone of radius 0.1 around the lepton direction. The measured cross sections are defined in a limited kinematic range for the Z/γ^* decay products.

(i) In the electron channel, the measured cross sections refer to the region: 66 GeV $< m_{e^+e^-} <$ 116 GeV, $E_{\mathrm{T}}^e > 20$ GeV, $|\eta^e| < 1.37$ or $1.52 < |\eta^e| < 2.47$, and ΔR(jet-electron) > 0.5.

(ii) Similarly, in the muon case the measurements are presented in the region: 66 GeV $< m_{\mu^+\mu^-} <$ 116 GeV, $p_{\mathrm{T}}^{\mu} > 20$ GeV, $|\eta^{\mu}| < 2.4$, and ΔR(jet- muon) > 0.5.

The ALPGEN samples for Z/γ^* + jets processes provide a satisfactory description of both lepton and jet distributions

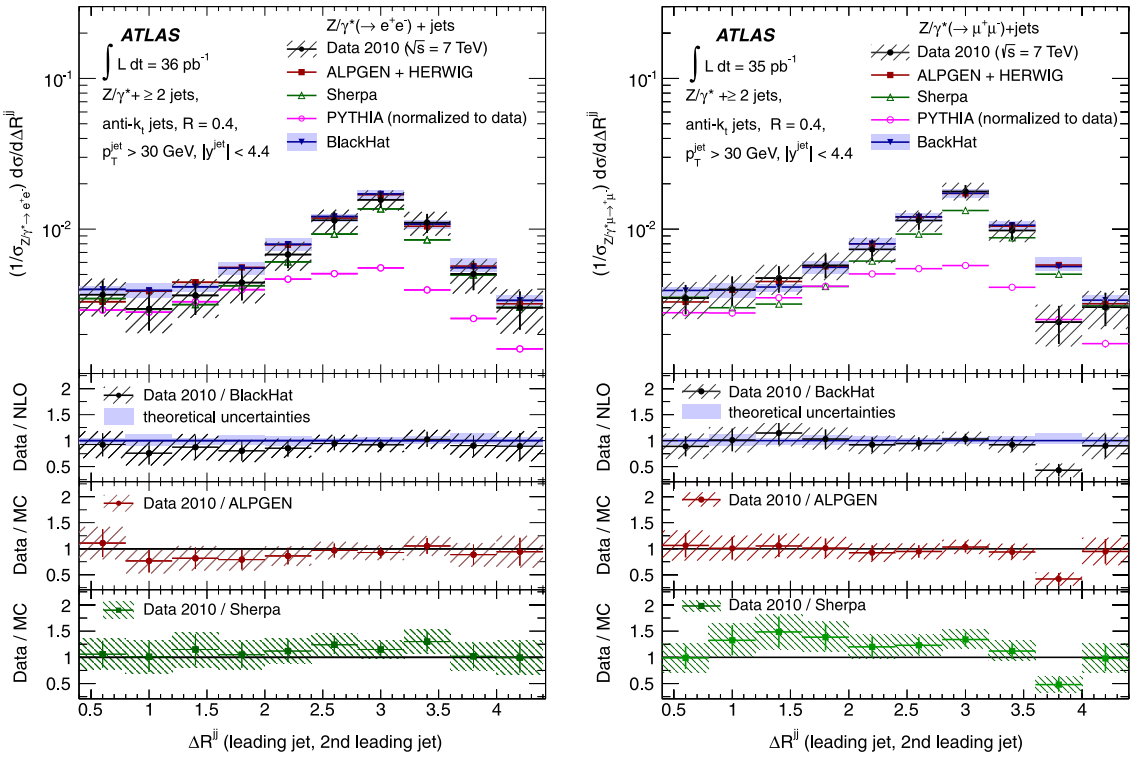

FIG. 14 (color online). Measured normalized dijet cross section $(1/\sigma_{Z/\gamma^*\rightarrow\ell^+\ell^-})d\sigma/d\Delta R^{jj}$ (black dots) in (left) $Z/\gamma^*(\rightarrow e^+e^-)$ + jets and (right) $Z/\gamma^*(\rightarrow \mu^+\mu^-)$ + jets production as a function of the angular separation ($y-\phi$ space) of the two leading jets ΔR^{jj}, in events with at least two jets with $p_T > 30$ GeV and $|y| < 4.4$ in the final state, and normalized by $\sigma_{Z/\gamma^*\rightarrow e^+e^-}$ and $\sigma_{Z/\gamma^*\rightarrow\mu^+\mu^-}$ Drell-Yan cross sections, respectively.

in data and are employed to compute the correction factors. For each observable ξ the bin-by-bin correction factors $U(\xi)$ are defined as the ratio between the simulated distribution, after all selection criteria are applied, and the corresponding distribution at the particle level defined in a limited fiducial kinematic region for the generated leptons and jets, as detailed above.

Correction factors are considered for the following measurements: the inclusive jet multiplicity, p_T and $|y|$ distributions; the p_T and $|y|$ distributions for the leading- and second-leading jets in events with at least one and two jets, respectively; and the invariant mass and angular separation distributions in the inclusive dijet sample. Typical correction factors are about 1.40 for the electron channel and about 1.15 for the muon channel (see below), where the difference is mainly attributed to the identification of the Z boson candidate in the final state.

The measured differential cross sections are defined as functions of a given ξ:

$$\frac{d\sigma}{d\xi} = \frac{1}{\mathcal{L}} \frac{1}{\Delta\xi}(N_{\text{data}} - N_{\text{backg}}) \times U(\xi) \tag{1}$$

where, for each bin in ξ, N_{data} and N_{backg} denote the number of entries (events or jets) observed in data and the background prediction, respectively, $\Delta\xi$ is the bin width, $U(\xi)$ is the correction factor, and $\mathcal{L}$ is the total integrated luminosity. The bin widths were chosen to be commensurate with the resolution, with typical correct-bin purities above 70%, and the cross section measurements are limited to bins in ξ that contain at least ten entries in the data.

A. Correction factors in the $Z/\gamma^* \to e^+e^-$ channel

In the case of the inclusive jet multiplicity, the correction factors vary with the number of jets and are between 1.40 and 1.50. The correction factors for the inclusive jet p_T distribution and the p_T distribution for the leading jet vary from 1.45 at p_T around 30 GeV and 1.50 at p_T about 60 GeV to 1.42 at very large p_T. The corresponding factors for the p_T distribution of the second-leading jet increase from about 1.40 to 1.55 with increasing p_T.

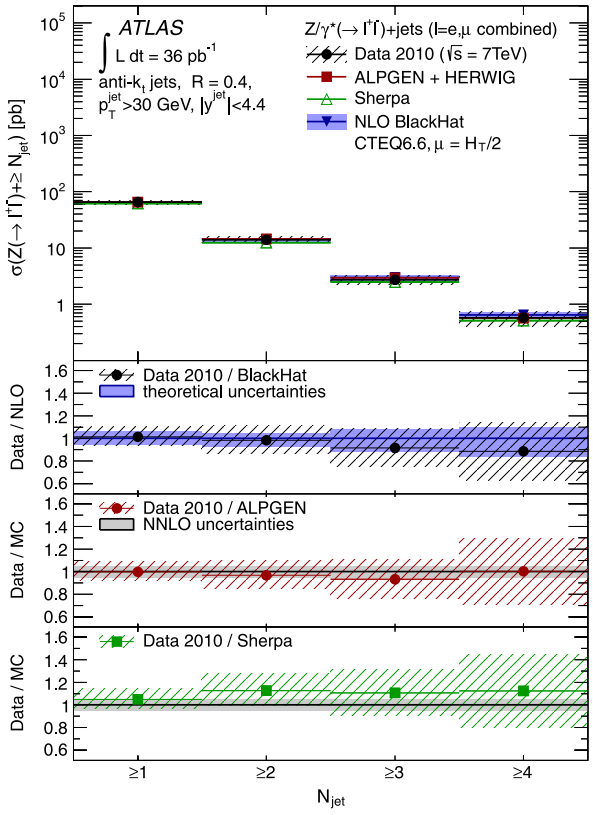

FIG. 15 (color online). Measured cross section $\sigma_{N_{\text{jet}}}$ (black dots) in $Z/\gamma^*(\to \ell^+\ell^-)$ + jets production as a function of the inclusive jet multiplicity, for events with at least one jet with $p_T >$ 30 GeV and $|y| < 4.4$ in the final state. In this and subsequent Figs. 16–26 the error bands indicate the total uncertainty from the combination of electron and muon results. The measurements are compared to NLO pQCD predictions from BLACKHAT, as well as the predictions from ALPGEN and SHERPA (both normalized to the FEWZ value for the total cross section).

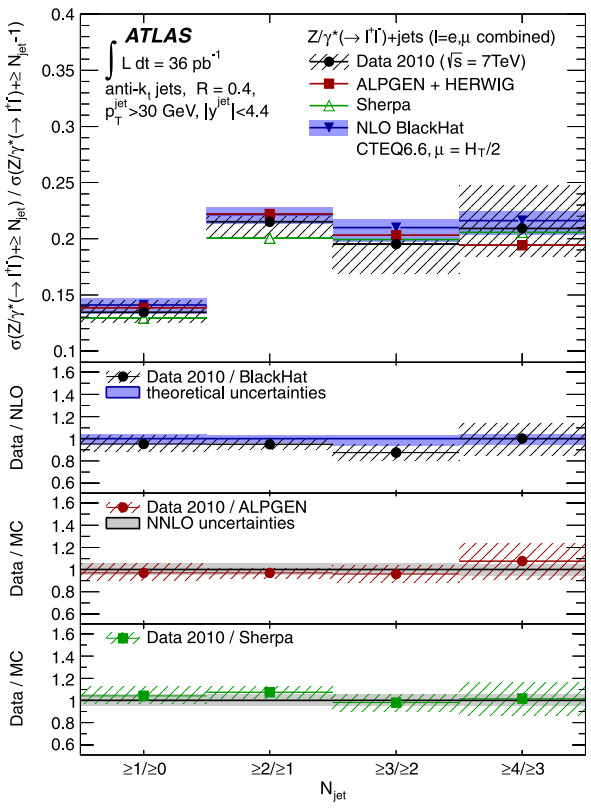

FIG. 16 (color online). Measured ratio of cross sections $(\sigma_{N_{\text{jet}}}/\sigma_{N_{\text{jet}}-1})$ (black dots) in $Z/\gamma^*(\to \ell^+\ell^-)$ + jets production as a function of the inclusive jet multiplicity, for events with at least one jet with $p_T > 30$ GeV and $|y| < 4.4$ in the final state.

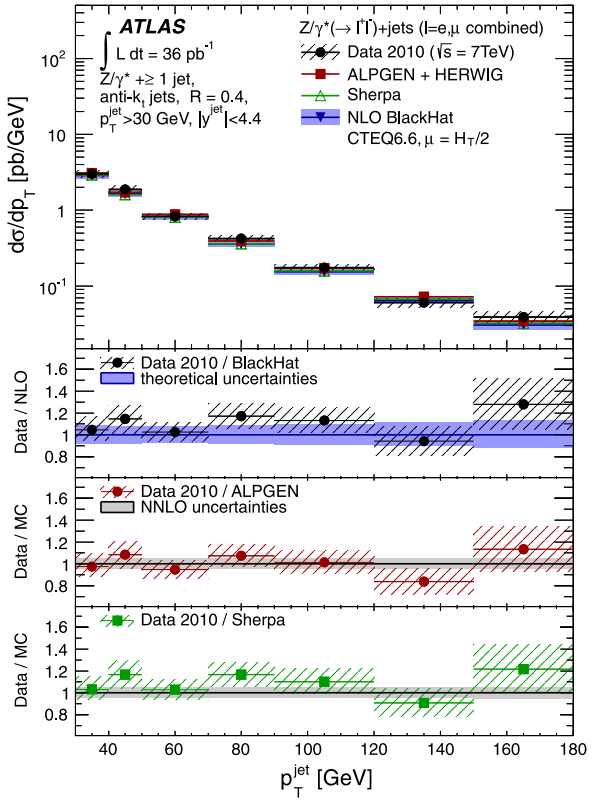

FIG. 17 (color online). Measured inclusive jet cross section $d\sigma/dp_T$ (black dots) in $Z/\gamma^*(\rightarrow \ell^+\ell^-)$ + jets production as a function of p_T, in events with at least one jet with $p_T > 30$ GeV and $|y| < 4.4$ in the final state.

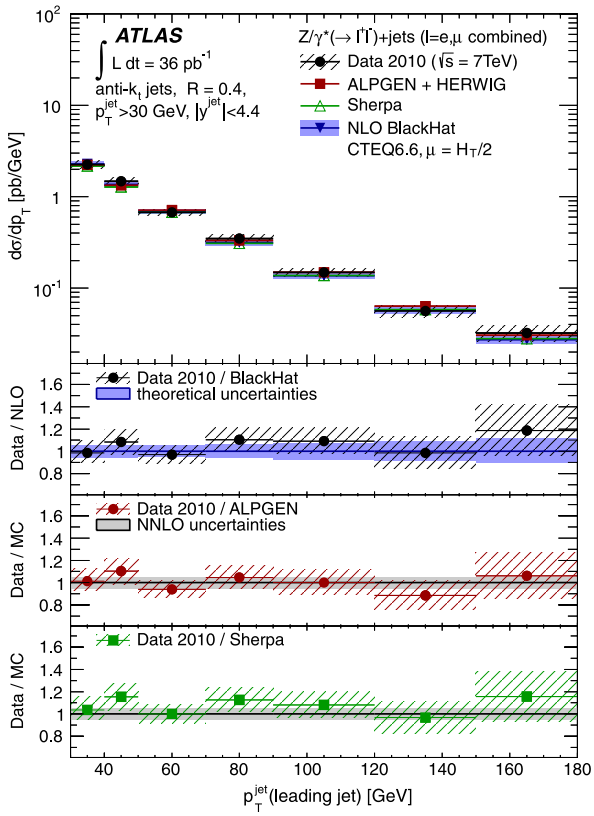

FIG. 18 (color online). Measured jet cross section $d\sigma/dp_T$ (black dots) in $Z/\gamma^*(\rightarrow \ell^+\ell^-)$ + jets production as a function of the leading jet p_T, in events with at least one jet with $p_T > 30$ GeV and $|y| < 4.4$ in the final state.

The correction factors for the inclusive $|y|$ distribution and the $|y|$ distribution of the leading jet vary from 1.40 for central jets to about 1.60 for very forward jets. The correction factors for the $|y|$ distribution of the second-leading jets are about 1.45 and show a mild rapidity dependence.

The correction factors for the Δy, $\Delta\phi$, and ΔR distributions between the two leading jets increase from 1.30 to 1.50 as the jet separation increases. Finally, the correction factor for the dijet invariant mass distribution varies between 1.40 and 1.55 as m^{jj} increases from 60 GeV to 300 GeV. At very low m^{jj}, the correction factors are about 0.90 and reflect a large sensitivity to the p_T thresholds applied in the analysis. Therefore, the cross section as a function of m^{jj} is only reported for $m^{jj} >$ 60 GeV.

B. Correction factors in the $Z/\gamma^* \rightarrow \mu^+\mu^-$ channel

The correction factors for the inclusive jet multiplicity decrease from 1.15 to 1.08 with increasing N_{jet}. The correction factors for the different p_T distributions increase from 1.10 to 1.20 as p_T increases from 30 GeV to 50 GeV and present a mild p_T dependence for $p_T > 50$ GeV. Similarly, the corresponding factors for the different jet $|y|$ distributions vary between 1.15 for central jets and 1.20 for forward jets.

The correction factors for the Δy, $\Delta\phi$, and ΔR distributions, for the two leading jets in events with at least two jets in the final state, vary between 1.10 and 1.20 as the jet separation increases. The correction factors for the m^{jj} distribution vary between 1.10 and 1.20 as m^{jj} increases. As in the electron case, the cross section as a function of m^{jj} is limited to the region $m^{jj} > 60$ GeV.

X. STUDY OF SYSTEMATIC UNCERTAINTIES

A detailed study of systematic uncertainties is carried out. In the following, a complete description is given for two of the observables: the inclusive cross section as a function of N_{jet} and the inclusive jet cross section as a function of p_T, in events with at least one jet in the final state (see Fig. 2). The same sources of systematic uncertainty are considered for the rest of the observables.

(i) The measured jet energies are increased and decreased by factors between 3% and 10%, depending on p_T and η, to account for the absolute jet energy scale (JES) uncertainty, as determined in inclusive jet studies [29]. For a given jet $|\eta|$, the jet energy uncertainty tends to decrease with increasing p_T,

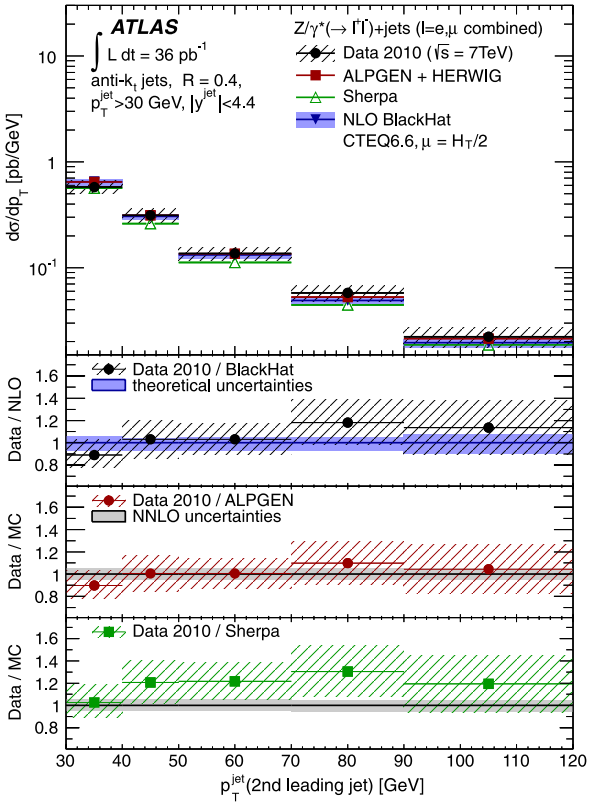

FIG. 19 (color online). Measured jet cross section $d\sigma/dp_T$ (black dots) in $Z/\gamma^*(\rightarrow \ell^+\ell^-)$ + jets production as a function of the second-leading jet p_T, in events with at least two jets with $p_T > 30$ GeV and $|y| < 4.4$ in the final state.

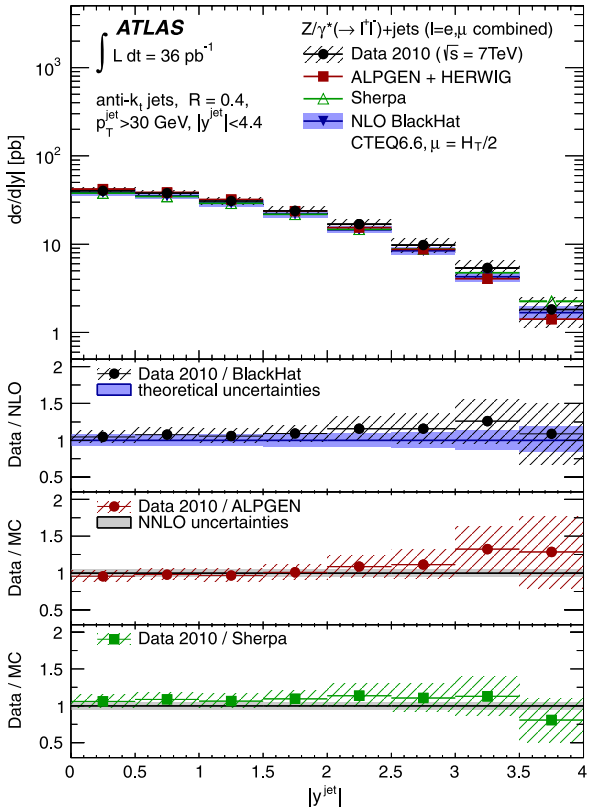

FIG. 20 (color online). Measured inclusive jet cross section $d\sigma/d|y|$ (black dots) in $Z/\gamma^*(\rightarrow \ell^+\ell^-)$ + jets production as a function of $|y|$, in events with at least one jet with $p_T > 30$ GeV and $|y| < 4.4$ in the final state.

while the uncertainties increase with increasing $|\eta|$. An additional 0.1% to 1.5% uncertainty on the jet energy, depending on p_T and $|\eta|$, is considered for each additional reconstructed primary vertex in the event to account for the uncertainty on the pileup offset subtraction, where the uncertainty decreases (increases) with increasing p_T ($|\eta|$). Additional uncertainties are included to account for the different quark- and gluon-jet relative population in multijets and Z/γ^* + jets processes and the presence of close-by jets in the final state, leading to a different average calorimeter response. These effects added in quadrature result in an uncertainty on the measured cross sections that increases from 7% to 22% as N_{jet} increases and from 8% to 12% as p_T increases, and constitutes the dominant source of systematic uncertainty for each of the measured distributions. The uncertainty on the jet energy resolution (JER) [29] translates into a 1% uncertainty on the cross section as a function of N_{jet} and into a 1% to 3% uncertainty on the measured cross sections with increasing jet p_T and $|y|$.

(ii) The uncertainty on the estimated multijets background in the electron channel translates into an uncertainty on the measured cross sections which rises from 0.6% to 2% as N_{jet} and p_T increase. In addition, the background contributions from top quark, W + jets, $Z/\gamma^*(\rightarrow \tau^+\tau^-)$ + jets, and diboson production processes are varied by $+7-9.6\%$, 5%, 5%, and 5%, respectively, to account for the uncertainty on the absolute normalization of the different MC samples. This translates into a less than 1% uncertainty in the measured cross sections. In the $Z/\gamma^*(\rightarrow \mu^+\mu^-)$ + jets measurements, the impact from the background uncertainties is negligible.

(iii) The correction factors are recomputed using SHERPA instead of ALPGEN to account for possible dependencies on the parton shower, underlying event and fragmentation models, and the PDF sets used in the MC samples. This introduces an uncertainty on the measured cross sections that increases from 0.4% to 4.5% with increasing N_{jet} and p_T. In addition, a Bayesian iterative method [31] is used to unfold the data, which accounts for the full migration matrix across bins for a given observable. The ALPGEN MC samples are used to construct the input migration matrices for the different measured distributions and up to three iterations are considered, as optimized separately for each observable using

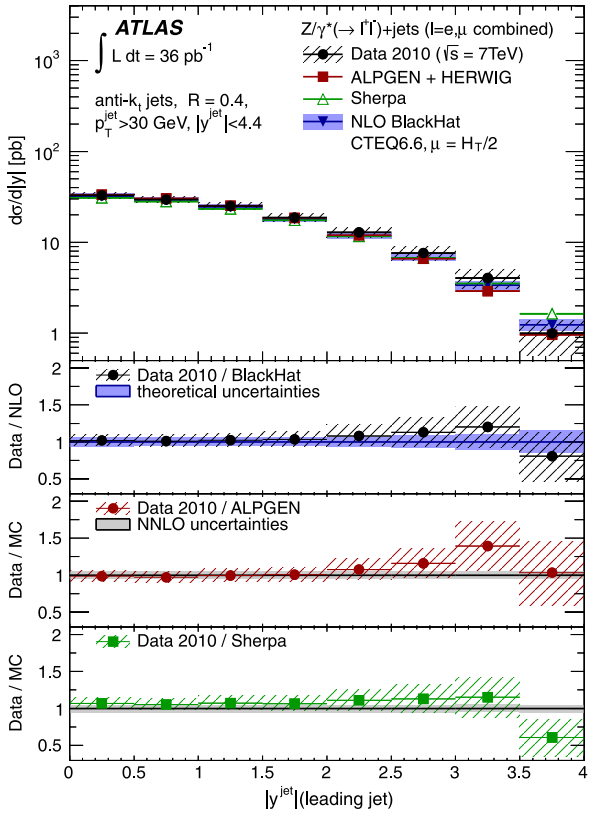

FIG. 21 (color online). Measured jet cross section $d\sigma/d|y|$ (black dots) in $Z/\gamma^*(\rightarrow \ell^+\ell^-)$ + jets production as a function of the leading jet $|y|$, in events with at least one jet with $p_T > 30$ GeV and $|y| < 4.4$ in the final state.

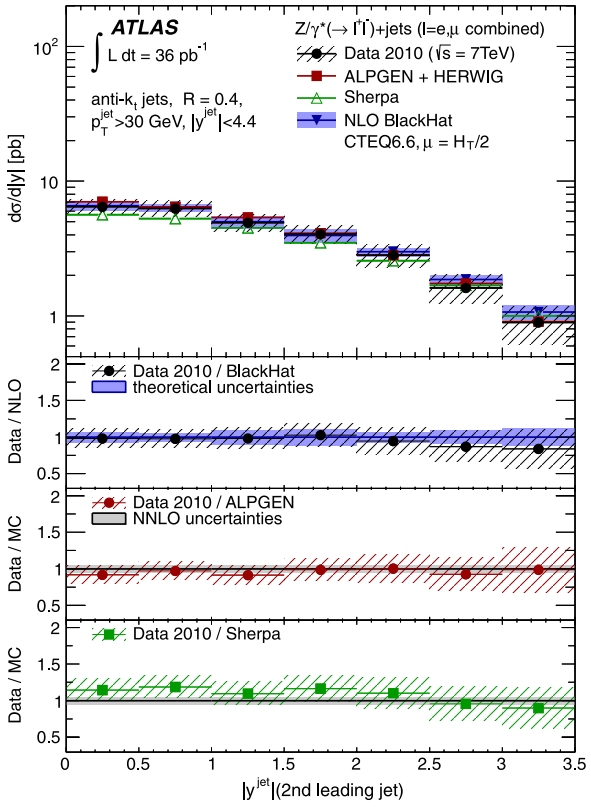

FIG. 22 (color online). Measured jet cross section $d\sigma/d|y|$ (black dots) in $Z/\gamma^*(\rightarrow \ell^+\ell^-)$ + jets production as a function of the second-leading jet $|y|$, in events with at least two jets with $p_T > 30$ GeV and $|y| < 4.4$ in the final state.

the simulation. The differences with respect to the nominal bin-by-bin correction factors are less than 1% except at very large p_T where they vary between 3% and 6%, and are included as an additional source of systematic uncertainty. Altogether, this introduces an uncertainty on the measured cross sections that increases from 0.7% to 7% with increasing N_{jet} and p_T.

(iv) The uncertainty on the electron selection is taken into account. It includes uncertainties on the electron absolute energy scale and energy resolution, the uncertainty on the electron identification efficiency, and the uncertainties on the electron reconstruction scale factors applied to the MC simulation. This translates into a 4% uncertainty in the measured $Z/\gamma^*(\rightarrow e^+e^-)$ + jets cross sections, approximately independent of N_{jet}, and jet p_T and η. The uncertainty on the measured cross sections due to the determination of the electron trigger efficiency is negligible.

(v) The uncertainty on the muon reconstruction efficiency, the muon momentum scale, and the muon momentum resolution translate into a conservative 2% uncertainty in the measured $Z/\gamma^*(\rightarrow \mu^+\mu^-)$ + jets cross sections, approximately independent of N_{jet}, and jet p_T and η. The uncertainty on the muon trigger efficiency introduces a less than 1% uncertainty on the measured cross sections.

For each channel, the different sources of systematic uncertainty are added in quadrature to the statistical uncertainty to obtain the total uncertainty. The total systematic uncertainty increases from 9% to 23% as N_{jet} increases; and from 10% at low p_T to 13% at very high p_T. Finally, the additional 3.4% uncertainty on the total integrated luminosity [32] is also taken into account.

XI. NEXT-TO-LEADING ORDER PQCD PREDICTIONS

NLO pQCD predictions for $Z/\gamma^*(\rightarrow e^+e^-)$ + jets and $Z/\gamma^*(\rightarrow \mu^+\mu^-)$ + jets production are computed using the BLACKHAT program [5]. CTEQ6.6 PDFs [16] are employed and renormalization and factorization scales are set to $\mu = H_T/2$, where H_T is defined event-by-event as the scalar sum of the p_T of all particles and partons in the final state. The anti-k_t algorithm with $R = 0.4$ is used to reconstruct jets at the parton level.

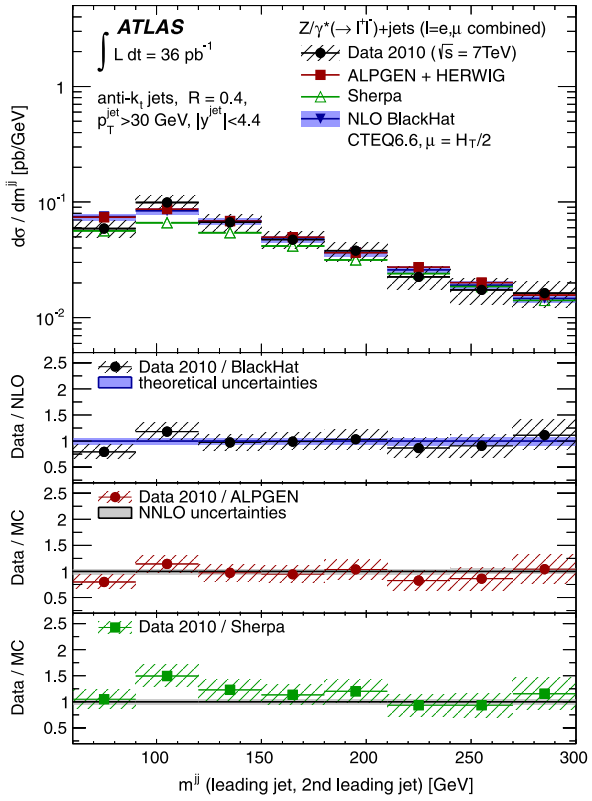

FIG. 23 (color online). Measured dijet cross section $d\sigma/dm^{jj}$ (black dots) in $Z/\gamma^*(\rightarrow \ell^+\ell^-)$ + jets production as a function of the invariant mass of the two leading jets m^{jj}, in events with at least two jets with $p_T > 30$ GeV and $|y| < 4.4$ in the final state.

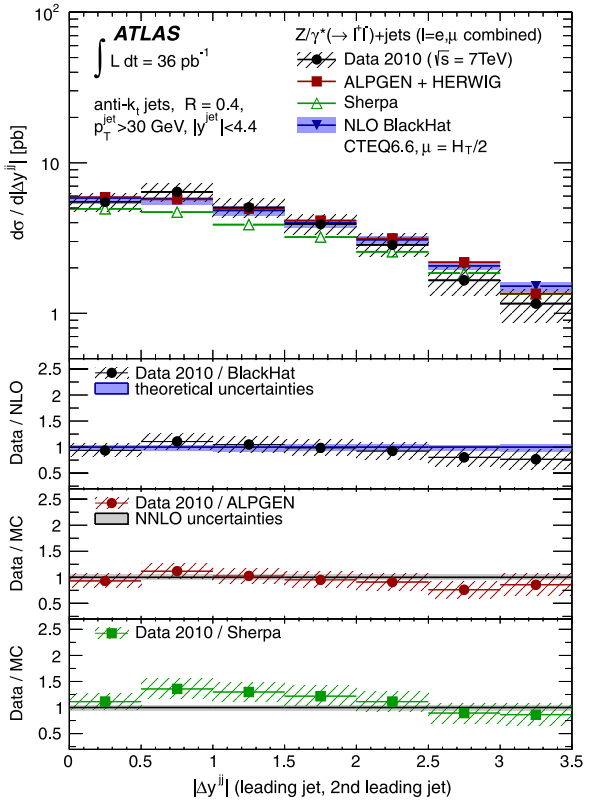

FIG. 24 (color online). Measured dijet cross section $d\sigma/d|\Delta y^{jj}|$ (black dots) in $Z/\gamma^*(\rightarrow \ell^+\ell^-)$ + jets production as a function of the rapidity separation of the two leading jets $|\Delta y^{jj}|$, in events with at least two jets with $p_T > 30$ GeV and $|y| < 4.4$ in the final state.

Systematic uncertainties on the predictions related to PDF uncertainties are computed using the Hessian method [33] and are defined as 90% confidence level uncertainties. For the total cross sections, they increase from 2% to 5% with increasing N_{jet}. Additional changes in the PDFs due to the variation of the input value for $\alpha_s(M_Z)$ by ± 0.002 around its nominal value $\alpha_s(M_Z) = 0.118$ introduce uncertainties on the measured cross sections that increase from 2% to 7% with increasing N_{jet}. These are added in quadrature to the PDF uncertainties. Variations of the renormalization and factorization scales by a factor of 2 (half) reduce (increase) the predicted cross sections by 4% to 14% as N_{jet} increases.

The theoretical predictions are corrected for QED radiation effects. The correction factors δ^{QED} are determined using ALPGEN MC samples with and without photon radiation in the final state, defined by the lepton four-momentum and photons within a cone of radius 0.1 around the lepton direction. The correction factors are about 2% for the electron and muon channels, and do not present a significant N_{jet} dependence.

The theoretical predictions include parton-to-hadron correction factors δ^{had} that approximately account for nonperturbative contributions from the underlying event and fragmentation into particles. In each measurement, the correction factor is estimated using HERWIG+JIMMY MC samples, as the ratio at the particle level between the nominal distribution and the one obtained by turning off both the interactions between proton remnants and the cluster fragmentation in the MC samples. The nonperturbative correction factors for the inclusive N_{jet} and p_T distributions are about 0.99 and exhibit a moderate N_{jet} and p_T dependence. However, for very forward jets δ^{had} is about 0.9. The nonperturbative corrections are also computed using PYTHIA-AMBT1 MC samples with different parton shower, fragmentation model, and UE settings. The uncertainty on δ^{had}, defined as the difference between the results obtained with HERWIG/JIMMY-AUET1 and PYTHIA-AMBT1, varies between 2% and 5%.

XII. RESULTS

As mentioned in Sec. IX, the measured cross sections refer to particle level jets identified using the anti-k_t algorithm with $R = 0.4$, for jets with $p_T > 30$ GeV and $|y| < 4.4$, and the results are defined in a limited kinematic range for the Z/γ^* decay products. The data are compared to the

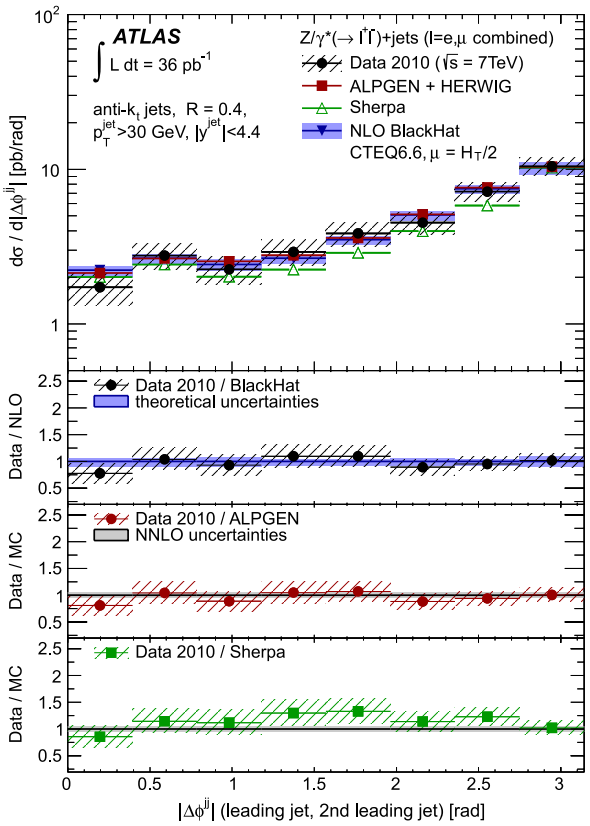

FIG. 25 (color online). Measured dijet cross section $d\sigma/d|\Delta\phi^{jj}|$ (black dots) in $Z/\gamma^*(\rightarrow \ell^+\ell^-)$ + jets production as a function of the azimuthal separation of the two leading jets $|\Delta\phi^{jj}|$, in events with at least two jets with $p_T > 30$ GeV and $|y| < 4.4$ in the final state.

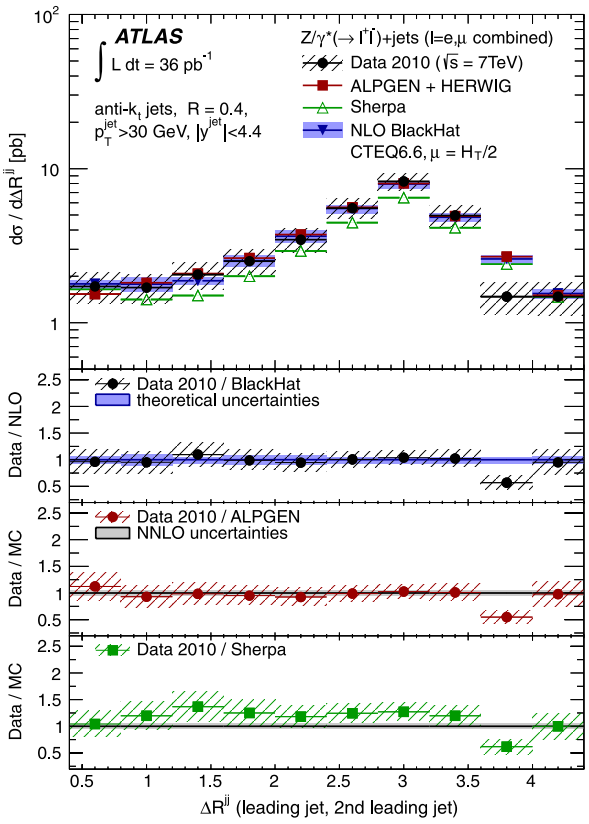

FIG. 26 (color online). Measured dijet cross section $d\sigma/d\Delta R^{jj}$ (black dots) in $Z/\gamma^*(\rightarrow \ell^+\ell^-)$ + jets production as a function of the angular separation ($y - \phi$ space) of the two leading jets ΔR^{jj}, in events with at least two jets with $p_T > 30$ GeV and $|y| < 4.4$ in the final state.

predictions from the different MC event generators implementing $Z/\gamma^*(\rightarrow e^+e^-)$ + jets and $Z/\gamma^*(\rightarrow \mu^+\mu^-)$ + jets production, as discussed in Sec. IV, as well as to NLO pQCD predictions, as discussed in Sec. XI. Tabulated values of the results are available in Tables II, III, IV, V, VI, VII, VIII, IX, X, XI, XII, and XIII and in the Durham HEP database [34].

A. Inclusive jet multiplicity

Figure 3 presents the measured cross sections as functions of the inclusive jet multiplicity ($\geq N_{\text{jet}}$) for $Z/\gamma^* \rightarrow e^+e^-$ and $Z/\gamma^* \rightarrow \mu^+\mu^-$ interactions, in events with up to at least four jets in the final state. The data are well described by the predictions from ALPGEN and SHERPA, and BLACKHAT NLO pQCD. ALPGEN and SHERPA predictions include a 5% uncertainty from the NNLO pQCD normalization, as discussed in Sec. IV, and the systematic uncertainty on the BLACKHAT NLO pQCD predictions is discussed in Sec. XI. In the case of PYTHIA, the LO pQCD ($q\bar{q} \rightarrow Z/\gamma^* g$ and $qg \rightarrow Z/\gamma^* q$ processes) MC predictions are multiplied by a factor 1.19, as determined from data and extracted from the average of electron and muon results in the ≥ 1 jet bin in Fig. 3. This brings the PYTHIA predictions close to the data. However, for larger N_{jet}, and despite the additional normalization applied, PYTHIA predictions underestimate the measured cross sections.

The measured ratio of cross sections for N_{jet} and $N_{\text{jet}} - 1$ is shown in Fig. 4, compared to the different theoretical predictions. This observable cancels part of the systematic uncertainty and constitutes an improved test of the SM. The ratio is sensitive to the value of the strong coupling, and to the details of the implementation of higher-order matrix elements and soft-gluon radiation contributions in the theoretical predictions. The data indicate that the cross sections decrease by a factor of 5 with the requirement of each additional jet in the final state. The electron and muon measurements are well described by ALPGEN and SHERPA, and the BLACKHAT NLO pQCD predictions. PYTHIA predictions underestimate the measured ratios.

B. $d\sigma/dp_T$ and $d\sigma/d|y|$

The inclusive jet differential cross section $d\sigma/dp_T$ as a function of p_T is presented in Fig. 5, for both electron and muon analyses, in events with at least one jet in the final state. The cross sections are divided by the corresponding inclusive Z/γ^* cross section times branching ratio $\sigma_{Z/\gamma^* \to \ell^+\ell^-}(\ell = e, \mu)$, separately for $Z/\gamma^* \to e^+e^-$ and $Z/\gamma^* \to \mu^+\mu^-$, measured in the same kinematic region for the leptons and consistent with the results in Ref. [30], with the aim of cancelling systematic uncertainties related to lepton identification and the luminosity. The measured differential cross sections decrease by more than 2 orders of magnitude as p_T increases between 30 GeV and 180 GeV. The data are well described by ALPGEN and SHERPA, and the BLACKHAT NLO pQCD predictions. PYTHIA predictions include the multiplicative factor 1.19 (as described above) and are then divided by the measured $\sigma_{Z/\gamma^* \to \ell^+\ell^-}$ cross sections in this analysis. This results in total normalization factors ($\times 0.0028$ pb^{-1}) and ($\times 0.0027$ pb^{-1}) for the electron and muon channels, respectively. PYTHIA shows a slightly softer jet p_T spectrum than the data. Similar conclusions are extracted from Fig. 6, where the differential cross sections are presented as a function of the leading-jet p_T.

Figure 7 shows the measured differential cross sections $(1/\sigma_{Z/\gamma^* \to \ell^+\ell^-})d\sigma/dp_T$, for electron and muon channels, as a function of p_T of the second leading jet for jets with 30 GeV $< p_T <$ 120 GeV, in events with at least two jets in the final state. The measured cross sections decrease with increasing p_T, and are again well described by ALPGEN and SHERPA, and the BLACKHAT NLO pQCD predictions, while PYTHIA does not describe the data. This is expected since PYTHIA only implements pQCD matrix elements for $Z/\gamma^* + 1$ jet production, with the additional parton radiation produced via parton shower.

Inclusive jet differential cross sections $(1/\sigma_{Z/\gamma^* \to \ell^+\ell^-}) \times d\sigma/d|y|$ as a function of $|y|$ for jets with $p_T > 30$ GeV are presented in Fig. 8, while Fig. 9 shows the jet measurements as a function of the rapidity of the leading jet. The measured cross sections decrease with increasing $|y|$ and are well described by ALPGEN and the BLACKHAT NLO pQCD predictions. SHERPA provides a good description of the data in the region $|y| < 3.5$ but predicts a slightly larger cross section than observed in data for very forward jets. PYTHIA provides a good description of the shape of the measured cross sections in the region $|y| < 2.5$ but predicts a smaller cross section than the data in the forward region. In Fig. 10, the measured differential cross sections are presented as functions of the $|y|$ of the second leading jet, for events with at least two jets in the final state. The data are described by the predictions from ALPGEN and SHERPA, and BLACKHAT NLO pQCD, while again PYTHIA does not describe the data.

C. $d\sigma/dm^{jj}$

The measured differential cross sections $(1/\sigma_{Z/\gamma^* \to \ell^+\ell^-})d\sigma/dm^{jj}$ as a function of the invariant mass of the two leading jets in the event for 60 GeV $< m^{jj} <$ 300 GeV are presented in Fig. 11 for both electron and muon channels. The shape of the measured cross section at low m^{jj} is affected by the jet p_T threshold in the cross section definition. For $m^{jj} > 100$ GeV, the measured cross sections decrease with increasing m^{jj}. The measurements are well described by ALPGEN and SHERPA, and the BLACKHAT NLO pQCD predictions. PYTHIA approximately reproduces the shape of the measured distribution but underestimates the measured cross sections.

D. $d\sigma/d|\Delta y^{jj}|$, $d\sigma/d|\Delta\phi^{jj}|$, and $d\sigma/d\Delta R^{jj}$

Inclusive dijet cross sections are also measured as a function of the spatial separation of the two leading jets in the final state. Figure 12 shows the measured differential cross section as a function of the rapidity separation of the jets $(1/\sigma_{Z/\gamma^* \to \ell^+\ell^-})d\sigma/d|\Delta y^{jj}|$, for both the electron and muon analysis, compared to the different predictions. The measured differential cross sections as a function of the azimuthal separation between jets $(1/\sigma_{Z/\gamma^* \to \ell^+\ell^-}) \times d\sigma/d|\Delta\phi^{jj}|$ are presented in Fig. 13 and 14 shows the measured differential cross sections $(1/\sigma_{Z/\gamma^* \to \ell^+\ell^-}) \times d\sigma/d\Delta R^{jj}$ as a function of the angular separation ΔR^{jj} between the two leading jets in the event. The measurements are well described by ALPGEN and SHERPA, and the BLACKHAT NLO pQCD predictions, while PYTHIA underestimates the measured cross sections. In particular, PYTHIA underestimates the data for large $|\Delta\phi^{jj}|$ values and for those topologies corresponding to well-separated jets.

E. Combination of electron and muon results

The measured cross section distributions for the $Z/\gamma^*(\to e^+e^-)$ + jets and $Z/\gamma^*(\to \mu^+\mu^-)$ + jets analyses are combined. In this case, the results are not normalized by the inclusive Z/γ^* cross section after the combination, with the aim to present also precise absolute jet cross section measurements.

As already discussed, the electron and muon measurements are performed in different fiducial regions for the rapidity of the leptons in the final state. In addition, the QED radiation effects are different in both channels. For each measured distribution, bin-by-bin correction factors, as extracted from ALPGEN $Z/\gamma^*(\to e^+e^-)$ + jets and $Z/\gamma^*(\to \mu^+\mu^-)$ + jets MC samples, are used to extrapolate the measurements to the region $p_T > 20$ GeV and $|\eta| < 2.5$ for the leptons, where the lepton kinematics are defined at the decay vertex of the Z boson. The increased acceptance in the lepton rapidities translates into about a 14% and a 5% increase of the measured cross sections in

the electron and muon channels, respectively. As already mentioned in Sec. XI, the correction for QED effects increases the cross sections by about 2%. The uncertainties on the acceptance corrections are at the per mille level, as determined by using SHERPA instead of ALPGEN, and by considering different PDFs among the CTEQ6.6 and MSTW sets. A χ^2 test is performed for each observable to quantify the agreement between the electron and muon results before they are combined, where the statistical and uncorrelated uncertainties are taken into account. The statistical tests lead to probabilities larger than 60% for the electron and muon measurements to be compatible with each other, consistent with slightly conservative systematic uncertainties.

The electron and muon results are combined using the BLUE (Best Linear Unbiased Estimate) [35] method, which considers the correlations between the systematic uncertainties in the two channels. The uncertainties related to the trigger, the lepton reconstruction, and the multijets background estimation are considered uncorrelated between the two channels, while the rest of the systematic uncertainties are treated as fully correlated. Figs. 15 to 26 show the combined results, and Tables II, III, IV, V, VI, VII, VIII, IX, X, XI, XII, and XIII collect the final measurements for the electron and muon channels and their combination, together with the multiplicative parton-to-hadron correction factors δ^{had} applied to the BLACKHAT NLO pQCD predictions (see Sec. XI). The measurements are well described by the BLACKHAT NLO pQCD predictions, and by the predictions from ALPGEN and SHERPA. The corresponding χ^2 tests relative to the different predictions, performed separately in each channel and for each observable, lead to χ^2 per degree of freedom values in the range between 0.05 and 2.70. Further details of the combination and the χ^2 tests are presented in the Appendix.

XIII. SUMMARY

In summary, results are reported for inclusive jet production in $Z/\gamma^* \to e^+e^-$ and $Z/\gamma^* \to \mu^+\mu^-$ events in proton-proton collisions at $\sqrt{s} = 7$ TeV. The analysis considers the data collected by the ATLAS detector in 2010 corresponding to a total integrated luminosity of about 36 pb^{-1}. Jets are defined using the anti-k_t algorithm with $R = 0.4$ and the measurements are performed for jets in the region $p_T > 30$ GeV and $|y| < 4.4$. Cross sections are measured as a function of the inclusive jet multiplicity, and the transverse momentum and rapidity of the jets in the final state. Measurements are also performed as a function of the dijet invariant mass and the angular separation between the two leading jets in events with at least two jets in the final state. The measured cross sections are well described by NLO pQCD predictions including nonperturbative corrections, as well as by predictions of LO matrix elements of up to $2 \to 5$ parton scatters, supplemented by parton showers, as implemented in the ALPGEN and SHERPA MC generators.

ACKNOWLEDGMENTS

We thank CERN for the very successful operation of the LHC, as well as the support staff from our institutions without whom ATLAS could not be operated efficiently. We acknowledge the support of ANPCyT, Argentina; YerPhI, Armenia; ARC, Australia; BMWF, Austria; ANAS, Azerbaijan; SSTC, Belarus; CNPq and FAPESP, Brazil; NSERC, NRC and CFI, Canada; CERN; CONICYT, Chile; CAS, MOST and NSFC, China; COLCIENCIAS, Colombia; MSMT CR, MPO CR and VSC CR, Czech Republic; DNRF, DNSRC and Lundbeck Foundation, Denmark; ARTEMIS, European Union; IN2P3-CNRS, CEA-DSM/IRFU, France; GNAS, Georgia; BMBF, DFG, HGF, MPG and AvH Foundation, Germany; GSRT, Greece; ISF, MINERVA, GIF, DIP and Benoziyo Center, Israel; INFN, Italy; MEXT and JSPS, Japan; CNRST, Morocco; FOM and NWO, Netherlands; RCN, Norway; MNiSW, Poland; GRICES and FCT, Portugal; MERYS (MECTS), Romania; MES of Russia and ROSATOM, Russian Federation; JINR; MSTD, Serbia; MSSR, Slovakia; ARRS and MVZT, Slovenia; DST/NRF, South Africa; MICINN, Spain; SRC and Wallenberg Foundation, Sweden; SER, SNSF and Cantons of Bern and Geneva, Switzerland; NSC, Taiwan; TAEK, Turkey; STFC, the Royal Society and Leverhulme Trust, United Kingdom; DOE and NSF, United States of America. The crucial computing support from all WLCG partners is acknowledged gratefully, in particular, from CERN and the ATLAS Tier-1 facilities at TRIUMF (Canada), NDGF (Denmark, Norway, Sweden), CC-IN2P3 (France), KIT/GridKA (Germany), INFN-CNAF (Italy), NL-T1 (Netherlands), PIC (Spain), ASGC (Taiwan), RAL (UK) and BNL (USA) and in the Tier-2 facilities worldwide.

APPENDIX—COMBINED RESULTS

The results for the electron and muon channels are extrapolated to a common acceptance region $p_T > 20$ GeV and $|\eta| < 2.5$ for the kinematics of the leptons, defined at the decay vertex of the Z boson before QED radiation. For each bin in a given observable ξ, the measured cross section $\sigma_\xi^{\text{fiducial}}$ in each channel is corrected according to

$$\sigma_\xi^{\text{extrapolated}} = \sigma_\xi^{\text{fiducial}} \times \delta^{\text{QED}} \times \mathcal{A}, \qquad \text{(A1)}$$

where δ^{QED} corrects for QED radiation effects back to the Born level and $\mathcal{A}$ extrapolates the result to the new lepton acceptance region. Tables XIV, XV, XVI, and XVII present the correction factors applied to the measured

TABLE XIV. Multiplicative correction factors, applied to the data in the electron and muon channels, that extrapolate the measured cross sections to the common acceptance region $p_T > 20$ GeV and $|\eta| < 2.5$ for the lepton kinematics, defined at the decay vertex of the Z boson before QED radiation.

		$\sigma_{N_{\text{jet}}}$		
N_{jet}	δ^{QED} (e-channel)	$\mathcal{A}$ (e-channel)	δ^{QED} (μ-channel)	$\mathcal{A}$ (μ-channel)
≥ 1 jet	1.024 ± 0.001	1.143 ± 0.003	1.024 ± 0.001	1.046 ± 0.003
≥ 2 jets	1.021 ± 0.001	1.144 ± 0.002	1.022 ± 0.001	1.045 ± 0.002
≥ 3 jets	1.021 ± 0.002	1.144 ± 0.003	1.021 ± 0.002	1.045 ± 0.002
≥ 4 jets	1.016 ± 0.003	1.151 ± 0.007	1.021 ± 0.002	1.048 ± 0.005
		$\sigma_{N_{\text{jet}}}/\sigma_{N_{\text{jet}}-1}$		
N_{jet}	δ^{QED} (e-channel)	$\mathcal{A}$ (e-channel)	δ^{QED} (μ-channel)	$\mathcal{A}$ (μ-channel)
≥ 1 jet	1.005 ± 0.003	1.001 ± 0.003	1.005 ± 0.003	0.994 ± 0.001
≥ 2 jets	0.997 ± 0.001	1.001 ± 0.003	0.998 ± 0.002	0.999 ± 0.001
≥ 3 jets	1.000 ± 0.001	1.001 ± 0.003	0.999 ± 0.001	1.001 ± 0.002
≥ 4 jets	0.996 ± 0.004	1.006 ± 0.006	1.001 ± 0.002	1.003 ± 0.003
		$d\sigma/dp_T$ (inclusive)		
p_T [GeV]	δ^{QED} (e-channel)	$\mathcal{A}$ (e-channel)	δ^{QED} (μ-channel)	$\mathcal{A}$ (μ-channel)
30–40	1.029 ± 0.001	1.142 ± 0.001	1.029 ± 0.001	1.048 ± 0.003
40–50	1.023 ± 0.003	1.144 ± 0.002	1.022 ± 0.005	1.048 ± 0.004
50–70	1.019 ± 0.001	1.143 ± 0.006	1.021 ± 0.001	1.046 ± 0.003
70–90	1.019 ± 0.003	1.145 ± 0.005	1.019 ± 0.003	1.043 ± 0.003
90–120	1.019 ± 0.003	1.143 ± 0.002	1.020 ± 0.003	1.040 ± 0.002
120–150	1.017 ± 0.004	1.144 ± 0.008	1.020 ± 0.004	1.040 ± 0.005
150–180	1.016 ± 0.002	1.142 ± 0.011	1.017 ± 0.004	1.036 ± 0.006
		$d\sigma/d\lvert y\rvert$ (inclusive)		
$\lvert y\rvert$	δ^{QED} (e-channel)	$\mathcal{A}$ (e-channel)	δ^{QED} (μ-channel)	$\mathcal{A}$ (μ-channel)
0.0–0.5	1.024 ± 0.003	1.135 ± 0.002	1.024 ± 0.002	1.035 ± 0.001
0.5–1.0	1.024 ± 0.001	1.139 ± 0.003	1.024 ± 0.001	1.039 ± 0.002
1.0–1.5	1.024 ± 0.001	1.140 ± 0.005	1.024 ± 0.002	1.047 ± 0.005
1.5–2.0	1.024 ± 0.002	1.148 ± 0.005	1.024 ± 0.001	1.056 ± 0.006
2.0–2.5	1.022 ± 0.001	1.160 ± 0.011	1.022 ± 0.001	1.059 ± 0.005
2.5–3.0	1.020 ± 0.001	1.158 ± 0.003	1.020 ± 0.001	1.067 ± 0.010
3.0–3.5	1.019 ± 0.001	1.152 ± 0.004	1.020 ± 0.006	1.068 ± 0.011
3.5–4.0	1.025 ± 0.007	1.163 ± 0.017	1.016 ± 0.002	1.065 ± 0.008

cross sections, separately for the electron and muon analyses.

The results are then combined using the BLUE [35] method that takes into account the correlations between systematic uncertainties in the two channels. The method assumes Gaussian χ^2 distributions and is not directly able to treat the asymmetric systematic uncertainties present in the measured cross sections. Therefore, a modified asymmetric iterative BLUE method is employed.

Three separate BLUE combinations are computed, using as an input the upper, the lower, and the average of the upper and lower uncertainties in the electron and muon channels, leading to three different results here denoted as $\sigma_\xi^{\text{up}} \pm \Delta\sigma_\xi^{\text{up}}$, $\sigma_\xi^{\text{low}} \pm \Delta\sigma_\xi^{\text{low}}$, and $\sigma_\xi^{\text{ave}} \pm \Delta\sigma_\xi^{\text{ave}}$, respectively. The central value for the combined cross section σ_ξ, and its upper and lower uncertainties, $\Delta^+\sigma_\xi$ and $\Delta^-\sigma_\xi$ respectively, are given by the expressions

$$\sigma_\xi = \sigma_\xi^{\text{ave}}, \tag{A2}$$

$$\Delta^+\sigma_\xi = 2 \times R \times \Delta\sigma_\xi^{\text{ave}}, \quad \text{and} \tag{A3}$$

$$\Delta^-\sigma_\xi = 2 \times (1 - R) \times \Delta\sigma_\xi^{\text{ave}}, \tag{A4}$$

with

TABLE XV. Multiplicative correction factors, applied to the data in the electron and muon channels, that extrapolate the measured cross sections to the common acceptance region $p_T > 20$ GeV and $|\eta| < 2.5$ for the lepton kinematics, defined at the decay vertex of the Z boson before QED radiation.

		$d\sigma/dp_T$ (leading jet)		
p_T [GeV]	δ^{QED} (e-channel)	$\mathcal{A}$ (e-channel)	δ^{QED} (μ-channel)	$\mathcal{A}$ (μ-channel)
30–40	1.031 ± 0.001	1.142 ± 0.001	1.031 ± 0.002	1.049 ± 0.003
40–50	1.023 ± 0.005	1.143 ± 0.004	1.022 ± 0.006	1.048 ± 0.004
50–70	1.020 ± 0.001	1.143 ± 0.005	1.021 ± 0.001	1.046 ± 0.004
70–90	1.020 ± 0.004	1.146 ± 0.006	1.019 ± 0.003	1.043 ± 0.003
90–120	1.019 ± 0.003	1.142 ± 0.003	1.020 ± 0.003	1.040 ± 0.002
120–150	1.017 ± 0.004	1.144 ± 0.010	1.020 ± 0.004	1.038 ± 0.003
150–180	1.016 ± 0.002	1.141 ± 0.014	1.016 ± 0.004	1.036 ± 0.008
		$d\sigma/d\lvert y\rvert$ (leading jet)		
$\lvert y\rvert$	δ^{QED} (e-channel)	$\mathcal{A}$ (e-channel)	δ^{QED} (μ-channel)	$\mathcal{A}$ (μ-channel)
0.0–0.5	1.024 ± 0.003	1.133 ± 0.004	1.025 ± 0.002	1.034 ± 0.001
0.5–1.0	1.025 ± 0.001	1.137 ± 0.003	1.024 ± 0.001	1.037 ± 0.002
1.0–1.5	1.025 ± 0.001	1.141 ± 0.005	1.025 ± 0.003	1.047 ± 0.005
1.5–2.0	1.025 ± 0.002	1.150 ± 0.005	1.024 ± 0.001	1.057 ± 0.006
2.0–2.5	1.023 ± 0.001	1.161 ± 0.010	1.022 ± 0.001	1.063 ± 0.006
2.5–3.0	1.020 ± 0.001	1.164 ± 0.006	1.020 ± 0.002	1.073 ± 0.010
3.0–3.5	1.019 ± 0.002	1.159 ± 0.006	1.021 ± 0.009	1.076 ± 0.015
3.5–4.0	1.025 ± 0.008	1.170 ± 0.016	1.017 ± 0.002	1.074 ± 0.012
		$d\sigma/dp_T$ (second-leading jet)		
p_T [GeV]	δ^{QED} (e-channel)	$\mathcal{A}$ (e-channel)	δ^{QED} (μ-channel)	$\mathcal{A}$ (μ-channel)
30–40	1.023 ± 0.001	1.141 ± 0.002	1.024 ± 0.001	1.045 ± 0.002
40–50	1.022 ± 0.003	1.147 ± 0.003	1.021 ± 0.003	1.046 ± 0.002
50–70	1.018 ± 0.001	1.146 ± 0.008	1.020 ± 0.001	1.043 ± 0.001
70–90	1.015 ± 0.002	1.142 ± 0.009	1.019 ± 0.005	1.045 ± 0.005
90–120	1.024 ± 0.009	1.148 ± 0.008	1.021 ± 0.008	1.040 ± 0.003
		$d\sigma/d\lvert y\rvert$ (second-leading jet)		
$\lvert y\rvert$	δ^{QED} (e-channel)	$\mathcal{A}$ (e-channel)	δ^{QED} (μ-channel)	$\mathcal{A}$ (μ-channel)
0.0–0.5	1.021 ± 0.002	1.142 ± 0.003	1.020 ± 0.002	1.038 ± 0.002
0.5–1.0	1.021 ± 0.002	1.148 ± 0.004	1.023 ± 0.002	1.042 ± 0.002
1.0–1.5	1.021 ± 0.002	1.137 ± 0.005	1.024 ± 0.002	1.047 ± 0.003
1.5–2.0	1.021 ± 0.002	1.142 ± 0.004	1.023 ± 0.002	1.053 ± 0.003
2.0–2.5	1.021 ± 0.007	1.155 ± 0.008	1.021 ± 0.002	1.048 ± 0.004
2.5–3.0	1.022 ± 0.003	1.140 ± 0.008	1.019 ± 0.004	1.048 ± 0.011
3.0–3.5	1.018 ± 0.004	1.143 ± 0.007	1.017 ± 0.005	1.051 ± 0.011

$$R = \frac{\Delta\sigma_{\xi}^{\mathrm{up}}}{\Delta\sigma_{\xi}^{\mathrm{up}} + \Delta\sigma_{\xi}^{\mathrm{low}}}. \tag{A5}$$

The BLUE method provides uncertainties on the combined measurement that include both statistical and systematic uncertainties.

Finally, χ^2 tests to the data points in each measured cross section before and after extrapolation are performed with respect to the NLO pQCD, ALPGEN, and SHERPA predictions, according to

$$\chi^2 = \sum_{j=1}^{\mathrm{bins}} \frac{[d_j - t_j(\vec{s})]^2}{[\delta d_j]^2 + [\delta t_j(\vec{s})]^2} + \sum_{i=1}^{7} [s_i]^2, \tag{A6}$$

TABLE XVI. Multiplicative correction factors, applied to the data in the electron and muon channels, that extrapolate the measured cross sections to the common acceptance region $p_T >$ 20 GeV and $|\eta| < 2.5$ for the lepton kinematics, defined at the decay vertex of the Z boson before QED radiation.

		$d\sigma/dm^{jj}$		
m^{jj} [GeV]	δ^{QED} (e-channel)	$\mathcal{A}$ (e-channel)	δ^{QED} (μ-channel)	$\mathcal{A}$ (μ-channel)
60–90	1.025 ± 0.004	1.148 ± 0.006	1.025 ± 0.005	1.044 ± 0.004
90–120	1.023 ± 0.002	1.141 ± 0.005	1.025 ± 0.002	1.046 ± 0.004
120–150	1.022 ± 0.002	1.138 ± 0.004	1.022 ± 0.002	1.047 ± 0.006
150–180	1.016 ± 0.002	1.146 ± 0.006	1.021 ± 0.002	1.043 ± 0.008
180–210	1.017 ± 0.003	1.149 ± 0.007	1.019 ± 0.004	1.042 ± 0.002
210–240	1.016 ± 0.002	1.141 ± 0.010	1.020 ± 0.004	1.049 ± 0.006
240–270	1.022 ± 0.006	1.140 ± 0.013	1.022 ± 0.007	1.045 ± 0.009
270–300	1.026 ± 0.015	1.154 ± 0.016	1.018 ± 0.005	1.041 ± 0.009
		$d\sigma/d\lvert\Delta y^{jj}\rvert$		
$\lvert\Delta y^{jj}\rvert$	δ^{QED} (e-channel)	$\mathcal{A}$ (e-channel)	δ^{QED} (μ-channel)	$\mathcal{A}$ (μ-channel)
0.0–0.5	1.021 ± 0.001	1.146 ± 0.004	1.023 ± 0.001	1.041 ± 0.001
0.5–1.0	1.021 ± 0.004	1.148 ± 0.009	1.024 ± 0.003	1.042 ± 0.004
1.0–1.5	1.022 ± 0.002	1.141 ± 0.004	1.021 ± 0.003	1.046 ± 0.004
1.5–2.0	1.022 ± 0.001	1.141 ± 0.004	1.022 ± 0.004	1.044 ± 0.002
2.0–2.5	1.021 ± 0.004	1.132 ± 0.010	1.022 ± 0.002	1.045 ± 0.004
2.5–3.0	1.017 ± 0.003	1.147 ± 0.008	1.017 ± 0.002	1.050 ± 0.003
3.0–3.5	1.019 ± 0.002	1.145 ± 0.009	1.023 ± 0.008	1.052 ± 0.007

TABLE XVII. Multiplicative correction factors, applied to the data in the electron and muon channels, that extrapolate the measured cross sections to the common acceptance region $p_T >$ 20 GeV and $|\eta| < 2.5$ for the lepton kinematics, defined at the decay vertex of the Z boson before QED radiation.

		$d\sigma/d\lvert\Delta\phi^{jj}\rvert$		
$\lvert\Delta\phi^{jj}\rvert$ [rad.]	δ^{QED} (e-channel)	$\mathcal{A}$ (e-channel)	δ^{QED} (μ-channel)	$\mathcal{A}$ (μ-channel)
$0 - \pi/8$	1.020 ± 0.006	1.138 ± 0.007	1.018 ± 0.004	1.034 ± 0.002
$\pi/8 - \pi/4$	1.020 ± 0.004	1.146 ± 0.007	1.022 ± 0.007	1.038 ± 0.004
$\pi/4 - 3\pi/8$	1.017 ± 0.002	1.144 ± 0.005	1.021 ± 0.002	1.037 ± 0.004
$3\pi/8 - \pi/2$	1.021 ± 0.002	1.137 ± 0.005	1.021 ± 0.002	1.040 ± 0.002
$\pi/2 - 5\pi/8$	1.021 ± 0.004	1.149 ± 0.014	1.021 ± 0.001	1.043 ± 0.003
$5\pi/8 - 3\pi/4$	1.022 ± 0.002	1.140 ± 0.003	1.026 ± 0.002	1.048 ± 0.009
$3\pi/4 - 7\pi/8$	1.022 ± 0.002	1.148 ± 0.004	1.024 ± 0.002	1.047 ± 0.003
$7\pi/8 - \pi$	1.022 ± 0.001	1.143 ± 0.002	1.021 ± 0.002	1.050 ± 0.003
		$d\sigma/d\lvert\Delta R^{jj}\rvert$		
ΔR^{jj}	δ^{QED} (e-channel)	$\mathcal{A}$ (e-channel)	δ^{QED} (μ-channel)	$\mathcal{A}$ (μ-channel)
0.4–0.8	1.018 ± 0.006	1.142 ± 0.006	1.017 ± 0.005	1.041 ± 0.011
0.8–1.2	1.016 ± 0.006	1.145 ± 0.012	1.021 ± 0.006	1.029 ± 0.007
1.2–1.6	1.021 ± 0.003	1.147 ± 0.016	1.019 ± 0.003	1.038 ± 0.004
1.6–2.0	1.022 ± 0.005	1.142 ± 0.004	1.025 ± 0.003	1.037 ± 0.004
2.0–2.4	1.022 ± 0.002	1.147 ± 0.004	1.024 ± 0.003	1.043 ± 0.005
2.4–2.8	1.023 ± 0.001	1.144 ± 0.003	1.025 ± 0.001	1.044 ± 0.002
2.8–3.2	1.022 ± 0.003	1.139 ± 0.005	1.023 ± 0.001	1.046 ± 0.003
3.2–3.6	1.019 ± 0.001	1.144 ± 0.011	1.020 ± 0.003	1.048 ± 0.002
3.6–4.0	1.020 ± 0.004	1.140 ± 0.013	1.020 ± 0.003	1.051 ± 0.006
4.0–4.4	1.020 ± 0.003	1.147 ± 0.009	1.021 ± 0.003	1.056 ± 0.007

TABLE XVIII. Results of χ^2 tests to the electron and muon data with respect to the NLO pQCD predictions. The results are tabulated for the original cross section measurements and after extrapolating to the Born level in a common region for the lepton kinematics.

χ^2 results (w.r.t. NLO pQCD predictions)			
e-channel			
Measurement	Degrees of freedom	χ^2/d.o.f	χ^2/d.o.f
	(d.o.f)	(Fiducial)	(Extrapolated)
$\sigma_{N_{\text{jet}}}$	4	1.43	1.43
$\sigma_{N_{\text{jet}}}/\sigma_{N_{\text{jet}}-1}$	4	1.54	1.59
$d\sigma/dp_T$ (inclusive)	7	0.17	0.18
$d\sigma/d\lvert y\rvert$ (inclusive)	8	0.79	0.74
$d\sigma/dp_T$ (leading jet)	7	0.28	0.29
$d\sigma/d\lvert y\rvert$ (leading jet)	8	1.19	1.16
$d\sigma/dp_T$ (second-leading jet)	5	0.05	0.06
$d\sigma/d\lvert y\rvert$ (second-leading jet)	7	0.79	0.85
$d\sigma/dm^{jj}$	8	0.98	0.98
$d\sigma/d\lvert\Delta y^{jj}\rvert$	7	0.32	0.34
$d\sigma/d\lvert\Delta\phi^{jj}\rvert$	8	0.43	0.44
$d\sigma/d\Delta R^{jj}$	10	0.14	0.16
μ-channel			
Measurement	Degrees of freedom (d.o.f)	χ^2/d.o.f (fiducial)	χ^2/d.o.f (extrapolated)
$\sigma_{N_{\text{jet}}}$	4	0.09	0.11
$\sigma_{N_{\text{jet}}}/\sigma_{N_{\text{jet}}-1}$	4	0.07	0.08
$d\sigma/dp_T$ (inclusive)	7	1.78	1.77
$d\sigma/d\lvert y\rvert$ (inclusive)	8	0.43	0.41
$d\sigma/dp_T$ (leading jet)	7	1.17	1.13
$d\sigma/d\lvert y\rvert$ (leading jet)	8	0.46	0.46
$d\sigma/dp_T$ (second-leading jet)	5	1.20	1.23
$d\sigma/d\lvert y\rvert$ (second-leading jet)	7	0.32	0.32
$d\sigma/dm^{jj}$	8	0.61	0.61
$d\sigma/d\lvert\Delta y^{jj}\rvert$	7	0.96	0.96
$d\sigma/d\lvert\Delta\phi^{jj}\rvert$	8	0.54	0.55
$d\sigma/d\Delta R^{jj}$	10	1.54	1.55

TABLE XIX. Results of χ^2 tests to the electron and muon data with respect to the ALPGEN predictions. The results are tabulated for the original cross section measurements and after extrapolating to the Born level in a common region for the lepton kinematics.

χ^2 results (w.r.t. ALPGEN predictions)			
e-channel			
Measurement	Degrees of freedom	χ^2/d.o.f	χ^2/d.o.f
	(d.o.f)	(Fiducial)	(Extrapolated)
$\sigma_{N_{\text{jet}}}$	4	0.99	0.99
$\sigma_{N_{\text{jet}}}/\sigma_{N_{\text{jet}}-1}$	4	1.55	1.55
$d\sigma/dp_T$ (inclusive)	7	0.13	0.13
$d\sigma/d\lvert y\rvert$ (inclusive)	8	0.97	0.97
$d\sigma/dp_T$ (leading jet)	7	0.17	0.17
$d\sigma/d\lvert y\rvert$ (leading jet)	8	1.33	1.33
$d\sigma/dp_T$ (second-leading jet)	5	0.07	0.07
$d\sigma/d\lvert y\rvert$ (second-leading jet)	7	0.63	0.63
$d\sigma/dm^{jj}$	8	0.87	0.87
$d\sigma/d\lvert\Delta y^{jj}\rvert$	7	0.42	0.42
$d\sigma/d\lvert\Delta\phi^{jj}\rvert$	8	0.44	0.44
$d\sigma/d\Delta R^{jj}$	10	0.25	0.25
μ-channel			
Measurement	Degrees of freedom (d.o.f)	χ^2/d.o.f (Fiducial)	χ^2/d.o.f (Extrapolated)
$\sigma_{N_{\text{jet}}}$	4	0.08	0.08
$\sigma_{N_{\text{jet}}}/\sigma_{N_{\text{jet}}-1}$	4	0.11	0.11
$d\sigma/dp_T$ (inclusive)	7	1.87	1.87
$d\sigma/d\lvert y\rvert$ (inclusive)	8	0.71	0.71
$d\sigma/dp_T$ (leading jet)	7	1.29	1.29
$d\sigma/d\lvert y\rvert$ (leading jet)	8	0.60	0.60
$d\sigma/dp_T$ (second-leading jet)	5	0.89	0.89
$d\sigma/d\lvert y\rvert$ (second-leading jet)	7	0.50	0.50
$d\sigma/dm^{jj}$	8	0.58	0.58
$d\sigma/d\lvert\Delta y^{jj}\rvert$	7	0.90	0.90
$d\sigma/d\lvert\Delta\phi^{jj}\rvert$	8	0.43	0.43
$d\sigma/d\Delta R^{jj}$	10	1.59	1.59

where d_j is the measured data point j, $t_j(\bar{s})$ is the corresponding prediction, and $\bar{s}$ denotes the vector of standard deviations, s_i, for the different independent sources of systematic uncertainty in data and theory, which are considered fully correlated across bins. For each measurement considered, the sums above run over the total number of data points and seven independent sources of systematic uncertainty, and the correlations

TABLE XX. Results of χ^2 tests to the electron and muon data with respect to the SHERPA predictions. The results are tabulated for the original cross section measurements and after extrapolating to the Born level in a common region for the lepton kinematics.

χ^2 results (w.r.t. SHERPA predictions)			
e-channel Measurement	Degrees of freedom	χ^2/d.o.f	χ^2/d.o.f
	(d.o.f)	(Fiducial)	(Extrapolated)
$\sigma_{N_{\text{jet}}}$	4	0.65	0.68
$\sigma_{N_{\text{jet}}}/\sigma_{N_{\text{jet}}-1}$	4	1.51	1.50
$d\sigma/dp_T$ (inclusive)	7	0.29	0.29
$d\sigma/d\lvert y\rvert$ (inclusive)	8	1.19	1.13
$d\sigma/dp_T$ (leading jet)	7	0.30	0.30
$d\sigma/d\lvert y\rvert$ (leading jet)	8	1.85	1.82
$d\sigma/dp_T$ (second-leading jet)	5	0.27	0.29
$d\sigma/d\lvert y\rvert$ (second-leading jet)	7	1.24	1.22
$d\sigma/dm^{jj}$	8	1.25	1.22
$d\sigma/d\lvert\Delta y^{jj}\rvert$	7	0.80	0.80
$d\sigma/d\lvert\Delta\phi^{jj}\rvert$	8	0.59	0.60
$d\sigma/d\Delta R^{jj}$	10	0.36	0.36
μ-channel Measurement	Degrees of freedom	χ^2/d.o.f	χ^2/d.o.f
	(d.o.f)	(Fiducial)	(Extrapolated)
$\sigma_{N_{\text{jet}}}$	4	0.37	0.38
$\sigma_{N_{\text{jet}}}/\sigma_{N_{\text{jet}}-1}$	4	0.31	0.32
$d\sigma/dp_T$ (inclusive)	7	2.10	2.08
$d\sigma/d\lvert y\rvert$ (inclusive)	8	0.73	0.74
$d\sigma/dp_T$ (leading jet)	7	1.24	1.21
$d\sigma/d\lvert y\rvert$ (leading jet)	8	1.02	1.06
$d\sigma/dp_T$ (second-leading jet)	5	1.40	1.40
$d\sigma/d\lvert y\rvert$ (second-leading jet)	7	0.62	0.62
$d\sigma/dm^{jj}$	8	1.01	1.02
$d\sigma/d\lvert\Delta y^{jj}\rvert$	7	1.86	1.85
$d\sigma/d\lvert\Delta\phi^{jj}\rvert$	8	1.02	1.03
$d\sigma/d\Delta R^{jj}$	10	2.70	2.70

among systematic uncertainties are taken into account in $t_j(\bar{s})$. The average of the upper and lower uncertainties in data and theory are employed, and the χ^2 is minimized with respect to $\bar{s}$. The results of the χ^2 tests are tabulated in Tables XVIII, XIX, and XX.

[1] V. M. Abazov *et al.* (The D0 Collaboration), Phys. Lett. B **678**, 45 (2009); V. M. Abazov *et al.* (The D0 Collaboration), Phys. Lett. B **682**, 370 (2010); T. Aaltonen *et al.* (The CDF Collaboration), Phys. Rev. Lett. **100**, 102001 (2008).

[2] The ATLAS Collaboration, Phys. Lett. B **708**, 221 (2012); The CMS Collaboration, arXiv:1110.3226 [J. High Energy Phys. (to be published)].

[3] The ATLAS reference system is a Cartesian right-handed coordinate system, with the nominal collision point at the

origin. The anticlockwise beam direction defines the positive z-axis, while the positive x-axis is defined as pointing from the collision point to the center of the LHC ring and the positive y-axis points upwards. The azimuthal angle ϕ is measured around the beam axis, and the polar angle θ is measured with respect to the z-axis. The pseudorapidity is defined as $\eta = -\ln(\tan(\theta/2))$. The rapidity is defined as $y = 0.5 \times \ln[(E + p_z)/(E - p_z)]$, where E denotes the energy and p_z is the component of the momentum along the beam direction.

[4] J. Campbell and R. K. Ellis, Phys. Rev. D **65**, 113007 (2002).
[5] C. F. Berger *et al.*, Phys. Rev. D **78**, 036003 (2008); C. F. Berger *et al.*, Phys. Rev. D **82**, 074002 (2010); H. Ita *et al.*, arXiv:1108.2229.
[6] The ATLAS Collaboration, JINST **3**, S08003 (2008).
[7] The ATLAS Collaboration, arXiv:1110.3174 [Eur. Phys. J. C (to be published)].
[8] The ATLAS Collaboration, J. High Energy Phys. 12 (2010) 060.
[9] The ATLAS Collaboration, Report No. ATLAS-CONF-2011-063, http://cdsweb.cern.ch/record/1345743.
[10] M. L. Mangano *et al.*, J. High Energy Phys. 07 (2003) 001.
[11] G. Corcella *et al.*, J. High Energy Phys. 01 (2001) 010.
[12] J. Butterworth, J. Forshaw, and M. Seymour, Z. Phys. C **72**, 637 (1996).
[13] T. Gleisberg, S. Hoeche, F. Krauss, M. Schoenherr, S. Schumann, F. Siegert, and J. Winter, J. High Energy Phys. 02 (2009) 007.
[14] T. Sjöstrand and M. van Zijl, Phys. Rev. D **36**, 2019 (1987).
[15] J. Pumplin *et al.*, J. High Energy Phys. 07 (2002) 012.
[16] P. M. Nadolsky *et al.*, Phys. Rev. D **78**, 013004 (2008).
[17] K. Melnikov and F. Petriello, Phys. Rev. D **74**, 114017 (2006).R. Gavin, Y. Li, F. Petriello *et al.*, Comput. Phys. Commun. **182**, 2388 (2011).
[18] T. Sjöstrand *et al.*, J. High Energy Phys. 05 (2006) 026.
[19] A. D. Martin, W. J. Stirling, R. S. Thorne, and G. Watt, Eur. Phys. J. C **63**, 189 (2009); A. Sherstnev and R. S. Thorne, Eur. Phys. J. C **55**, 553 (2008).
[20] The ATLAS Collaboration, Report No. ATL-PHYS-PUB-2010-014, 2010, http://cdsweb.cern.ch/record/1303025.
[21] The ATLAS Collaboration, Report No. ATLAS-CONF-2010-031, http://cdsweb.cern.ch/record/1277665.
[22] N. Davidson *et al.*, Report No. IFJPAN-IV-2009-10.
[23] S. Frixione, B. R. Webber, Report No. Cavendish-HEP-08/14.
[24] The ATLAS Collaboration, Eur. Phys. J. C **70**, 823 (2010).
[25] S. Agostinelli *et al.*, Nucl. Instrum. Methods Phys. Res., Sect. A **506**, 250 (2003).
[26] M. Cacciari, G. P. Salam, and G. Soyez, J. High Energy Phys. 04 (2008) 063; M. Cacciari and G. P. Salam, Phys. Lett. B **641**, 57 (2006); M. Cacciari, G. P. Salam, and G. Soyez, http://fastjet.fr/.
[27] The hadronic final state in the MC generators is defined using all particles with lifetime above 10^{-11} s, after excluding the Z/γ^* decay products.
[28] The ATLAS Collaboration, Report No. ATLAS-CONF-2011-030, http://cdsweb.cern.ch/record/1337780.
[29] The ATLAS Collaboration, Report No. ATLAS-CONF-2011-007, http://cdsweb.cern.ch/record/1330713.The ATLAS Collaboration, Report No. ATLAS-CONF-2010-056, http://cdsweb.cern.ch/record/1281329.
[30] The ATLAS Collaboration, arXiv:1109.5141 [Phys. Rev. D (to be published)].
[31] G. D'Agostini, CERN Report No. 99-03, 1999.
[32] The ATLAS Collaboration, Eur. Phys. J. C **71**, 1630 (2011).The ATLAS Collaboration, Report No. ATLAS-CONF-2011-011, http://cdsweb.cern.ch/record/1334563.
[33] J. Pumplin *et al.*, Phys. Rev. D **65**, 014013 (2001).
[34] A complete set of tables with the full results are available at the DurhamHepDatarepository (http://hepdata.cedar.ac.uk).
[35] L. Lyons, D. Gibaut, and P. Clifford, Nucl. Instrum. Methods Phys. Res., Sect. A **270**, 110 (1988).

G. Aad,[47] B. Abbott,[110] J. Abdallah,[11] A. A. Abdelalim,[48] A. Abdesselam,[117] O. Abdinov,[10] B. Abi,[111] M. Abolins,[87] H. Abramowicz,[152] H. Abreu,[114] E. Acerbi,[88a,88b] B. S. Acharya,[163a,163b] D. L. Adams,[24] T. N. Addy,[55] J. Adelman,[174] M. Aderholz,[98] S. Adomeit,[97] P. Adragna,[74] T. Adye,[128] S. Aefsky,[22] J. A. Aguilar-Saavedra,[123b,b] M. Aharrouche,[80] S. P. Ahlen,[21] F. Ahles,[47] A. Ahmad,[147] M. Ahsan,[40] G. Aielli,[132a,132b] T. Akdogan,[18a] T. P. A. Åkesson,[78] G. Akimoto,[154] A. V. Akimov,[93] A. Akiyama,[66] M. S. Alam,[1] M. A. Alam,[75] J. Albert,[168] S. Albrand,[54] M. Aleksa,[29] I. N. Aleksandrov,[64] F. Alessandria,[88a] C. Alexa,[25a] G. Alexander,[152] G. Alexandre,[48] T. Alexopoulos,[9] M. Alhroob,[20] M. Aliev,[15] G. Alimonti,[88a] J. Alison,[119] M. Aliyev,[10] P. P. Allport,[72] S. E. Allwood-Spiers,[52] J. Almond,[81] A. Aloisio,[101a,101b] R. Alon,[170] A. Alonso,[78] M. G. Alviggi,[101a,101b] K. Amako,[65] P. Amaral,[29] C. Amelung,[22] V. V. Ammosov,[127] A. Amorim,[123a,c] G. Amorós,[166] N. Amram,[152] C. Anastopoulos,[29] L. S. Ancu,[16] N. Andari,[114] T. Andeen,[34] C. F. Anders,[20] G. Anders,[57a] K. J. Anderson,[30] A. Andreazza,[88a,88b] V. Andrei,[57a] M-L. Andrieux,[54] X. S. Anduaga,[69] A. Angerami,[34] F. Anghinolfi,[29] N. Anjos,[123a] A. Annovi,[46] A. Antonaki,[8] M. Antonelli,[46] A. Antonov,[95] J. Antos,[143b] F. Anulli,[131a] S. Aoun,[82] L. Aperio Bella,[4] R. Apolle,[117,d] G. Arabidze,[87] I. Aracena,[142] Y. Arai,[65] A. T. H. Arce,[44] J. P. Archambault,[28] S. Arfaoui,[29,e] J-F. Arguin,[14] E. Arik,[18a,a] M. Arik,[18a] A. J. Armbruster,[86] O. Arnaez,[80] C. Arnault,[114] A. Artamonov,[94] G. Artoni,[131a,131b] D. Arutinov,[20] S. Asai,[154] R. Asfandiyarov,[171] S. Ask,[27] B. Åsman,[145a,145b] L. Asquith,[5] K. Assamagan,[24] A. Astbury,[168] A. Astvatsatourov,[51] G. Atoian,[174] B. Aubert,[4] E. Auge,[114] K. Augsten,[126] M. Aurousseau,[144a] N. Austin,[72] G. Avolio,[162] R. Avramidou,[9] D. Axen,[167] C. Ay,[53] G. Azuelos,[92,f] Y. Azuma,[154]

M. A. Baak,[29] G. Baccaglioni,[88a] C. Bacci,[133a,133b] A. M. Bach,[14] H. Bachacou,[135] K. Bachas,[29] G. Bachy,[29] M. Backes,[48] M. Backhaus,[20] E. Badescu,[25a] P. Bagnaia,[131a,131b] S. Bahinipati,[2] Y. Bai,[32a] D. C. Bailey,[157] T. Bain,[157] J. T. Baines,[128] O. K. Baker,[174] M. D. Baker,[24] S. Baker,[76] E. Banas,[38] P. Banerjee,[92] Sw. Banerjee,[171] D. Banfi,[29] A. Bangert,[136] V. Bansal,[168] H. S. Bansil,[17] L. Barak,[170] S. P. Baranov,[93] A. Barashkou,[64] A. Barbaro Galtieri,[14] T. Barber,[27] E. L. Barberio,[85] D. Barberis,[49a,49b] M. Barbero,[20] D. Y. Bardin,[64] T. Barillari,[98] M. Barisonzi,[173] T. Barklow,[142] N. Barlow,[27] B. M. Barnett,[128] R. M. Barnett,[14] A. Baroncelli,[133a] G. Barone,[48] A. J. Barr,[117] F. Barreiro,[79] J. Barreiro Guimarães da Costa,[56] P. Barrillon,[114] R. Bartoldus,[142] A. E. Barton,[70] D. Bartsch,[20] V. Bartsch,[148] R. L. Bates,[52] L. Batkova,[143a] J. R. Batley,[27] A. Battaglia,[16] M. Battistin,[29] G. Battistoni,[88a] F. Bauer,[135] H. S. Bawa,[142,g] B. Beare,[157] T. Beau,[77] P. H. Beauchemin,[117] R. Beccherle,[49a] P. Bechtle,[41] H. P. Beck,[16] M. Beckingham,[47] K. H. Becks,[173] A. J. Beddall,[18c] A. Beddall,[18c] S. Bedikian,[174] V. A. Bednyakov,[64] C. P. Bee,[82] M. Begel,[24] S. Behar Harpaz,[151] P. K. Behera,[62] M. Beimforde,[98] C. Belanger-Champagne,[84] P. J. Bell,[48] W. H. Bell,[48] G. Bella,[152] L. Bellagamba,[19a] F. Bellina,[29] M. Bellomo,[29] A. Belloni,[56] O. Beloborodova,[106] K. Belotskiy,[95] O. Beltramello,[29] S. Ben Ami,[151] O. Benary,[152] D. Benchekroun,[134a] C. Benchouk,[82] M. Bendel,[80] N. Benekos,[164] Y. Benhammou,[152] D. P. Benjamin,[44] M. Benoit,[114] J. R. Bensinger,[22] K. Benslama,[129] S. Bentvelsen,[104] D. Berge,[29] E. Bergeaas Kuutmann,[41] N. Berger,[4] F. Berghaus,[168] E. Berglund,[48] J. Beringer,[14] K. Bernardet,[82] P. Bernat,[76] R. Bernhard,[47] C. Bernius,[24] T. Berry,[75] A. Bertin,[19a,19b] F. Bertinelli,[29] F. Bertolucci,[121a,121b] M. I. Besana,[88a,88b] N. Besson,[135] S. Bethke,[98] W. Bhimji,[45] R. M. Bianchi,[29] M. Bianco,[71a,71b] O. Biebel,[97] S. P. Bieniek,[76] K. Bierwagen,[53] J. Biesiada,[14] M. Biglietti,[133a,133b] H. Bilokon,[46] M. Bindi,[19a,19b] S. Binet,[114] A. Bingul,[18c] C. Bini,[131a,131b] C. Biscarat,[176] U. Bitenc,[47] K. M. Black,[21] R. E. Blair,[5] J.-B. Blanchard,[114] G. Blanchot,[29] T. Blazek,[143a] C. Blocker,[22] J. Blocki,[38] A. Blondel,[48] W. Blum,[80] U. Blumenschein,[53] G. J. Bobbink,[104] V. B. Bobrovnikov,[106] S. S. Bocchetta,[78] A. Bocci,[44] C. R. Boddy,[117] M. Boehler,[41] J. Boek,[173] N. Boelaert,[35] S. Böser,[76] J. A. Bogaerts,[29] A. Bogdanchikov,[106] A. Bogouch,[89,a] C. Bohm,[145a] V. Boisvert,[75] T. Bold,[162,h] V. Boldea,[25a] N. M. Bolnet,[135] M. Bona,[74] V. G. Bondarenko,[95] M. Bondioli,[162] M. Boonekamp,[135] G. Boorman,[75] C. N. Booth,[138] S. Bordoni,[77] C. Borer,[16] A. Borisov,[127] G. Borissov,[70] I. Borjanovic,[12a] S. Borroni,[86] K. Bos,[104] D. Boscherini,[19a] M. Bosman,[11] H. Boterenbrood,[104] D. Botterill,[128] J. Bouchami,[92] J. Boudreau,[122] E. V. Bouhova-Thacker,[70] C. Bourdarios,[114] N. Bousson,[82] A. Boveia,[30] J. Boyd,[29] I. R. Boyko,[64] N. I. Bozhko,[127] I. Bozovic-Jelisavcic,[12b] J. Bracinik,[17] A. Braem,[29] P. Branchini,[133a] G. W. Brandenburg,[56] A. Brandt,[7] G. Brandt,[15] O. Brandt,[53] U. Bratzler,[155] B. Brau,[83] J. E. Brau,[113] H. M. Braun,[173] B. Brelier,[157] J. Bremer,[29] R. Brenner,[165] S. Bressler,[151] D. Breton,[114] D. Britton,[52] F. M. Brochu,[27] I. Brock,[20] R. Brock,[87] T. J. Brodbeck,[70] E. Brodet,[152] F. Broggi,[88a] C. Bromberg,[87] G. Brooijmans,[34] W. K. Brooks,[31b] G. Brown,[81] H. Brown,[7] P. A. Bruckman de Renstrom,[38] D. Bruncko,[143b] R. Bruneliere,[47] S. Brunet,[60] A. Bruni,[19a] G. Bruni,[19a] M. Bruschi,[19a] T. Buanes,[13] F. Bucci,[48] J. Buchanan,[117] N. J. Buchanan,[2] P. Buchholz,[140] R. M. Buckingham,[117] A. G. Buckley,[45] S. I. Buda,[25a] I. A. Budagov,[64] B. Budick,[107] V. Büscher,[80] L. Bugge,[116] D. Buira-Clark,[117] O. Bulekov,[95] M. Bunse,[42] T. Buran,[116] H. Burckhart,[29] S. Burdin,[72] T. Burgess,[13] S. Burke,[128] E. Busato,[33] P. Bussey,[52] C. P. Buszello,[165] F. Butin,[29] B. Butler,[142] J. M. Butler,[21] C. M. Buttar,[52] J. M. Butterworth,[76] W. Buttinger,[27] T. Byatt,[76] S. Cabrera Urbán,[166] D. Caforio,[19a,19b] O. Cakir,[3a] P. Calafiura,[14] G. Calderini,[77] P. Calfayan,[97] R. Calkins,[105] L. P. Caloba,[23a] R. Caloi,[131a,131b] D. Calvet,[33] S. Calvet,[33] R. Camacho Toro,[33] P. Camarri,[132a,132b] M. Cambiaghi,[118a,118b] D. Cameron,[116] S. Campana,[29] M. Campanelli,[76] V. Canale,[101a,101b] F. Canelli,[30,i] A. Canepa,[158a] J. Cantero,[79] L. Capasso,[101a,101b] M. D. M. Capeans Garrido,[29] I. Caprini,[25a] M. Caprini,[25a] D. Capriotti,[98] M. Capua,[36a,36b] R. Caputo,[147] R. Cardarelli,[132a] T. Carli,[29] G. Carlino,[101a] L. Carminati,[88a,88b] B. Caron,[158a] S. Caron,[47] G. D. Carrillo Montoya,[171] A. A. Carter,[74] J. R. Carter,[27] J. Carvalho,[123a,j] D. Casadei,[107] M. P. Casado,[11] M. Cascella,[121a,121b] C. Caso,[49a,49b,a] A. M. Castaneda Hernandez,[171] E. Castaneda-Miranda,[171] V. Castillo Gimenez,[166] N. F. Castro,[123a] G. Cataldi,[71a] F. Cataneo,[29] A. Catinaccio,[29] J. R. Catmore,[70] A. Cattai,[29] G. Cattani,[132a,132b] S. Caughron,[87] D. Cauz,[163a,163c] P. Cavalleri,[77] D. Cavalli,[88a] M. Cavalli-Sforza,[11] V. Cavasinni,[121a,121b] F. Ceradini,[133a,133b] A. S. Cerqueira,[23a] A. Cerri,[29] L. Cerrito,[74] F. Cerutti,[46] S. A. Cetin,[18b] F. Cevenini,[101a,101b] A. Chafaq,[134a] D. Chakraborty,[105] K. Chan,[2] B. Chapleau,[84] J. D. Chapman,[27] J. W. Chapman,[86] E. Chareyre,[77] D. G. Charlton,[17] V. Chavda,[81] C. A. Chavez Barajas,[29] S. Cheatham,[84] S. Chekanov,[5] S. V. Chekulaev,[158a] G. A. Chelkov,[64] M. A. Chelstowska,[103] C. Chen,[63] H. Chen,[24] S. Chen,[32c] T. Chen,[32c] X. Chen,[171] S. Cheng,[32a] A. Cheplakov,[64] V. F. Chepurnov,[64] R. Cherkaoui El Moursli,[134e] V. Chernyatin,[24] E. Cheu,[6] S. L. Cheung,[157] L. Chevalier,[135] G. Chiefari,[101a,101b] L. Chikovani,[50a] J. T. Childers,[57a] A. Chilingarov,[70] G. Chiodini,[71a] M. V. Chizhov,[64] G. Choudalakis,[30]

S. Chouridou,[136] I. A. Christidi,[76] A. Christov,[47] D. Chromek-Burckhart,[29] M. L. Chu,[150] J. Chudoba,[124] G. Ciapetti,[131a,131b] K. Ciba,[37] A. K. Ciftci,[3a] R. Ciftci,[3a] D. Cinca,[33] V. Cindro,[73] M. D. Ciobotaru,[162] C. Ciocca,[19a] A. Ciocio,[14] M. Cirilli,[86] M. Ciubancan,[25a] A. Clark,[48] P. J. Clark,[45] W. Cleland,[122] J. C. Clemens,[82] B. Clement,[54] C. Clement,[145a,145b] R. W. Clifft,[128] Y. Coadou,[82] M. Cobal,[163a,163c] A. Coccaro,[49a,49b] J. Cochran,[63] P. Coe,[117] J. G. Cogan,[142] J. Coggeshall,[164] E. Cogneras,[176] C. D. Cojocaru,[28] J. Colas,[4] A. P. Colijn,[104] C. Collard,[114] N. J. Collins,[17] C. Collins-Tooth,[52] J. Collot,[54] G. Colon,[83] P. Conde Muiño,[123a] E. Coniavitis,[117] M. C. Conidi,[11] M. Consonni,[103] V. Consorti,[47] S. Constantinescu,[25a] C. Conta,[118a,118b] F. Conventi,[101a,i] J. Cook,[29] M. Cooke,[14] B. D. Cooper,[76] A. M. Cooper-Sarkar,[117] N. J. Cooper-Smith,[75] K. Copic,[34] T. Cornelissen,[173] M. Corradi,[19a] F. Corriveau,[84,j] A. Cortes-Gonzalez,[164] G. Cortiana,[98] G. Costa,[88a] M. J. Costa,[166] D. Costanzo,[138] T. Costin,[30] D. Côté,[29] L. Courneyea,[168] G. Cowan,[75] C. Cowden,[27] B. E. Cox,[81] K. Cranmer,[107] F. Crescioli,[121a,121b] M. Cristinziani,[20] G. Crosetti,[36a,36b] R. Crupi,[71a,71b] S. Crépé-Renaudin,[54] C.-M. Cuciuc,[25a] C. Cuenca Almenar,[174] T. Cuhadar Donszelmann,[138] M. Curatolo,[46] C. J. Curtis,[17] P. Cwetanski,[60] H. Czirr,[140] Z. Czyczula,[174] S. D'Auria,[52] M. D'Onofrio,[72] A. D'Orazio,[131a,131b] P. V. M. Da Silva,[23a] C. Da Via,[81] W. Dabrowski,[37] T. Dai,[86] C. Dallapiccola,[83] M. Dam,[35] M. Dameri,[49a,49b] D. S. Damiani,[136] H. O. Danielsson,[29] D. Dannheim,[98] V. Dao,[48] G. Darbo,[49a] G. L. Darlea,[25b] C. Daum,[104] J. P. Dauvergne,[29] W. Davey,[85] T. Davidek,[125] N. Davidson,[85] R. Davidson,[70] E. Davies,[117,d] M. Davies,[92] A. R. Davison,[76] Y. Davygora,[57a] E. Dawe,[141] I. Dawson,[138] J. W. Dawson,[5,a] R. K. Daya,[39] K. De,[7] R. de Asmundis,[101a] S. De Castro,[19a,19b] P. E. De Castro Faria Salgado,[24] S. De Cecco,[77] J. de Graat,[97] N. De Groot,[103] P. de Jong,[104] C. De La Taille,[114] H. De la Torre,[79] B. De Lotto,[163a,163c] L. De Mora,[70] L. De Nooij,[104] D. De Pedis,[131a] A. De Salvo,[131a] U. De Sanctis,[163a,163c] A. De Santo,[148] J. B. De Vivie De Regie,[114] S. Dean,[76] R. Debbe,[24] D. V. Dedovich,[64] J. Degenhardt,[119] M. Dehchar,[117] C. Del Papa,[163a,163c] J. Del Peso,[79] T. Del Prete,[121a,121b] M. Deliyergiyev,[73] A. Dell'Acqua,[29] L. Dell'Asta,[88a,88b] M. Della Pietra,[101a,k] D. della Volpe,[101a,101b] M. Delmastro,[29] P. Delpierre,[82] N. Delruelle,[29] P. A. Delsart,[54] C. Deluca,[147] S. Demers,[174] M. Demichev,[64] B. Demirkoz,[11,l] J. Deng,[162] S. P. Denisov,[127] D. Derendarz,[38] J. E. Derkaoui,[134d] F. Derue,[77] P. Dervan,[72] K. Desch,[20] E. Devetak,[147] P. O. Deviveiros,[157] A. Dewhurst,[128] B. DeWilde,[147] S. Dhaliwal,[157] R. Dhullipudi,[24,m] A. Di Ciaccio,[132a,132b] L. Di Ciaccio,[4] A. Di Girolamo,[29] B. Di Girolamo,[29] S. Di Luise,[133a,133b] A. Di Mattia,[171] B. Di Micco,[29] R. Di Nardo,[132a,132b] A. Di Simone,[132a,132b] R. Di Sipio,[19a,19b] M. A. Diaz,[31a] F. Diblen,[18c] E. B. Diehl,[86] J. Dietrich,[41] T. A. Dietzsch,[57a] S. Diglio,[114] K. Dindar Yagci,[39] J. Dingfelder,[20] C. Dionisi,[131a,131b] P. Dita,[25a] S. Dita,[25a] F. Dittus,[29] F. Djama,[82] T. Djobava,[50b] M. A. B. do Vale,[23a] A. Do Valle Wemans,[123a] T. K. O. Doan,[4] M. Dobbs,[84] R. Dobinson,[29,a] D. Dobos,[29] E. Dobson,[29] M. Dobson,[162] J. Dodd,[34] C. Doglioni,[117] T. Doherty,[52] Y. Doi,[65,a] J. Dolejsi,[125] I. Dolenc,[73] Z. Dolezal,[125] B. A. Dolgoshein,[95,a] T. Dohmae,[154] M. Donadelli,[23d] M. Donega,[119] J. Donini,[54] J. Dopke,[29] A. Doria,[101a] A. Dos Anjos,[171] M. Dosil,[11] A. Dotti,[121a,121b] M. T. Dova,[69] J. D. Dowell,[17] A. D. Doxiadis,[104] A. T. Doyle,[52] Z. Drasal,[125] J. Drees,[173] N. Dressnandt,[119] H. Drevermann,[29] C. Driouichi,[35] M. Dris,[9] J. Dubbert,[98] T. Dubbs,[136] S. Dube,[14] E. Duchovni,[170] G. Duckeck,[97] A. Dudarev,[29] F. Dudziak,[63] M. Dührssen,[29] I. P. Duerdoth,[81] L. Duflot,[114] M-A. Dufour,[84] M. Dunford,[29] H. Duran Yildiz,[3b] R. Duxfield,[138] M. Dwuznik,[37] F. Dydak,[29] M. Düren,[51] W. L. Ebenstein,[44] J. Ebke,[97] S. Eckert,[47] S. Eckweiler,[80] K. Edmonds,[80] C. A. Edwards,[75] N. C. Edwards,[52] W. Ehrenfeld,[41] T. Ehrich,[98] T. Eifert,[29] G. Eigen,[13] K. Einsweiler,[14] E. Eisenhandler,[74] T. Ekelof,[165] M. El Kacimi,[134c] M. Ellert,[165] S. Elles,[4] F. Ellinghaus,[80] K. Ellis,[74] N. Ellis,[29] J. Elmsheuser,[97] M. Elsing,[29] D. Emeliyanov,[128] R. Engelmann,[147] A. Engl,[97] B. Epp,[61] A. Eppig,[86] J. Erdmann,[53] A. Ereditato,[16] D. Eriksson,[145a] J. Ernst,[1] M. Ernst,[24] J. Ernwein,[135] D. Errede,[164] S. Errede,[164] E. Ertel,[80] M. Escalier,[114] C. Escobar,[122] X. Espinal Curull,[11] B. Esposito,[46] F. Etienne,[82] A. I. Etienvre,[135] E. Etzion,[152] D. Evangelakou,[53] H. Evans,[60] L. Fabbri,[19a,19b] C. Fabre,[29] R. M. Fakhrutdinov,[127] S. Falciano,[131a] Y. Fang,[171] M. Fanti,[88a,88b] A. Farbin,[7] A. Farilla,[133a] J. Farley,[147] T. Farooque,[157] S. M. Farrington,[117] P. Farthouat,[29] P. Fassnacht,[29] D. Fassouliotis,[8] B. Fatholahzadeh,[157] A. Favareto,[88a,88b] L. Fayard,[114] S. Fazio,[36a,36b] R. Febbraro,[33] P. Federic,[143a] O. L. Fedin,[120] W. Fedorko,[87] M. Fehling-Kaschek,[47] L. Feligioni,[82] D. Fellmann,[5] C. U. Felzmann,[85] C. Feng,[32d] E. J. Feng,[30] A. B. Fenyuk,[127] J. Ferencei,[143b] J. Ferland,[92] W. Fernando,[108] S. Ferrag,[52] J. Ferrando,[52] V. Ferrara,[41] A. Ferrari,[165] P. Ferrari,[104] R. Ferrari,[118a] A. Ferrer,[166] M. L. Ferrer,[46] D. Ferrere,[48] C. Ferretti,[86] A. Ferretto Parodi,[49a,49b] M. Fiascaris,[30] F. Fiedler,[80] A. Filipčič,[73] A. Filippas,[9] F. Filthaut,[103] M. Fincke-Keeler,[168] M. C. N. Fiolhais,[123a,j] L. Fiorini,[166] A. Firan,[39] G. Fischer,[41] P. Fischer,[20] M. J. Fisher,[108] S. M. Fisher,[128] M. Flechl,[47] I. Fleck,[140] J. Fleckner,[80] P. Fleischmann,[172] S. Fleischmann,[173] T. Flick,[173] L. R. Flores Castillo,[171] M. J. Flowerdew,[98] M. Fokitis,[9] T. Fonseca Martin,[16] D. A. Forbush,[137] A. Formica,[135] A. Forti,[81] D. Fortin,[158a] J. M. Foster,[81] D. Fournier,[114] A. Foussat,[29] A. J. Fowler,[44]

K. Fowler,[136] H. Fox,[70] P. Francavilla,[121a,121b] S. Franchino,[118a,118b] D. Francis,[29] T. Frank,[170] M. Franklin,[56] S. Franz,[29] M. Fraternali,[118a,118b] S. Fratina,[119] S. T. French,[27] F. Friedrich,[43] R. Froeschl,[29] D. Froidevaux,[29] J. A. Frost,[27] C. Fukunaga,[155] E. Fullana Torregrosa,[29] J. Fuster,[166] C. Gabaldon,[29] O. Gabizon,[170] T. Gadfort,[24] S. Gadomski,[48] G. Gagliardi,[49a,49b] P. Gagnon,[60] C. Galea,[97] E. J. Gallas,[117] V. Gallo,[16] B. J. Gallop,[128] P. Gallus,[124] E. Galyaev,[40] K. K. Gan,[108] Y. S. Gao,[142,g] V. A. Gapienko,[127] A. Gaponenko,[14] F. Garberson,[174] M. Garcia-Sciveres,[14] C. García,[166] J. E. García Navarro,[48] R. W. Gardner,[30] N. Garelli,[29] H. Garitaonandia,[104] V. Garonne,[29] J. Garvey,[17] C. Gatti,[46] G. Gaudio,[118a] O. Gaumer,[48] B. Gaur,[140] L. Gauthier,[135] I. L. Gavrilenko,[93] C. Gay,[167] G. Gaycken,[20] J-C. Gayde,[29] E. N. Gazis,[9] P. Ge,[32d] C. N. P. Gee,[128] D. A. A. Geerts,[104] Ch. Geich-Gimbel,[20] K. Gellerstedt,[145a,145b] C. Gemme,[49a] A. Gemmell,[52] M. H. Genest,[97] S. Gentile,[131a,131b] M. George,[53] S. George,[75] P. Gerlach,[173] A. Gershon,[152] C. Geweniger,[57a] H. Ghazlane,[134b] P. Ghez,[4] N. Ghodbane,[33] B. Giacobbe,[19a] S. Giagu,[131a,131b] V. Giakoumopoulou,[8] V. Giangiobbe,[121a,121b] F. Gianotti,[29] B. Gibbard,[24] A. Gibson,[157] S. M. Gibson,[29] L. M. Gilbert,[117] V. Gilewsky,[90] D. Gillberg,[28] A. R. Gillman,[128] D. M. Gingrich,[2,f] J. Ginzburg,[152] N. Giokaris,[8] M. P. Giordani,[163c] R. Giordano,[101a,101b] F. M. Giorgi,[15] P. Giovannini,[98] P. F. Giraud,[135] D. Giugni,[88a] M. Giunta,[92] P. Giusti,[19a] B. K. Gjelsten,[116] L. K. Gladilin,[96] C. Glasman,[79] J. Glatzer,[47] A. Glazov,[41] K. W. Glitza,[173] G. L. Glonti,[64] J. Godfrey,[141] J. Godlewski,[29] M. Goebel,[41] T. Göpfert,[43] C. Goeringer,[80] C. Gössling,[42] T. Göttfert,[98] S. Goldfarb,[86] T. Golling,[174] S. N. Golovnia,[127] A. Gomes,[123a,c] L. S. Gomez Fajardo,[41] R. Gonçalo,[75] J. Goncalves Pinto Firmino Da Costa,[41] L. Gonella,[20] A. Gonidec,[29] S. Gonzalez,[171] S. González de la Hoz,[166] M. L. Gonzalez Silva,[26] S. Gonzalez-Sevilla,[48] J. J. Goodson,[147] L. Goossens,[29] P. A. Gorbounov,[94] H. A. Gordon,[24] I. Gorelov,[102] G. Gorfine,[173] B. Gorini,[29] E. Gorini,[71a,71b] A. Gorišek,[73] E. Gornicki,[38] S. A. Gorokhov,[127] V. N. Goryachev,[127] B. Gosdzik,[41] M. Gosselink,[104] M. I. Gostkin,[64] I. Gough Eschrich,[162] M. Gouighri,[134a] D. Goujdami,[134c] M. P. Goulette,[48] A. G. Goussiou,[137] C. Goy,[4] I. Grabowska-Bold,[162,h] P. Grafström,[29] C. Grah,[173] K-J. Grahn,[41] F. Grancagnolo,[71a] S. Grancagnolo,[15] V. Grassi,[147] V. Gratchev,[120] N. Grau,[34] H. M. Gray,[29] J. A. Gray,[147] E. Graziani,[133a] O. G. Grebenyuk,[120] D. Greenfield,[128] T. Greenshaw,[72] Z. D. Greenwood,[24,m] K. Gregersen,[35] I. M. Gregor,[41] P. Grenier,[142] J. Griffiths,[137] N. Grigalashvili,[64] A. A. Grillo,[136] S. Grinstein,[11] Y. V. Grishkevich,[96] J.-F. Grivaz,[114] M. Groh,[98] E. Gross,[170] J. Grosse-Knetter,[53] J. Groth-Jensen,[170] K. Grybel,[140] V. J. Guarino,[5] D. Guest,[174] C. Guicheney,[33] A. Guida,[71a,71b] T. Guillemin,[4] S. Guindon,[53] H. Guler,[84,n] J. Gunther,[124] B. Guo,[157] J. Guo,[34] A. Gupta,[30] Y. Gusakov,[64] V. N. Gushchin,[127] A. Gutierrez,[92] P. Gutierrez,[110] N. Guttman,[152] O. Gutzwiller,[171] C. Guyot,[135] C. Gwenlan,[117] C. B. Gwilliam,[72] A. Haas,[142] S. Haas,[29] C. Haber,[14] R. Hackenburg,[24] H. K. Hadavand,[39] D. R. Hadley,[17] P. Haefner,[98] F. Hahn,[29] S. Haider,[29] Z. Hajduk,[38] H. Hakobyan,[175] J. Haller,[53] K. Hamacher,[173] P. Hamal,[112] A. Hamilton,[48] S. Hamilton,[160] H. Han,[32a] L. Han,[32b] K. Hanagaki,[115] M. Hance,[119] C. Handel,[80] P. Hanke,[57a] J. R. Hansen,[35] J. B. Hansen,[35] J. D. Hansen,[35] P. H. Hansen,[35] P. Hansson,[142] K. Hara,[159] G. A. Hare,[136] T. Harenberg,[173] S. Harkusha,[89] D. Harper,[86] R. D. Harrington,[45] O. M. Harris,[137] K. Harrison,[17] J. Hartert,[47] F. Hartjes,[104] T. Haruyama,[65] A. Harvey,[55] S. Hasegawa,[100] Y. Hasegawa,[139] S. Hassani,[135] M. Hatch,[29] D. Hauff,[98] S. Haug,[16] M. Hauschild,[29] R. Hauser,[87] M. Havranek,[20] B. M. Hawes,[117] C. M. Hawkes,[17] R. J. Hawkings,[29] D. Hawkins,[162] T. Hayakawa,[66] D. Hayden,[75] H. S. Hayward,[72] S. J. Haywood,[128] E. Hazen,[21] M. He,[32d] S. J. Head,[17] V. Hedberg,[78] L. Heelan,[7] S. Heim,[87] B. Heinemann,[14] S. Heisterkamp,[35] L. Helary,[4] S. Hellman,[145a,145b] D. Hellmich,[20] C. Helsens,[11] R. C. W. Henderson,[70] M. Henke,[57a] A. Henrichs,[53] A. M. Henriques Correia,[29] S. Henrot-Versille,[114] F. Henry-Couannier,[82] C. Hensel,[53] T. Henß,[173] C. M. Hernandez,[7] Y. Hernández Jiménez,[166] R. Herrberg,[15] A. D. Hershenhorn,[151] G. Herten,[47] R. Hertenberger,[97] L. Hervas,[29] N. P. Hessey,[104] A. Hidvegi,[145a] E. Higón-Rodriguez,[166] D. Hill,[5,a] J. C. Hill,[27] N. Hill,[5] K. H. Hiller,[41] S. Hillert,[20] S. J. Hillier,[17] I. Hinchliffe,[14] E. Hines,[119] M. Hirose,[115] F. Hirsch,[42] D. Hirschbuehl,[173] J. Hobbs,[147] N. Hod,[152] M. C. Hodgkinson,[138] P. Hodgson,[138] A. Hoecker,[29] M. R. Hoeferkamp,[102] J. Hoffman,[39] D. Hoffmann,[82] M. Hohlfeld,[80] M. Holder,[140] S. O. Holmgren,[145a] T. Holy,[126] J. L. Holzbauer,[87] Y. Homma,[66] T. M. Hong,[119] L. Hooft van Huysduynen,[107] T. Horazdovsky,[126] C. Horn,[142] S. Horner,[47] K. Horton,[117] J-Y. Hostachy,[54] S. Hou,[150] M. A. Houlden,[72] A. Hoummada,[134a] J. Howarth,[81] D. F. Howell,[117] I. Hristova,[15] J. Hrivnac,[114] I. Hruska,[124] T. Hryn'ova,[4] P. J. Hsu,[174] S.-C. Hsu,[14] G. S. Huang,[110] Z. Hubacek,[126] F. Hubaut,[82] F. Huegging,[20] T. B. Huffman,[117] E. W. Hughes,[34] G. Hughes,[70] R. E. Hughes-Jones,[81] M. Huhtinen,[29] P. Hurst,[56] M. Hurwitz,[14] U. Husemann,[41] N. Huseynov,[64,o] J. Huston,[87] J. Huth,[56] G. Iacobucci,[48] G. Iakovidis,[9] M. Ibbotson,[81] I. Ibragimov,[140] R. Ichimiya,[66] L. Iconomidou-Fayard,[114] J. Idarraga,[114] P. Iengo,[101a,101b] O. Igonkina,[104] Y. Ikegami,[65] M. Ikeno,[65] Y. Ilchenko,[39] D. Iliadis,[153] D. Imbault,[77] M. Imori,[154] T. Ince,[20] J. Inigo-Golfin,[29] P. Ioannou,[8] M. Iodice,[133a] A. Irles Quiles,[166]

A. Ishikawa,[66] M. Ishino,[67] R. Ishmukhametov,[39] C. Issever,[117] S. Istin,[18a] A. V. Ivashin,[127] W. Iwanski,[38] H. Iwasaki,[65] J. M. Izen,[40] V. Izzo,[101a] B. Jackson,[119] J. N. Jackson,[72] P. Jackson,[142] M. R. Jaekel,[29] V. Jain,[60] K. Jakobs,[47] S. Jakobsen,[35] J. Jakubek,[126] D. K. Jana,[110] E. Jankowski,[157] E. Jansen,[76] A. Jantsch,[98] M. Janus,[20] G. Jarlskog,[78] L. Jeanty,[56] K. Jelen,[37] I. Jen-La Plante,[30] P. Jenni,[29] A. Jeremie,[4] P. Jež,[35] S. Jézéquel,[4] M. K. Jha,[19a] H. Ji,[171] W. Ji,[80] J. Jia,[147] Y. Jiang,[32b] M. Jimenez Belenguer,[41] G. Jin,[32b] S. Jin,[32a] O. Jinnouchi,[156] M. D. Joergensen,[35] D. Joffe,[39] L. G. Johansen,[13] M. Johansen,[145a,145b] K. E. Johansson,[145a] P. Johansson,[138] S. Johnert,[41] K. A. Johns,[6] K. Jon-And,[145a,145b] G. Jones,[81] R. W. L. Jones,[70] T. W. Jones,[76] T. J. Jones,[72] O. Jonsson,[29] C. Joram,[29] P. M. Jorge,[123a,c] J. Joseph,[14] T. Jovin,[12b] X. Ju,[129] C. A. Jung,[42] V. Juranek,[124] P. Jussel,[61] A. Juste Rozas,[11] V. V. Kabachenko,[127] S. Kabana,[16] M. Kaci,[166] A. Kaczmarska,[38] P. Kadlecik,[35] M. Kado,[114] H. Kagan,[108] M. Kagan,[56] S. Kaiser,[98] E. Kajomovitz,[151] S. Kalinin,[173] L. V. Kalinovskaya,[64] S. Kama,[39] N. Kanaya,[154] M. Kaneda,[29] T. Kanno,[156] V. A. Kantserov,[95] J. Kanzaki,[65] B. Kaplan,[174] A. Kapliy,[30] J. Kaplon,[29] D. Kar,[43] M. Karagoz,[117] M. Karnevskiy,[41] K. Karr,[5] V. Kartvelishvili,[70] A. N. Karyukhin,[127] L. Kashif,[171] A. Kasmi,[39] R. D. Kass,[108] A. Kastanas,[13] M. Kataoka,[4] Y. Kataoka,[154] E. Katsoufis,[9] J. Katzy,[41] V. Kaushik,[6] K. Kawagoe,[66] T. Kawamoto,[154] G. Kawamura,[80] M. S. Kayl,[104] V. A. Kazanin,[106] M. Y. Kazarinov,[64] J. R. Keates,[81] R. Keeler,[168] R. Kehoe,[39] M. Keil,[53] G. D. Kekelidze,[64] M. Kelly,[81] J. Kennedy,[97] C. J. Kenney,[142] M. Kenyon,[52] O. Kepka,[124] N. Kerschen,[29] B. P. Kerševan,[73] S. Kersten,[173] K. Kessoku,[154] C. Ketterer,[47] J. Keung,[157] M. Khakzad,[28] F. Khalil-zada,[10] H. Khandanyan,[164] A. Khanov,[111] D. Kharchenko,[64] A. Khodinov,[95] A. G. Kholodenko,[127] A. Khomich,[57a] T. J. Khoo,[27] G. Khoriauli,[20] A. Khoroshilov,[173] N. Khovanskiy,[64] V. Khovanskiy,[94] E. Khramov,[64] J. Khubua,[50b] H. Kim,[7] M. S. Kim,[2] P. C. Kim,[142] S. H. Kim,[159] N. Kimura,[169] O. Kind,[15] B. T. King,[72] M. King,[66] R. S. B. King,[117] J. Kirk,[128] L. E. Kirsch,[22] A. E. Kiryunin,[98] T. Kishimoto,[66] D. Kisielewska,[37] T. Kittelmann,[122] A. M. Kiver,[127] E. Kladiva,[143b] J. Klaiber-Lodewigs,[42] M. Klein,[72] U. Klein,[72] K. Kleinknecht,[80] M. Klemetti,[84] A. Klier,[170] A. Klimentov,[24] R. Klingenberg,[42] E. B. Klinkby,[35] T. Klioutchnikova,[29] P. F. Klok,[103] S. Klous,[104] E.-E. Kluge,[57a] T. Kluge,[72] P. Kluit,[104] S. Kluth,[98] N. S. Knecht,[157] E. Kneringer,[61] J. Knobloch,[29] E. B. F. G. Knoops,[82] A. Knue,[53] B. R. Ko,[44] T. Kobayashi,[154] M. Kobel,[43] M. Kocian,[142] A. Kocnar,[112] P. Kodys,[125] K. Köneke,[29] A. C. König,[103] S. Koenig,[80] L. Köpke,[80] F. Koetsveld,[103] P. Koevesarki,[20] T. Koffas,[28] E. Koffeman,[104] F. Kohn,[53] Z. Kohout,[126] T. Kohriki,[65] T. Koi,[142] T. Kokott,[20] G. M. Kolachev,[106] H. Kolanoski,[15] V. Kolesnikov,[64] I. Koletsou,[88a] J. Koll,[87] D. Kollar,[29] M. Kollefrath,[47] S. D. Kolya,[81] A. A. Komar,[93] Y. Komori,[154] T. Kondo,[65] T. Kono,[41,p] A. I. Kononov,[47] R. Konoplich,[107,q] N. Konstantinidis,[76] A. Kootz,[173] S. Koperny,[37] S. V. Kopikov,[127] K. Korcyl,[38] K. Kordas,[153] V. Koreshev,[127] A. Korn,[117] A. Korol,[106] I. Korolkov,[11] E. V. Korolkova,[138] V. A. Korotkov,[127] O. Kortner,[98] S. Kortner,[98] V. V. Kostyukhin,[20] M. J. Kotamäki,[29] S. Kotov,[98] V. M. Kotov,[64] A. Kotwal,[44] C. Kourkoumelis,[8] V. Kouskoura,[153] A. Koutsman,[104] R. Kowalewski,[168] T. Z. Kowalski,[37] W. Kozanecki,[135] A. S. Kozhin,[127] V. Kral,[126] V. A. Kramarenko,[96] G. Kramberger,[73] M. W. Krasny,[77] A. Krasznahorkay,[107] J. Kraus,[87] A. Kreisel,[152] F. Krejci,[126] J. Kretzschmar,[72] N. Krieger,[53] P. Krieger,[157] K. Kroeninger,[53] H. Kroha,[98] J. Kroll,[119] J. Kroseberg,[20] J. Krstic,[12a] U. Kruchonak,[64] H. Krüger,[20] T. Kruker,[16] Z. V. Krumshteyn,[64] A. Kruth,[20] T. Kubota,[85] S. Kuehn,[47] A. Kugel,[57c] T. Kuhl,[41] D. Kuhn,[61] V. Kukhtin,[64] Y. Kulchitsky,[89] S. Kuleshov,[31b] C. Kummer,[97] M. Kuna,[77] N. Kundu,[117] J. Kunkle,[119] A. Kupco,[124] H. Kurashige,[66] M. Kurata,[159] Y. A. Kurochkin,[89] V. Kus,[124] M. Kuze,[156] P. Kuzhir,[90] J. Kvita,[29] R. Kwee,[15] A. La Rosa,[171] L. La Rotonda,[36a,36b] L. Labarga,[79] J. Labbe,[4] S. Lablak,[134a] C. Lacasta,[166] F. Lacava,[131a,131b] H. Lacker,[15] D. Lacour,[77] V. R. Lacuesta,[166] E. Ladygin,[64] R. Lafaye,[4] B. Laforge,[77] T. Lagouri,[79] S. Lai,[47] E. Laisne,[54] M. Lamanna,[29] C. L. Lampen,[6] W. Lampl,[6] E. Lancon,[135] U. Landgraf,[47] M. P. J. Landon,[74] H. Landsman,[151] J. L. Lane,[81] C. Lange,[41] A. J. Lankford,[162] F. Lanni,[24] K. Lantzsch,[173] S. Laplace,[77] C. Lapoire,[20] J. F. Laporte,[135] T. Lari,[88a] A. V. Larionov,[127] A. Larner,[117] C. Lasseur,[29] M. Lassnig,[29] P. Laurelli,[46] W. Lavrijsen,[14] P. Laycock,[72] A. B. Lazarev,[64] O. Le Dortz,[77] E. Le Guirriec,[82] C. Le Maner,[157] E. Le Menedeu,[135] C. Lebel,[92] T. LeCompte,[5] F. Ledroit-Guillon,[54] H. Lee,[104] J. S. H. Lee,[149] S. C. Lee,[150] L. Lee,[174] M. Lefebvre,[168] M. Legendre,[135] A. Leger,[48] B. C. LeGeyt,[119] F. Legger,[97] C. Leggett,[14] M. Lehmacher,[20] G. Lehmann Miotto,[29] X. Lei,[6] M. A. L. Leite,[23d] R. Leitner,[125] D. Lellouch,[170] M. Leltchouk,[34] B. Lemmer,[53] V. Lendermann,[57a] K. J. C. Leney,[144b] T. Lenz,[104] G. Lenzen,[173] B. Lenzi,[29] K. Leonhardt,[43] S. Leontsinis,[9] C. Leroy,[92] J-R. Lessard,[168] J. Lesser,[145a] C. G. Lester,[27] A. Leung Fook Cheong,[171] J. Levêque,[4] D. Levin,[86] L. J. Levinson,[170] M. S. Levitski,[127] M. Lewandowska,[21] A. Lewis,[117] G. H. Lewis,[107] A. M. Leyko,[20] M. Leyton,[15] B. Li,[82] H. Li,[171] S. Li,[32b,e] X. Li,[86] Z. Liang,[39] Z. Liang,[117,r] H. Liao,[33] B. Liberti,[132a] P. Lichard,[29] M. Lichtnecker,[97] K. Lie,[164] W. Liebig,[13] R. Lifshitz,[151] J. N. Lilley,[17] C. Limbach,[20] A. Limosani,[85] M. Limper,[62] S. C. Lin,[150,s] F. Linde,[104]

J. T. Linnemann,[87] E. Lipeles,[119] L. Lipinsky,[124] A. Lipniacka,[13] T. M. Liss,[164] D. Lissauer,[24] A. Lister,[48] A. M. Litke,[136] C. Liu,[28] D. Liu,[150,t] H. Liu,[86] J. B. Liu,[86] M. Liu,[32b] S. Liu,[2] Y. Liu,[32b] M. Livan,[118a,118b] S. S. A. Livermore,[117] A. Lleres,[54] J. Llorente Merino,[79] S. L. Lloyd,[74] E. Lobodzinska,[41] P. Loch,[6] W. S. Lockman,[136] T. Loddenkoetter,[20] F. K. Loebinger,[81] A. Loginov,[174] C. W. Loh,[167] T. Lohse,[15] K. Lohwasser,[47] M. Lokajicek,[124] J. Loken,[117] V. P. Lombardo,[4] R. E. Long,[70] L. Lopes,[123a,c] D. Lopez Mateos,[56] M. Losada,[161] P. Loscutoff,[14] F. Lo Sterzo,[131a,131b] M. J. Losty,[158a] X. Lou,[40] A. Lounis,[114] K. F. Loureiro,[161] J. Love,[21] P. A. Love,[70] A. J. Lowe,[142,g] F. Lu,[32a] H. J. Lubatti,[137] C. Luci,[131a,131b] A. Lucotte,[54] A. Ludwig,[43] D. Ludwig,[41] I. Ludwig,[47] J. Ludwig,[47] F. Luehring,[60] G. Luijckx,[104] D. Lumb,[47] L. Luminari,[131a] E. Lund,[116] B. Lund-Jensen,[146] B. Lundberg,[78] J. Lundberg,[145a,145b] J. Lundquist,[35] M. Lungwitz,[80] A. Lupi,[121a,121b] G. Lutz,[98] D. Lynn,[24] J. Lys,[14] E. Lytken,[78] H. Ma,[24] L. L. Ma,[171] J. A. Macana Goia,[92] G. Maccarrone,[46] A. Macchiolo,[98] B. Maček,[73] J. Machado Miguens,[123a] R. Mackeprang,[35] R. J. Madaras,[14] W. F. Mader,[43] R. Maenner,[57c] T. Maeno,[24] P. Mättig,[173] S. Mättig,[41] L. Magnoni,[29] E. Magradze,[53] Y. Mahalalel,[152] K. Mahboubi,[47] G. Mahout,[17] C. Maiani,[131a,131b] C. Maidantchik,[23a] A. Maio,[123a,c] S. Majewski,[24] Y. Makida,[65] N. Makovec,[114] P. Mal,[6] Pa. Malecki,[38] P. Malecki,[38] V. P. Maleev,[120] F. Malek,[54] U. Mallik,[62] D. Malon,[5] C. Malone,[142] S. Maltezos,[9] V. Malyshev,[106] S. Malyukov,[29] R. Mameghani,[97] J. Mamuzic,[12b] A. Manabe,[65] L. Mandelli,[88a] I. Mandić,[73] R. Mandrysch,[15] J. Maneira,[123a] P. S. Mangeard,[87] I. D. Manjavidze,[64] A. Mann,[53] P. M. Manning,[136] A. Manousakis-Katsikakis,[8] B. Mansoulie,[135] A. Manz,[98] A. Mapelli,[29] L. Mapelli,[29] L. March,[79] J. F. Marchand,[29] F. Marchese,[132a,132b] G. Marchiori,[77] M. Marcisovsky,[124] A. Marin,[21,a] C. P. Marino,[60] F. Marroquim,[23a] R. Marshall,[81] Z. Marshall,[29] F. K. Martens,[157] S. Marti-Garcia,[166] A. J. Martin,[174] B. Martin,[29] B. Martin,[87] F. F. Martin,[119] J. P. Martin,[92] Ph. Martin,[54] T. A. Martin,[17] V. J. Martin,[45] B. Martin dit Latour,[48] S. Martin-Haugh,[148] M. Martinez,[11] V. Martinez Outschoorn,[56] A. C. Martyniuk,[81] M. Marx,[81] F. Marzano,[131a] A. Marzin,[110] L. Masetti,[80] T. Mashimo,[154] R. Mashinistov,[93] J. Masik,[81] A. L. Maslennikov,[106] I. Massa,[19a,19b] G. Massaro,[104] N. Massol,[4] P. Mastrandrea,[131a,131b] A. Mastroberardino,[36a,36b] T. Masubuchi,[154] M. Mathes,[20] P. Matricon,[114] H. Matsumoto,[154] H. Matsunaga,[154] T. Matsushita,[66] C. Mattravers,[117,d] J. M. Maugain,[29] S. J. Maxfield,[72] D. A. Maximov,[106] E. N. May,[5] A. Mayne,[138] R. Mazini,[150] M. Mazur,[20] M. Mazzanti,[88a] E. Mazzoni,[121a,121b] S. P. Mc Kee,[86] A. McCarn,[164] R. L. McCarthy,[147] T. G. McCarthy,[28] N. A. McCubbin,[128] K. W. McFarlane,[55] J. A. Mcfayden,[138] H. McGlone,[52] G. Mchedlidze,[50b] R. A. McLaren,[29] T. Mclaughlan,[17] S. J. McMahon,[128] R. A. McPherson,[168,u] A. Meade,[83] J. Mechnich,[104] M. Mechtel,[173] M. Medinnis,[41] R. Meera-Lebbai,[110] T. Meguro,[115] R. Mehdiyev,[92] S. Mehlhase,[35] A. Mehta,[72] K. Meier,[57a] J. Meinhardt,[47] B. Meirose,[78] C. Melachrinos,[30] B. R. Mellado Garcia,[171] L. Mendoza Navas,[161] Z. Meng,[150,t] A. Mengarelli,[19a,19b] S. Menke,[98] C. Menot,[29] E. Meoni,[11] K. M. Mercurio,[56] P. Mermod,[117] L. Merola,[101a,101b] C. Meroni,[88a] F. S. Merritt,[30] A. Messina,[29] J. Metcalfe,[102] A. S. Mete,[63] C. Meyer,[80] J-P. Meyer,[135] J. Meyer,[172] J. Meyer,[53] T. C. Meyer,[29] W. T. Meyer,[63] J. Miao,[32d] S. Michal,[29] L. Micu,[25a] R. P. Middleton,[128] P. Miele,[29] S. Migas,[72] L. Mijović,[41] G. Mikenberg,[170] M. Mikestikova,[124] M. Mikuž,[73] D. W. Miller,[30] R. J. Miller,[87] W. J. Mills,[167] C. Mills,[56] A. Milov,[170] D. A. Milstead,[145a,145b] D. Milstein,[170] A. A. Minaenko,[127] M. Miñano,[166] I. A. Minashvili,[64] A. I. Mincer,[107] B. Mindur,[37] M. Mineev,[64] Y. Ming,[129] L. M. Mir,[11] G. Mirabelli,[131a] L. Miralles Verge,[11] A. Misiejuk,[75] J. Mitrevski,[136] G. Y. Mitrofanov,[127] V. A. Mitsou,[166] S. Mitsui,[65] P. S. Miyagawa,[138] K. Miyazaki,[66] J. U. Mjörnmark,[78] T. Moa,[145a,145b] P. Mockett,[137] S. Moed,[56] V. Moeller,[27] K. Mönig,[41] N. Möser,[20] S. Mohapatra,[147] W. Mohr,[47] S. Mohrdieck-Möck,[98] A. M. Moisseev,[127,a] R. Moles-Valls,[166] J. Molina-Perez,[29] J. Monk,[76] E. Monnier,[82] S. Montesano,[88a,88b] F. Monticelli,[69] S. Monzani,[19a,19b] R. W. Moore,[2] G. F. Moorhead,[85] C. Mora Herrera,[48] A. Moraes,[52] N. Morange,[135] J. Morel,[53] G. Morello,[36a,36b] D. Moreno,[80] M. Moreno Llácer,[166] P. Morettini,[49a] M. Morii,[56] J. Morin,[74] A. K. Morley,[29] G. Mornacchi,[29] S. V. Morozov,[95] J. D. Morris,[74] L. Morvaj,[100] H. G. Moser,[98] M. Mosidze,[50b] J. Moss,[108] R. Mount,[142] E. Mountricha,[135] S. V. Mouraviev,[93] E. J. W. Moyse,[83] M. Mudrinic,[12b] F. Mueller,[57a] J. Mueller,[122] K. Mueller,[20] T. A. Müller,[97] D. Muenstermann,[29] A. Muir,[167] Y. Munwes,[152] W. J. Murray,[128] I. Mussche,[104] E. Musto,[101a,101b] A. G. Myagkov,[127] M. Myska,[124] J. Nadal,[11] K. Nagai,[159] K. Nagano,[65] Y. Nagasaka,[59] A. M. Nairz,[29] Y. Nakahama,[29] K. Nakamura,[154] T. Nakamura,[154] I. Nakano,[109] G. Nanava,[20] A. Napier,[160] M. Nash,[76,d] N. R. Nation,[21] T. Nattermann,[20] T. Naumann,[41] G. Navarro,[161] H. A. Neal,[86] E. Nebot,[79] P. Yu. Nechaeva,[93] A. Negri,[118a,118b] G. Negri,[29] S. Nektarijevic,[48] A. Nelson,[63] S. Nelson,[142] T. K. Nelson,[142] S. Nemecek,[124] P. Nemethy,[107] A. A. Nepomuceno,[23a] M. Nessi,[29,v] S. Y. Nesterov,[120] M. S. Neubauer,[164] A. Neusiedl,[80] R. M. Neves,[107] P. Nevski,[24] P. R. Newman,[17] V. Nguyen Thi Hong,[135] R. B. Nickerson,[117] R. Nicolaidou,[135] L. Nicolas,[138] B. Nicquevert,[29] F. Niedercorn,[114] J. Nielsen,[136] T. Niinikoski,[29] N. Nikiforou,[34]

A. Nikiforov,[15] V. Nikolaenko,[127] K. Nikolaev,[64] I. Nikolic-Audit,[77] K. Nikolics,[48] K. Nikolopoulos,[24] H. Nilsen,[47] P. Nilsson,[7] Y. Ninomiya,[154] A. Nisati,[131a] T. Nishiyama,[66] R. Nisius,[98] L. Nodulman,[5] M. Nomachi,[115] I. Nomidis,[153] M. Nordberg,[29] B. Nordkvist,[145a,145b] P. R. Norton,[128] J. Novakova,[125] M. Nozaki,[65] M. Nožička,[41] L. Nozka,[112] I. M. Nugent,[158a] A.-E. Nuncio-Quiroz,[20] G. Nunes Hanninger,[85] T. Nunnemann,[97] E. Nurse,[76] T. Nyman,[29] B. J. O'Brien,[45] S. W. O'Neale,[17,a] D. C. O'Neil,[141] V. O'Shea,[52] F. G. Oakham,[28,f] H. Oberlack,[98] J. Ocariz,[77] A. Ochi,[66] S. Oda,[154] S. Odaka,[65] J. Odier,[82] H. Ogren,[60] A. Oh,[81] S. H. Oh,[44] C. C. Ohm,[145a,145b] T. Ohshima,[100] H. Ohshita,[139] T. Ohsugi,[58] S. Okada,[66] H. Okawa,[162] Y. Okumura,[100] T. Okuyama,[154] M. Olcese,[49a] A. G. Olchevski,[64] M. Oliveira,[123a,j] D. Oliveira Damazio,[24] E. Oliver Garcia,[166] D. Olivito,[119] A. Olszewski,[38] J. Olszowska,[38] C. Omachi,[66] A. Onofre,[123a,w] P. U. E. Onyisi,[30] C. J. Oram,[158a] M. J. Oreglia,[30] Y. Oren,[152] D. Orestano,[133a,133b] I. Orlov,[106] C. Oropeza Barrera,[52] R. S. Orr,[157] B. Osculati,[49a,49b] R. Ospanov,[119] C. Osuna,[11] G. Otero y Garzon,[26] J. P. Ottersbach,[104] M. Ouchrif,[134d] F. Ould-Saada,[116] A. Ouraou,[135] Q. Ouyang,[32a] M. Owen,[81] S. Owen,[138] V. E. Ozcan,[18a] N. Ozturk,[7] A. Pacheco Pages,[11] C. Padilla Aranda,[11] S. Pagan Griso,[14] E. Paganis,[138] F. Paige,[24] K. Pajchel,[116] G. Palacino,[158b] C. P. Paleari,[6] S. Palestini,[29] D. Pallin,[33] A. Palma,[123a,c] J. D. Palmer,[17] Y. B. Pan,[171] E. Panagiotopoulou,[9] B. Panes,[31a] N. Panikashvili,[86] S. Panitkin,[24] D. Pantea,[25a] M. Panuskova,[124] V. Paolone,[122] A. Papadelis,[145a] Th. D. Papadopoulou,[9] A. Paramonov,[5] W. Park,[24,x] M. A. Parker,[27] F. Parodi,[49a,49b] J. A. Parsons,[34] U. Parzefall,[47] E. Pasqualucci,[131a] A. Passeri,[133a] F. Pastore,[133a,133b] Fr. Pastore,[75] G. Pásztor,[48,y] S. Pataraia,[173] N. Patel,[149] J. R. Pater,[81] S. Patricelli,[101a,101b] T. Pauly,[29] M. Pecsy,[143a] M. I. Pedraza Morales,[171] S. V. Peleganchuk,[106] H. Peng,[32b] R. Pengo,[29] A. Penson,[34] J. Penwell,[60] M. Perantoni,[23a] K. Perez,[34,z] T. Perez Cavalcanti,[41] E. Perez Codina,[11] M. T. Pérez García-Estañ,[166] V. Perez Reale,[34] L. Perini,[88a,88b] H. Pernegger,[29] R. Perrino,[71a] P. Perrodo,[4] S. Persembe,[3a] V. D. Peshekhonov,[64] B. A. Petersen,[29] J. Petersen,[29] T. C. Petersen,[35] E. Petit,[82] A. Petridis,[153] C. Petridou,[153] E. Petrolo,[131a] F. Petrucci,[133a,133b] D. Petschull,[41] M. Petteni,[141] R. Pezoa,[31b] A. Phan,[85] A. W. Phillips,[27] P. W. Phillips,[128] G. Piacquadio,[29] E. Piccaro,[74] M. Piccinini,[19a,19b] A. Pickford,[52] S. M. Piec,[41] R. Piegaia,[26] J. E. Pilcher,[30] A. D. Pilkington,[81] J. Pina,[123a,c] M. Pinamonti,[163a,163c] A. Pinder,[117] J. L. Pinfold,[2] J. Ping,[32c] B. Pinto,[123a,c] O. Pirotte,[29] C. Pizio,[88a,88b] R. Placakyte,[41] M. Plamondon,[168] M.-A. Pleier,[24] A. V. Pleskach,[127] A. Poblaguev,[24] S. Poddar,[57a] F. Podlyski,[33] L. Poggioli,[114] T. Poghosyan,[20] M. Pohl,[48] F. Polci,[54] G. Polesello,[118a] A. Policicchio,[137] A. Polini,[19a] J. Poll,[74] V. Polychronakos,[24] D. M. Pomarede,[135] D. Pomeroy,[22] K. Pommès,[29] L. Pontecorvo,[131a] B. G. Pope,[87] G. A. Popeneciu,[25a] D. S. Popovic,[12a] A. Poppleton,[29] X. Portell Bueso,[29] R. Porter,[162] C. Posch,[21] G. E. Pospelov,[98] S. Pospisil,[126] I. N. Potrap,[98] C. J. Potter,[148] C. T. Potter,[113] G. Poulard,[29] J. Poveda,[171] R. Prabhu,[76] P. Pralavorio,[82] S. Prasad,[56] R. Pravahan,[7] S. Prell,[63] K. Pretzl,[16] L. Pribyl,[29] D. Price,[60] L. E. Price,[5] M. J. Price,[29] P. M. Prichard,[72] D. Prieur,[122] M. Primavera,[71a] K. Prokofiev,[107] F. Prokoshin,[31b] S. Protopopescu,[24] J. Proudfoot,[5] X. Prudent,[43] H. Przysiezniak,[4] S. Psoroulas,[20] E. Ptacek,[113] E. Pueschel,[83] J. Purdham,[86] M. Purohit,[24,x] P. Puzo,[114] Y. Pylypchenko,[116] J. Qian,[86] Z. Qian,[82] Z. Qin,[41] A. Quadt,[53] D. R. Quarrie,[14] W. B. Quayle,[171] F. Quinonez,[31a] M. Raas,[103] V. Radescu,[57b] B. Radics,[20] T. Rador,[18a] F. Ragusa,[88a,88b] G. Rahal,[176] A. M. Rahimi,[108] D. Rahm,[24] S. Rajagopalan,[24] M. Rammensee,[47] M. Rammes,[140] M. Ramstedt,[145a,145b] A. S. Randle-Conde,[39] K. Randrianarivony,[28] P. N. Ratoff,[70] F. Rauscher,[97] E. Rauter,[98] M. Raymond,[29] A. L. Read,[116] D. M. Rebuzzi,[118a,118b] A. Redelbach,[172] G. Redlinger,[24] R. Reece,[119] K. Reeves,[40] A. Reichold,[104] E. Reinherz-Aronis,[152] A. Reinsch,[113] I. Reisinger,[42] D. Reljic,[12a] C. Rembser,[29] Z. L. Ren,[150] A. Renaud,[114] P. Renkel,[39] M. Rescigno,[131a] S. Resconi,[88a] B. Resende,[135] P. Reznicek,[97] R. Rezvani,[157] A. Richards,[76] R. Richter,[98] E. Richter-Was,[4,aa] M. Ridel,[77] S. Rieke,[80] M. Rijpstra,[104] M. Rijssenbeek,[147] A. Rimoldi,[118a,118b] L. Rinaldi,[19a] R. R. Rios,[39] I. Riu,[11] G. Rivoltella,[88a,88b] F. Rizatdinova,[111] E. Rizvi,[74] S. H. Robertson,[84,u] A. Robichaud-Veronneau,[117] D. Robinson,[27] J. E. M. Robinson,[76] M. Robinson,[113] A. Robson,[52] J. G. Rocha de Lima,[105] C. Roda,[121a,121b] D. Roda Dos Santos,[29] S. Rodier,[79] D. Rodriguez,[161] A. Roe,[53] S. Roe,[29] O. Røhne,[116] V. Rojo,[1] S. Rolli,[160] A. Romaniouk,[95] V. M. Romanov,[64] G. Romeo,[26] L. Roos,[77] E. Ros,[166] S. Rosati,[131a,131b] K. Rosbach,[48] A. Rose,[148] M. Rose,[75] G. A. Rosenbaum,[157] E. I. Rosenberg,[63] P. L. Rosendahl,[13] O. Rosenthal,[140] L. Rosselet,[48] V. Rossetti,[11] E. Rossi,[131a,131b] L. P. Rossi,[49a] L. Rossi,[88a,88b] M. Rotaru,[25a] I. Roth,[170] J. Rothberg,[137] D. Rousseau,[114] C. R. Royon,[135] A. Rozanov,[82] Y. Rozen,[151] X. Ruan,[114] I. Rubinskiy,[41] B. Ruckert,[97] N. Ruckstuhl,[104] V. I. Rud,[96] C. Rudolph,[43] G. Rudolph,[61] F. Rühr,[6] F. Ruggieri,[133a,133b] A. Ruiz-Martinez,[63] E. Rulikowska-Zarebska,[37] V. Rumiantsev,[90,a] L. Rumyantsev,[64] K. Runge,[47] O. Runolfsson,[20] Z. Rurikova,[47] N. A. Rusakovich,[64] D. R. Rust,[60] J. P. Rutherfoord,[6] C. Ruwiedel,[14] P. Ruzicka,[124] Y. F. Ryabov,[120] V. Ryadovikov,[127] P. Ryan,[87] M. Rybar,[125] G. Rybkin,[114] N. C. Ryder,[117] S. Rzaeva,[10] A. F. Saavedra,[149] I. Sadeh,[152]

H. F-W. Sadrozinski,[136] R. Sadykov,[64] F. Safai Tehrani,[131a,131b] H. Sakamoto,[154] G. Salamanna,[74] A. Salamon,[132a] M. Saleem,[110] D. Salihagic,[98] A. Salnikov,[142] J. Salt,[166] B. M. Salvachua Ferrando,[5] D. Salvatore,[36a,36b] F. Salvatore,[148] A. Salvucci,[103] A. Salzburger,[29] D. Sampsonidis,[153] B. H. Samset,[116] A. Sanchez,[101a,101b] H. Sandaker,[13] H. G. Sander,[80] M. P. Sanders,[97] M. Sandhoff,[173] T. Sandoval,[27] C. Sandoval,[161] R. Sandstroem,[98] S. Sandvoss,[173] D. P. C. Sankey,[128] A. Sansoni,[46] C. Santamarina Rios,[84] C. Santoni,[33] R. Santonico,[132a,132b] H. Santos,[123a] J. G. Saraiva,[123a,c] T. Sarangi,[171] E. Sarkisyan-Grinbaum,[7] F. Sarri,[121a,121b] G. Sartisohn,[173] O. Sasaki,[65] T. Sasaki,[65] N. Sasao,[67] I. Satsounkevitch,[89] G. Sauvage,[4] E. Sauvan,[4] J. B. Sauvan,[114] P. Savard,[157,f] V. Savinov,[122] D. O. Savu,[29] P. Savva,[9] L. Sawyer,[24,m] D. H. Saxon,[52] L. P. Says,[33] C. Sbarra,[19a] A. Sbrizzi,[19a,19b] O. Scallon,[92] D. A. Scannicchio,[162] J. Schaarschmidt,[114] P. Schacht,[98] U. Schäfer,[80] S. Schaepe,[20] S. Schaetzel,[57b] A. C. Schaffer,[114] D. Schaile,[97] R. D. Schamberger,[147] A. G. Schamov,[106] V. Scharf,[57a] V. A. Schegelsky,[120] D. Scheirich,[86] M. Schernau,[162] M. I. Scherzer,[14] C. Schiavi,[49a,49b] J. Schieck,[97] M. Schioppa,[36a,36b] S. Schlenker,[29] J. L. Schlereth,[5] E. Schmidt,[47] K. Schmieden,[20] C. Schmitt,[80] S. Schmitt,[57b] M. Schmitz,[20] A. Schöning,[57b] M. Schott,[29] D. Schouten,[158a] J. Schovancova,[124] M. Schram,[84] C. Schroeder,[80] N. Schroer,[57c] S. Schuh,[29] G. Schuler,[29] J. Schultes,[173] H.-C. Schultz-Coulon,[57a] H. Schulz,[15] J. W. Schumacher,[20] M. Schumacher,[47] B. A. Schumm,[136] Ph. Schune,[135] C. Schwanenberger,[81] A. Schwartzman,[142] Ph. Schwemling,[77] R. Schwienhorst,[87] R. Schwierz,[43] J. Schwindling,[135] T. Schwindt,[20] W. G. Scott,[128] J. Searcy,[113] E. Sedykh,[120] E. Segura,[11] S. C. Seidel,[102] A. Seiden,[136] F. Seifert,[43] J. M. Seixas,[23a] G. Sekhniaidze,[101a] D. M. Seliverstov,[120] B. Sellden,[145a] G. Sellers,[72] M. Seman,[143b] N. Semprini-Cesari,[19a,19b] C. Serfon,[97] L. Serin,[114] R. Seuster,[98] H. Severini,[110] M. E. Sevior,[85] A. Sfyrla,[29] E. Shabalina,[53] M. Shamim,[113] L. Y. Shan,[32a] J. T. Shank,[21] Q. T. Shao,[85] M. Shapiro,[14] P. B. Shatalov,[94] L. Shaver,[6] K. Shaw,[163a,163c] D. Sherman,[174] P. Sherwood,[76] A. Shibata,[107] H. Shichi,[100] S. Shimizu,[29] M. Shimojima,[99] T. Shin,[55] A. Shmeleva,[93] M. J. Shochet,[30] D. Short,[117] M. A. Shupe,[6] P. Sicho,[124] A. Sidoti,[131a,131b] A. Siebel,[173] F. Siegert,[47] Dj. Sijacki,[12a] O. Silbert,[170] J. Silva,[123a,c] Y. Silver,[152] D. Silverstein,[142] S. B. Silverstein,[145a] V. Simak,[126] O. Simard,[135] Lj. Simic,[12a] S. Simion,[114] B. Simmons,[76] M. Simonyan,[35] P. Sinervo,[157] N. B. Sinev,[113] V. Sipica,[140] G. Siragusa,[172] A. Sircar,[24] A. N. Sisakyan,[64] S. Yu. Sivoklokov,[96] J. Sjölin,[145a,145b] T. B. Sjursen,[13] L. A. Skinnari,[14] H. P. Skottowe,[56] K. Skovpen,[106] P. Skubic,[110] N. Skvorodnev,[22] M. Slater,[17] T. Slavicek,[126] K. Sliwa,[160] J. Sloper,[29] V. Smakhtin,[170] S. Yu. Smirnov,[95] L. N. Smirnova,[96] O. Smirnova,[78] B. C. Smith,[56] D. Smith,[142] K. M. Smith,[52] M. Smizanska,[70] K. Smolek,[126] A. A. Snesarev,[93] S. W. Snow,[81] J. Snow,[110] J. Snuverink,[104] S. Snyder,[24] M. Soares,[123a] R. Sobie,[168,u] J. Sodomka,[126] A. Soffer,[152] C. A. Solans,[166] M. Solar,[126] J. Solc,[126] E. Soldatov,[95] U. Soldevila,[166] E. Solfaroli Camillocci,[131a,131b] A. A. Solodkov,[127] O. V. Solovyanov,[127] J. Sondericker,[24] N. Soni,[2] V. Sopko,[126] B. Sopko,[126] M. Sorbi,[88a,88b] M. Sosebee,[7] R. Soualah,[163a,163c] A. Soukharev,[106] S. Spagnolo,[71a,71b] F. Spanò,[75] R. Spighi,[19a] G. Spigo,[29] F. Spila,[131a,131b] E. Spiriti,[133a] R. Spiwoks,[29] M. Spousta,[125] T. Spreitzer,[157] B. Spurlock,[7] R. D. St. Denis,[52] T. Stahl,[140] J. Stahlman,[119] R. Stamen,[57a] E. Stanecka,[29] R. W. Stanek,[5] C. Stanescu,[133a] S. Stapnes,[116] E. A. Starchenko,[127] J. Stark,[54] P. Staroba,[124] P. Starovoitov,[90] A. Staude,[97] P. Stavina,[143a] G. Stavropoulos,[14] G. Steele,[52] P. Steinbach,[43] P. Steinberg,[24] I. Stekl,[126] B. Stelzer,[141] H. J. Stelzer,[87] O. Stelzer-Chilton,[158a] H. Stenzel,[51] K. Stevenson,[74] G. A. Stewart,[29] J. A. Stillings,[20] T. Stockmanns,[20] M. C. Stockton,[29] K. Stoerig,[47] G. Stoicea,[25a] S. Stonjek,[98] P. Strachota,[125] A. R. Stradling,[7] A. Straessner,[43] J. Strandberg,[146] S. Strandberg,[145a,145b] A. Strandlie,[116] M. Strang,[108] E. Strauss,[142] M. Strauss,[110] P. Strizenec,[143b] R. Ströhmer,[172] D. M. Strom,[113] J. A. Strong,[75,a] R. Stroynowski,[39] J. Strube,[128] B. Stugu,[13] I. Stumer,[24,a] J. Stupak,[147] P. Sturm,[173] D. A. Soh,[150,r] D. Su,[142] HS. Subramania,[2] A. Succurro,[11] Y. Sugaya,[115] T. Sugimoto,[100] C. Suhr,[105] K. Suita,[66] M. Suk,[125] V. V. Sulin,[93] S. Sultansoy,[3d] T. Sumida,[29] X. Sun,[54] J. E. Sundermann,[47] K. Suruliz,[138] S. Sushkov,[11] G. Susinno,[36a,36b] M. R. Sutton,[148] Y. Suzuki,[65] Y. Suzuki,[66] M. Svatos,[124] Yu. M. Sviridov,[127] S. Swedish,[167] I. Sykora,[143a] T. Sykora,[125] B. Szeless,[29] J. Sánchez,[166] D. Ta,[104] K. Tackmann,[41] A. Taffard,[162] R. Tafirout,[158a] N. Taiblum,[152] Y. Takahashi,[100] H. Takai,[24] R. Takashima,[68] H. Takeda,[66] T. Takeshita,[139] M. Talby,[82] A. Talyshev,[106] M. C. Tamsett,[24] J. Tanaka,[154] R. Tanaka,[114] S. Tanaka,[130] S. Tanaka,[65] Y. Tanaka,[99] K. Tani,[66] N. Tannoury,[82] G. P. Tappern,[29] S. Tapprogge,[80] D. Tardif,[157] S. Tarem,[151] F. Tarrade,[28] G. F. Tartarelli,[88a] P. Tas,[125] M. Tasevsky,[124] E. Tassi,[36a,36b] M. Tatarkhanov,[14] Y. Tayalati,[134d] C. Taylor,[76] F. E. Taylor,[91] G. N. Taylor,[85] W. Taylor,[158b] M. Teinturier,[114] M. Teixeira Dias Castanheira,[74] P. Teixeira-Dias,[75] K. K. Temming,[47] H. Ten Kate,[29] P. K. Teng,[150] S. Terada,[65] K. Terashi,[154] J. Terron,[79] M. Terwort,[41,p] M. Testa,[46] R. J. Teuscher,[157,u] J. Thadome,[173] J. Therhaag,[20] T. Theveneaux-Pelzer,[77] M. Thioye,[174] S. Thoma,[47] J. P. Thomas,[17] E. N. Thompson,[83] P. D. Thompson,[17] P. D. Thompson,[157] A. S. Thompson,[52] E. Thomson,[119] M. Thomson,[27] R. P. Thun,[86] F. Tian,[34]

T. Tic,[124] V. O. Tikhomirov,[93] Y. A. Tikhonov,[106] C. J. W. P. Timmermans,[103] P. Tipton,[174] F. J. Tique Aires Viegas,[29] S. Tisserant,[82] J. Tobias,[47] B. Toczek,[37] T. Todorov,[4] S. Todorova-Nova,[160] B. Toggerson,[162] J. Tojo,[65] S. Tokár,[143a] K. Tokunaga,[66] K. Tokushuku,[65] K. Tollefson,[87] M. Tomoto,[100] L. Tompkins,[14] K. Toms,[102] G. Tong,[32a] A. Tonoyan,[13] C. Topfel,[16] N. D. Topilin,[64] I. Torchiani,[29] E. Torrence,[113] H. Torres,[77] E. Torró Pastor,[166] J. Toth,[82,y] F. Touchard,[82] D. R. Tovey,[138] D. Traynor,[74] T. Trefzger,[172] L. Tremblet,[29] A. Tricoli,[29] I. M. Trigger,[158a] S. Trincaz-Duvoid,[77] T. N. Trinh,[77] M. F. Tripiana,[69] W. Trischuk,[157] A. Trivedi,[24,x] B. Trocmé,[54] C. Troncon,[88a] M. Trottier-McDonald,[141] A. Trzupek,[38] C. Tsarouchas,[29] J. C-L. Tseng,[117] M. Tsiakiris,[104] P. V. Tsiareshka,[89] D. Tsionou,[4] G. Tsipolitis,[9] V. Tsiskaridze,[47] E. G. Tskhadadze,[50a] I. I. Tsukerman,[94] V. Tsulaia,[14] J.-W. Tsung,[20] S. Tsuno,[65] D. Tsybychev,[147] A. Tua,[138] J. M. Tuggle,[30] M. Turala,[38] D. Turecek,[126] I. Turk Cakir,[3e] E. Turlay,[104] R. Turra,[88a,88b] P. M. Tuts,[34] A. Tykhonov,[73] M. Tylmad,[145a,145b] M. Tyndel,[128] H. Tyrvainen,[29] G. Tzanakos,[8] K. Uchida,[20] I. Ueda,[154] R. Ueno,[28] M. Ugland,[13] M. Uhlenbrock,[20] M. Uhrmacher,[53] F. Ukegawa,[159] G. Unal,[29] D. G. Underwood,[5] A. Undrus,[24] G. Unel,[162] Y. Unno,[65] D. Urbaniec,[34] E. Urkovsky,[152] P. Urrejola,[31a] G. Usai,[7] M. Uslenghi,[118a,118b] L. Vacavant,[82] V. Vacek,[126] B. Vachon,[84] S. Vahsen,[14] J. Valenta,[124] P. Valente,[131a] S. Valentinetti,[19a,19b] S. Valkar,[125] E. Valladolid Gallego,[166] S. Vallecorsa,[151] J. A. Valls Ferrer,[166] H. van der Graaf,[104] E. van der Kraaij,[104] R. Van Der Leeuw,[104] E. van der Poel,[104] D. van der Ster,[29] N. van Eldik,[83] P. van Gemmeren,[5] Z. van Kesteren,[104] I. van Vulpen,[104] M. Vanadia,[98] W. Vandelli,[29] G. Vandoni,[29] A. Vaniachine,[5] P. Vankov,[41] F. Vannucci,[77] F. Varela Rodriguez,[29] R. Vari,[131a] D. Varouchas,[14] A. Vartapetian,[7] K. E. Varvell,[149] V. I. Vassilakopoulos,[55] F. Vazeille,[33] G. Vegni,[88a,88b] J. J. Veillet,[114] C. Vellidis,[8] F. Veloso,[123a] R. Veness,[29] S. Veneziano,[131a] A. Ventura,[71a,71b] D. Ventura,[137] M. Venturi,[47] N. Venturi,[16] V. Vercesi,[118a] M. Verducci,[137] W. Verkerke,[104] J. C. Vermeulen,[104] A. Vest,[43] M. C. Vetterli,[141,f] I. Vichou,[164] T. Vickey,[144b,bb] O. E. Vickey Boeriu,[144b] G. H. A. Viehhauser,[117] S. Viel,[167] M. Villa,[19a,19b] M. Villaplana Perez,[166] E. Vilucchi,[46] M. G. Vincter,[28] E. Vinek,[29] V. B. Vinogradov,[64] M. Virchaux,[135,a] J. Virzi,[14] O. Vitells,[170] M. Viti,[41] I. Vivarelli,[47] F. Vives Vaque,[2] S. Vlachos,[9] M. Vlasak,[126] N. Vlasov,[20] A. Vogel,[20] P. Vokac,[126] G. Volpi,[46] M. Volpi,[85] G. Volpini,[88a] H. von der Schmitt,[98] J. von Loeben,[98] H. von Radziewski,[47] E. von Toerne,[20] V. Vorobel,[125] A. P. Vorobiev,[127] V. Vorwerk,[11] M. Vos,[166] R. Voss,[29] T. T. Voss,[173] J. H. Vossebeld,[72] N. Vranjes,[12a] M. Vranjes Milosavljevic,[104] V. Vrba,[124] M. Vreeswijk,[104] T. Vu Anh,[80] R. Vuillermet,[29] I. Vukotic,[114] W. Wagner,[173] P. Wagner,[119] H. Wahlen,[173] J. Wakabayashi,[100] J. Walbersloh,[42] S. Walch,[86] J. Walder,[70] R. Walker,[97] W. Walkowiak,[140] R. Wall,[174] P. Waller,[72] C. Wang,[44] H. Wang,[171] H. Wang,[32b,cc] J. Wang,[150] J. Wang,[32d] J. C. Wang,[137] R. Wang,[102] S. M. Wang,[150] A. Warburton,[84] C. P. Ward,[27] M. Warsinsky,[47] P. M. Watkins,[17] A. T. Watson,[17] M. F. Watson,[17] G. Watts,[137] S. Watts,[81] A. T. Waugh,[149] B. M. Waugh,[76] J. Weber,[42] M. Weber,[128] M. S. Weber,[16] P. Weber,[53] A. R. Weidberg,[117] P. Weigell,[98] J. Weingarten,[53] C. Weiser,[47] H. Wellenstein,[22] P. S. Wells,[29] M. Wen,[46] T. Wenaus,[24] S. Wendler,[122] Z. Weng,[150,r] T. Wengler,[29] S. Wenig,[29] N. Wermes,[20] M. Werner,[47] P. Werner,[29] M. Werth,[162] M. Wessels,[57a] C. Weydert,[54] K. Whalen,[28] S. J. Wheeler-Ellis,[162] S. P. Whitaker,[21] A. White,[7] M. J. White,[85] S. R. Whitehead,[117] D. Whiteson,[162] D. Whittington,[60] F. Wicek,[114] D. Wicke,[173] F. J. Wickens,[128] W. Wiedenmann,[171] M. Wielers,[128] P. Wienemann,[20] C. Wiglesworth,[74] L. A. M. Wiik,[47] P. A. Wijeratne,[76] A. Wildauer,[166] M. A. Wildt,[41,p] I. Wilhelm,[125] H. G. Wilkens,[29] J. Z. Will,[97] E. Williams,[34] H. H. Williams,[119] W. Willis,[34] S. Willocq,[83] J. A. Wilson,[17] M. G. Wilson,[142] A. Wilson,[86] I. Wingerter-Seez,[4] S. Winkelmann,[47] F. Winklmeier,[29] M. Wittgen,[142] M. W. Wolter,[38] H. Wolters,[123a,j] W. C. Wong,[40] G. Wooden,[86] B. K. Wosiek,[38] J. Wotschack,[29] M. J. Woudstra,[83] K. Wraight,[52] C. Wright,[52] B. Wrona,[72] S. L. Wu,[171] X. Wu,[48] Y. Wu,[32b,dd] E. Wulf,[34] R. Wunstorf,[42] B. M. Wynne,[45] L. Xaplanteris,[9] S. Xella,[35] S. Xie,[47] Y. Xie,[32a] C. Xu,[32b,ee] D. Xu,[138] G. Xu,[32a] B. Yabsley,[149] S. Yacoob,[144b] M. Yamada,[65] H. Yamaguchi,[154] A. Yamamoto,[65] K. Yamamoto,[63] S. Yamamoto,[154] T. Yamamura,[154] T. Yamanaka,[154] J. Yamaoka,[44] T. Yamazaki,[154] Y. Yamazaki,[66] Z. Yan,[21] H. Yang,[86] U. K. Yang,[81] Y. Yang,[60] Y. Yang,[32a] Z. Yang,[145a,145b] S. Yanush,[90] Y. Yao,[14] Y. Yasu,[65] G. V. Ybeles Smit,[129] J. Ye,[39] S. Ye,[24] M. Yilmaz,[3c] R. Yoosoofmiya,[122] K. Yorita,[169] R. Yoshida,[5] C. Young,[142] S. Youssef,[21] D. Yu,[24] J. Yu,[7] J. Yu,[32c,ee] L. Yuan,[32a,ff] A. Yurkewicz,[147] V. G. Zaets,[127] R. Zaidan,[62] A. M. Zaitsev,[127] Z. Zajacova,[29] Yo. K. Zalite,[120] L. Zanello,[131a,131b] P. Zarzhitsky,[39] A. Zaytsev,[106] C. Zeitnitz,[173] M. Zeller,[174] M. Zeman,[124] A. Zemla,[38] C. Zendler,[20] O. Zenin,[127] T. Ženiš,[143a] Z. Zenonos,[121a,121b] S. Zenz,[14] D. Zerwas,[114] G. Zevi della Porta,[56] Z. Zhan,[32d] D. Zhang,[32b,cc] H. Zhang,[87] J. Zhang,[5] X. Zhang,[32d] Z. Zhang,[114] L. Zhao,[107] T. Zhao,[137] Z. Zhao,[32b] A. Zhemchugov,[64] S. Zheng,[32a] J. Zhong,[150,gg] B. Zhou,[86] N. Zhou,[162] Y. Zhou,[150] C. G. Zhu,[32d] H. Zhu,[41] J. Zhu,[86] Y. Zhu,[171] X. Zhuang,[97] V. Zhuravlov,[98] D. Zieminska,[60] R. Zimmermann,[20]

S. Zimmermann,[20] S. Zimmermann,[47] M. Ziolkowski,[140] R. Zitoun,[4] L. Živković,[34] V. V. Zmouchko,[127,a] G. Zobernig,[171] A. Zoccoli,[19a,19b] Y. Zolnierowski,[4] A. Zsenei,[29] M. zur Nedden,[15] V. Zutshi,[105] and L. Zwalinski[29]

(ATLAS Collaboration)

[1]*University at Albany, Albany, New York, USA*
[2]*Department of Physics, University of Alberta, Edmonton AB, Canada*
[3a]*Department of Physics, Ankara University, Ankara, Turkey*
[3b]*Department of Physics, Dumlupinar University, Kutahya, Turkey*
[3c]*Department of Physics, Gazi University, Ankara, Turkey*
[3d]*Division of Physics, TOBB University of Economics and Technology, Ankara, Turkey*
[3e]*Turkish Atomic Energy Authority, Ankara, Turkey*
[4]*LAPP, CNRS/IN2P3 and Université de Savoie, Annecy-le-Vieux, France*
[5]*High Energy Physics Division, Argonne National Laboratory, Argonne, Illinois, USA*
[6]*Department of Physics, University of Arizona, Tucson, Arizona, USA*
[7]*Department of Physics, The University of Texas at Arlington, Arlington, Texas, USA*
[8]*Physics Department, University of Athens, Athens, Greece*
[9]*Physics Department, National Technical University of Athens, Zografou, Greece*
[10]*Institute of Physics, Azerbaijan Academy of Sciences, Baku, Azerbaijan*
[11]*Institut de Física d'Altes Energies and Departament de Física de la Universitat Autònoma de Barcelona and ICREA, Barcelona, Spain*
[12a]*Institute of Physics, University of Belgrade, Belgrade, Serbia*
[12b]*Vinca Institute of Nuclear Sciences, Belgrade, Serbia*
[13]*Department for Physics and Technology, University of Bergen, Bergen, Norway*
[14]*Physics Division, Lawrence Berkeley National Laboratory and University of California, Berkeley, California, USA*
[15]*Department of Physics, Humboldt University, Berlin, Germany*
[16]*Albert Einstein Center for Fundamental Physics and Laboratory for High Energy Physics, University of Bern, Bern, Switzerland*
[17]*School of Physics and Astronomy, University of Birmingham, Birmingham, United Kingdom*
[18a]*Department of Physics, Bogazici University, Istanbul, Turkey*
[18b]*Division of Physics, Dogus University, Istanbul, Turkey*
[18c]*Department of Physics Engineering, Gaziantep University, Gaziantep, Turkey*
[18d]*Department of Physics, Istanbul Technical University, Istanbul, Turkey*
[19a]*INFN Sezione di Bologna, Italy*
[19b]*Dipartimento di Fisica, Università di Bologna, Bologna, Italy*
[20]*Physikalisches Institut, University of Bonn, Bonn, Germany*
[21]*Department of Physics, Boston University, Boston, Massachusetts, USA*
[22]*Department of Physics, Brandeis University, Waltham, Massachusetts, USA*
[23a]*Universidade Federal do Rio De Janeiro COPPE/EE/IF, Rio de Janeiro, Brazil*
[23b]*Federal University of Juiz de Fora (UFJF), Juiz de Fora, Brazil*
[23c]*Federal University of Sao Joao del Rei (UFSJ), Sao Joao del Rei, Brazil*
[23d]*Instituto de Fisica, Universidade de Sao Paulo, Sao Paulo, Brazil*
[24]*Physics Department, Brookhaven National Laboratory, Upton, New York, USA*
[25a]*National Institute of Physics and Nuclear Engineering, Bucharest, Romania*
[25b]*University Politehnica Bucharest, Bucharest, Romania*
[25c]*West University in Timisoara, Timisoara, Romania*
[26]*Departamento de Física, Universidad de Buenos Aires, Buenos Aires, Argentina*
[27]*Cavendish Laboratory, University of Cambridge, Cambridge, United Kingdom*
[28]*Department of Physics, Carleton University, Ottawa ON, Canada*
[29]*CERN, Geneva, Switzerland*
[30]*Enrico Fermi Institute, University of Chicago, Chicago, Illinois, USA*
[31a]*Departamento de Fisica, Pontificia Universidad Católica de Chile, Santiago, Chile*
[31b]*Departamento de Física, Universidad Técnica Federico Santa María, Valparaíso, Chile*
[32a]*Institute of High Energy Physics, Chinese Academy of Sciences, Beijing, China*
[32b]*Department of Modern Physics, University of Science and Technology of China, Anhui, China*
[32c]*Department of Physics, Nanjing University, Jiangsu, China*
[32d]*High Energy Physics Group, Shandong University, Shandong, China*
[33]*Laboratoire de Physique Corpusculaire, Clermont Université and Université Blaise Pascal and CNRS/IN2P3, Aubiere Cedex, France*
[34]*Nevis Laboratory, Columbia University, Irvington, New York, USA*
[35]*Niels Bohr Institute, University of Copenhagen, Kobenhavn, Denmark*

[36a]INFN Gruppo Collegato di Cosenza, Italy
[36b]Dipartimento di Fisica, Università della Calabria, Arcavata di Rende, Italy
[37]Faculty of Physics and Applied Computer Science, AGH-University of Science and Technology, Krakow, Poland
[38]The Henryk Niewodniczanski Institute of Nuclear Physics, Polish Academy of Sciences, Krakow, Poland
[39]Physics Department, Southern Methodist University, Dallas, Texas, USA
[40]Physics Department, University of Texas at Dallas, Richardson, Texas, USA
[41]DESY, Hamburg and Zeuthen, Germany
[42]Institut für Experimentelle Physik IV, Technische Universität Dortmund, Dortmund, Germany
[43]Institut für Kern- und Teilchenphysik, Technical University Dresden, Dresden, Germany
[44]Department of Physics, Duke University, Durham, North Carolina, USA
[45]SUPA - School of Physics and Astronomy, University of Edinburgh, Edinburgh, United Kingdom
[46]INFN Laboratori Nazionali di Frascati, Frascati, Italy
[47]Fakultät für Mathematik und Physik, Albert-Ludwigs-Universität, Freiburg i.Br., Germany
[48]Section de Physique, Université de Genève, Geneva, Switzerland
[49a]INFN Sezione di Genova, Italy
[49b]Dipartimento di Fisica, Università di Genova, Genova, Italy
[50a]E. Andronikashvili Institute of Physics, Georgian Academy of Sciences, Tbilisi, Georgia
[50b]High Energy Physics Institute, Tbilisi State University, Tbilisi, Georgia
[51]II Physikalisches Institut, Justus-Liebig-Universität Giessen, Giessen, Germany
[52]SUPA - School of Physics and Astronomy, University of Glasgow, Glasgow, United Kingdom
[53]II Physikalisches Institut, Georg-August-Universität, Göttingen, Germany
[54]Laboratoire de Physique Subatomique et de Cosmologie, Université Joseph Fourier and CNRS/IN2P3 and Institut National Polytechnique de Grenoble, Grenoble, France
[55]Department of Physics, Hampton University, Hampton, Virginia, USA
[56]Laboratory for Particle Physics and Cosmology, Harvard University, Cambridge, Massachusetts, USA
[57a]Kirchhoff-Institut für Physik, Ruprecht-Karls-Universität Heidelberg, Heidelberg, Germany
[57b]Physikalisches Institut, Ruprecht-Karls-Universität Heidelberg, Heidelberg, Germany
[57c]ZITI Institut für technische Informatik, Ruprecht-Karls-Universität Heidelberg, Mannheim, Germany
[58]Faculty of Science, Hiroshima University, Hiroshima, Japan
[59]Faculty of Applied Information Science, Hiroshima Institute of Technology, Hiroshima, Japan
[60]Department of Physics, Indiana University, Bloomington, Indiana, USA
[61]Institut für Astro- und Teilchenphysik, Leopold-Franzens-Universität, Innsbruck, Austria
[62]University of Iowa, Iowa City Iowa, USA
[63]Department of Physics and Astronomy, Iowa State University, Ames, Iowa, USA
[64]Joint Institute for Nuclear Research, JINR Dubna, Dubna, Russia
[65]KEK, High Energy Accelerator Research Organization, Tsukuba, Japan
[66]Graduate School of Science, Kobe University, Kobe, Japan
[67]Faculty of Science, Kyoto University, Kyoto, Japan
[68]Kyoto University of Education, Kyoto, Japan
[69]Instituto de Física La Plata, Universidad Nacional de La Plata and CONICET, La Plata, Argentina
[70]Physics Department, Lancaster University, Lancaster, United Kingdom
[71a]INFN Sezione di Lecce, Italy
[71b]Dipartimento di Fisica, Università del Salento, Lecce, Italy
[72]Oliver Lodge Laboratory, University of Liverpool, Liverpool, United Kingdom
[73]Department of Physics, Jožef Stefan Institute and University of Ljubljana, Ljubljana, Slovenia
[74]Department of Physics, Queen Mary University of London, London, United Kingdom
[75]Department of Physics, Royal Holloway University of London, Surrey, United Kingdom
[76]Department of Physics and Astronomy, University College London, London, United Kingdom
[77]Laboratoire de Physique Nucléaire et de Hautes Energies, UPMC and Université Paris-Diderot and CNRS/IN2P3, Paris, France
[78]Fysiska institutionen, Lunds universitet, Lund, Sweden
[79]Departamento de Fisica Teorica C-15, Universidad Autonoma de Madrid, Madrid, Spain
[80]Institut für Physik, Universität Mainz, Mainz, Germany
[81]School of Physics and Astronomy, University of Manchester, Manchester, United Kingdom
[82]CPPM, Aix-Marseille Université and CNRS/IN2P3, Marseille, France
[83]Department of Physics, University of Massachusetts, Amherst, Massachusetts, USA
[84]Department of Physics, McGill University, Montreal QC, Canada
[85]School of Physics, University of Melbourne, Victoria, Australia
[86]Department of Physics, The University of Michigan, Ann Arbor, Michigan, USA
[87]Department of Physics and Astronomy, Michigan State University, East Lansing, Michigan, USA
[88a]INFN Sezione di Milano, Italy

[88b]*Dipartimento di Fisica, Università di Milano, Milano, Italy*
[89]*B.I. Stepanov Institute of Physics, National Academy of Sciences of Belarus, Minsk, Republic of Belarus*
[90]*National Scientific and Educational Centre for Particle and High Energy Physics, Minsk, Republic of Belarus*
[91]*Department of Physics, Massachusetts Institute of Technology, Cambridge, Massachusetts, USA*
[92]*Group of Particle Physics, University of Montreal, Montreal QC, Canada*
[93]*P.N. Lebedev Institute of Physics, Academy of Sciences, Moscow, Russia*
[94]*Institute for Theoretical and Experimental Physics (ITEP), Moscow, Russia*
[95]*Moscow Engineering and Physics Institute (MEPhI), Moscow, Russia*
[96]*Skobeltsyn Institute of Nuclear Physics, Lomonosov Moscow State University, Moscow, Russia*
[97]*Fakultät für Physik, Ludwig-Maximilians-Universität München, München, Germany*
[98]*Max-Planck-Institut für Physik (Werner-Heisenberg-Institut), München, Germany*
[99]*Nagasaki Institute of Applied Science, Nagasaki, Japan*
[100]*Graduate School of Science, Nagoya University, Nagoya, Japan*
[101a]*INFN Sezione di Napoli, Italy*
[101b]*Dipartimento di Scienze Fisiche, Università di Napoli, Napoli, Italy*
[102]*Department of Physics and Astronomy, University of New Mexico, Albuquerque, New Mexico, USA*
[103]*Institute for Mathematics, Astrophysics and Particle Physics, Radboud University Nijmegen/Nikhef, Nijmegen, Netherlands*
[104]*Nikhef National Institute for Subatomic Physics and University of Amsterdam, Amsterdam, Netherlands*
[105]*Department of Physics, Northern Illinois University, DeKalb, Illinois, USA*
[106]*Budker Institute of Nuclear Physics (BINP), Novosibirsk, Russia*
[107]*Department of Physics, New York University, New York, New York, USA*
[108]*Ohio State University, Columbus, Ohio, USA*
[109]*Faculty of Science, Okayama University, Okayama, Japan*
[110]*Homer L. Dodge Department of Physics and Astronomy, University of Oklahoma, Norman, Oklahoma, USA*
[111]*Department of Physics, Oklahoma State University, Stillwater, Oklahoma, USA*
[112]*Palacký University, RCPTM, Olomouc, Czech Republic*
[113]*Center for High Energy Physics, University of Oregon, Eugene, Oregon, USA*
[114]*LAL, Univ. Paris-Sud and CNRS/IN2P3, Orsay, France*
[115]*Graduate School of Science, Osaka University, Osaka, Japan*
[116]*Department of Physics, University of Oslo, Oslo, Norway*
[117]*Department of Physics, Oxford University, Oxford, United Kingdom*
[118a]*INFN Sezione di Pavia, Italy*
[118b]*Dipartimento di Fisica Nucleare e Teorica, Università di Pavia, Pavia, Italy*
[119]*Department of Physics, University of Pennsylvania, Philadelphia, Pennsylvania, USA*
[120]*Petersburg Nuclear Physics Institute, Gatchina, Russia*
[121a]*INFN Sezione di Pisa, Italy*
[121b]*Dipartimento di Fisica E. Fermi, Università di Pisa, Pisa, Italy*
[122]*Department of Physics and Astronomy, University of Pittsburgh, Pittsburgh, Pennsylvania, USA*
[123a]*Laboratorio de Instrumentacao e Fisica Experimental de Particulas - LIP, Lisboa, Portugal*
[123b]*Departamento de Fisica Teorica y del Cosmos and CAFPE, Universidad de Granada, Granada, Portugal*
[124]*Institute of Physics, Academy of Sciences of the Czech Republic, Praha, Czech Republic*
[125]*Faculty of Mathematics and Physics, Charles University in Prague, Praha, Czech Republic*
[126]*Czech Technical University in Prague, Praha, Czech Republic*
[127]*State Research Center Institute for High Energy Physics, Protvino, Russia*
[128]*Particle Physics Department, Rutherford Appleton Laboratory, Didcot, United Kingdom*
[129]*Physics Department, University of Regina, Regina SK, Canada*
[130]*Ritsumeikan University, Kusatsu, Shiga, Japan*
[131a]*INFN Sezione di Roma I, Italy*
[131b]*Dipartimento di Fisica, Università La Sapienza, Roma, Italy*
[132a]*INFN Sezione di Roma Tor Vergata, Italy*
[132b]*Dipartimento di Fisica, Università di Roma Tor Vergata, Roma, Italy*
[133a]*INFN Sezione di Roma Tre, Italy*
[133b]*Dipartimento di Fisica, Università Roma Tre, Roma, Italy*
[134a]*Faculté des Sciences Ain Chock, Réseau Universitaire de Physique des Hautes Energies - Université Hassan II, Casablanca, Morocco*
[134b]*Centre National de l'Energie des Sciences Techniques Nucleaires, Rabat, Morocco*
[134c]*Université Cadi Ayyad, Faculté des sciences Semlalia Département de Physique, B.P. 2390 Marrakech 40000, Morocco*
[134d]*Faculté des Sciences, Université Mohamed Premier and LPTPM, Oujda, Morocco*
[134e]*Faculté des Sciences, Université Mohammed V, Rabat, Morocco*
[135]*DSM/IRFU (Institut de Recherches sur les Lois Fondamentales de l'Univers), CEA Saclay (Commissariat a l'Energie Atomique), Gif-sur-Yvette, France*

[136]Santa Cruz Institute for Particle Physics, University of California Santa Cruz, Santa Cruz, California, USA
[137]Department of Physics, University of Washington, Seattle, Washington, USA
[138]Department of Physics and Astronomy, University of Sheffield, Sheffield, United Kingdom
[139]Department of Physics, Shinshu University, Nagano, Japan
[140]Fachbereich Physik, Universität Siegen, Siegen, Germany
[141]Department of Physics, Simon Fraser University, Burnaby BC, Canada
[142]SLAC National Accelerator Laboratory, Stanford, California, USA
[143a]Faculty of Mathematics, Physics & Informatics, Comenius University, Bratislava, Slovak Republic
[143b]Department of Subnuclear Physics, Institute of Experimental Physics of the Slovak Academy of Sciences, Kosice, Slovak Republic
[144a]Department of Physics, University of Johannesburg, Johannesburg, South Africa
[144b]School of Physics, University of the Witwatersrand, Johannesburg, South Africa
[145a]Department of Physics, Stockholm University, Sweden
[145b]The Oskar Klein Centre, Stockholm, Sweden
[146]Physics Department, Royal Institute of Technology, Stockholm, Sweden
[147]Department of Physics and Astronomy, Stony Brook University, Stony Brook, New York, USA
[148]Department of Physics and Astronomy, University of Sussex, Brighton, United Kingdom
[149]School of Physics, University of Sydney, Sydney, Australia
[150]Institute of Physics, Academia Sinica, Taipei, Taiwan
[151]Department of Physics, Technion: Israel Inst. of Technology, Haifa, Israel
[152]Raymond and Beverly Sackler School of Physics and Astronomy, Tel Aviv University, Tel Aviv, Israel
[153]Department of Physics, Aristotle University of Thessaloniki, Thessaloniki, Greece
[154]International Center for Elementary Particle Physics and Department of Physics, The University of Tokyo, Tokyo, Japan
[155]Graduate School of Science and Technology, Tokyo Metropolitan University, Tokyo, Japan
[156]Department of Physics, Tokyo Institute of Technology, Tokyo, Japan
[157]Department of Physics, University of Toronto, Toronto ON, Canada
[158a]TRIUMF, Vancouver BC, Canada
[158b]Department of Physics and Astronomy, York University, Toronto ON, Canada
[159]Institute of Pure and Applied Sciences, University of Tsukuba, Ibaraki, Japan
[160]Science and Technology Center, Tufts University, Medford, Massachusetts, USA
[161]Centro de Investigaciones, Universidad Antonio Narino, Bogota, Colombia
[162]Department of Physics and Astronomy, University of California Irvine, Irvine, California, USA
[163a]INFN Gruppo Collegato di Udine, Italy
[163b]ICTP, Trieste, Italy
[163c]Dipartimento di Chimica, Fisica e Ambiente, Università di Udine, Udine, Italy
[164]Department of Physics, University of Illinois, Urbana, Illinois, USA
[165]Department of Physics and Astronomy, University of Uppsala, Uppsala, Sweden
[166]Instituto de Física Corpuscular (IFIC) and Departamento de Física Atómica, Molecular y Nuclear and Departamento de Ingeniera Electrónica and Instituto de Microelectrónica de Barcelona (IMB-CNM), University of Valencia and CSIC, Valencia, Spain
[167]Department of Physics, University of British Columbia, Vancouver BC, Canada
[168]Department of Physics and Astronomy, University of Victoria, Victoria BC, Canada
[169]Waseda University, Tokyo, Japan
[170]Department of Particle Physics, The Weizmann Institute of Science, Rehovot, Israel
[171]Department of Physics, University of Wisconsin, Madison, Wisconsin, USA
[172]Fakultät für Physik und Astronomie, Julius-Maximilians-Universität, Würzburg, Germany
[173]Fachbereich C Physik, Bergische Universität Wuppertal, Wuppertal, Germany
[174]Department of Physics, Yale University, New Haven, Connecticut, USA
[175]Yerevan Physics Institute, Yerevan, Armenia
[176]Domaine scientifique de la Doua, Centre de Calcul CNRS/IN2P3, Villeurbanne Cedex, France

[a]Deceased.
[b]Also at Laboratorio de Instrumentacao e Fisica Experimental de Particulas—LIP, Lisboa, Portugal.
[c]Also at Faculdade de Ciencias and CFNUL, Universidade de Lisboa, Lisboa, Portugal.
[d]Also at Particle Physics Department, Rutherford Appleton Laboratory, Didcot, United Kingdom.
[e]Also at CPPM, Aix-Marseille Université and CNRS/IN2P3, Marseille, France.
[f]Also at TRIUMF, Vancouver BC, Canada.
[g]Also at Department of Physics, California State University, Fresno, CA, USA.
[h]Also at Faculty of Physics and Applied Computer Science, AGH-University of Science and Technology, Krakow, Poland.
[i]Also at Fermilab, Batavia, IL, USA.

[j]Also at Department of Physics, University of Coimbra, Coimbra, Portugal.
[k]Also at Università di Napoli Parthenope, Napoli, Italy.
[l]Also at Department of Physics, Middle East Technical University, Ankara, Turkey.
[m]Also at Louisiana Tech University, Ruston, LA, USA.
[n]Also at Group of Particle Physics, University of Montreal, Montreal, QC, Canada.
[o]Also at Institute of Physics, Azerbaijan Academy of Sciences, Baku, Azerbaijan.
[p]Also at Institut für Experimentalphysik, Universität Hamburg, Hamburg, Germany.
[q]Also at Manhattan College, New York, NY, USA.
[r]Also at School of Physics and Engineering, Sun Yat-sen University, Guanzhou, China.
[s]Also at Academia Sinica Grid Computing, Institute of Physics, Academia Sinica, Taipei, Taiwan.
[t]Also at High Energy Physics Group, Shandong University, Shandong, China.
[u]Also at Institute of Particle Physics (IPP), Canada.
[v]Also at Section de Physique, Université de Genève, Geneva, Switzerland.
[w]Also at Departamento de Fisica, Universidade de Minho, Braga, Portugal.
[x]Also at Department of Physics and Astronomy, University of South Carolina, Columbia, SC, USA.
[y]Also at KFKI Research Institute for Particle and Nuclear Physics, Budapest, Hungary.
[z]Also at California Institute of Technology, Pasadena, CA, USA.
[aa]Also at Institute of Physics, Jagiellonian University, Krakow, Poland.
[bb]Also at Department of Physics, Oxford University, Oxford, United Kingdom.
[cc]Also at Institute of Physics, Academia Sinica, Taipei, Taiwan
[dd]Also at Department of Physics, The University of Michigan, Ann Arbor, MI, USA.
[ee]Also at DSM/IRFU (Institut de Recherches sur les Lois Fondamentales de l'Univers), CEA Saclay (Commissariat a l'Energie Atomique), Gif-sur-Yvette, France.
[ff]Also at Laboratoire de Physique Nucléaire et de Hautes Energies, UPMC and Université Paris-Diderot and CNRS/IN2P3, Paris, France.
[gg]Also at Department of Physics, Nanjing University, Jiangsu, China.